# Functional organization of the perirhinal-lateral entorhinal circuit

**Babak Tahvildari**

**Department of Neurology and Neurosurgery**

**McGill University, Montreal**

**May 2007**

A thesis submitted to McGill University in partial fulfillment of the requirements of the degree of Doctor of Philosophy

*Your file Votre référence*
*ISBN: 978-0-494-32389-2*
*Our file Notre référence*
*ISBN: 978-0-494-32389-2*

**To my lovely parents: Amanollah Tahvildari and Louise Tahvildari**

*"Of one essence is the human race, thus has creation put the base;*

*One limb impacted is sufficient, for all others to feel the mace."*

(Saadi 1184-1283)

# Table of contents

# List of figures and tables

# Abstract

The perirhinal cortex (PRC) and the lateral entorhinal cortex (LEC) are essential components of the medial temporal lobe memory system, but the functional organization and interconnectivity of these structures is poorly defined. In this thesis, novel *in-vitro* and *in-vivo* approaches were developed to investigate the synaptic organization, intrinsic properties and cholinergic modulation of neurons in the PRC and LEC. *In-vivo* and *in-vitro* field potential profiles, combined with current-source density analysis and *in-vitro* intracellular recordings, demonstrated the existence of bi-directional excitatory synaptic interactions between the PRC and the LEC. Intracellular recordings and dye injection were also used to perform a morphological and electrophysiological characterization of principal neurons located in layers II and III of the LEC. These studies revealed that principal neurons in layer II of the LEC possess more heterogeneous morphological and electrophysiological properties than those in layer III. Moreover, layer III principal neurons display extensively arborized basal and apical dendrites that extend into layers I, II, III and V. This widespread arborization may allow these neurons to integrate neural signals destined for, and coming from, the hippocampus. We also discovered that muscarinic cholinergic receptor activation allows principal neurons in layer III of the LEC to generate persistent activity at a fixed frequency following an excitatory stimulus. This activity can be terminated by the application of another excitatory stimulus, allowing the cells to toggle between "On" and "Off" states. Finally, pharmacological and ionic substitution experiments *in-vitro* established that the

"On" and "Off" states of these cells are respectively dependent on $Ca^{2+}$-dependent non-specific channels, and BK-type $Ca^{2+}$-dependent $K^{+}$ channels. These studies expand our understanding of the network and cellular mechanisms by which neurons in the PRC and LEC may contribute to long-term and short term memory.

# Résumé

Le cortex perirhinal (CPR) et le cortex entorhinal latéral (CEL) représentent des composantes essentielles du système mnésique au niveau du lobe temporal médian mais dont l'organisation fonctionnelle et les interconnexions restent relativement peu comprises. Durant cette thèse, de nouvelles approches *in vitro* et *in vivo,* ont été développées dans le but d'explorer l'organisation synaptique, les propriétés intrinsèques et la modulation cholinergique des neurones du CPR et du CEL. En combinant la méthode du potentiel du champ *in vivo* et *in vitro* à l'analyse de densité du courant-source et à l'enregistrement intracellulaire *in vitro*, nous avons démontré l'existence d'une interaction synaptique excitatrice bidirectionnelle entre le CPR et le CEL. De plus, des injections de marqueur ont été couplées à des enregistrements intracellulaires pour déterminer les caractéristiques morphologiques et électrophysiologiques des principaux neurones situés au niveau des couches II et III du CEL. Nos résultats révèlent que les neurones de la couche II du CEL possèdent des propriétés morphologiques et électrophysiologiques beaucoup plus hétérogènes que les neurones de la couche III. Par ailleurs, les neurones principaux de la couche III montrent une importante arborisation des dendrites apicales et basales, qui s'étendent le long des couches I, II, III et V du cortex. Cette vaste arborisation peut permettre à ces neurones d'intégrer les différents signaux neuronaux émanant de et allant à l'hippocampe. Nous avons également découvert que l'activation des récepteurs cholinergiques de type muscariniques permet aux neurones principaux de la couche III du CEL de générer une activité persistante à fréquence fixe à la

suite de l'application d'un stimulus excitateur. Cette activité peut être stoppée par l'application d'un autre stimulus excitateur, ce qui permet aux cellules de basculer entre les états "On" et "Off". Finalement, des expériences de substitution pharmacologique et ionique *in vitro* ont permis d'établir que les états "On" et "Off" de ces neurones sont respectivement dépendant de canaux dépendant du $Ca^{2+}$ non spécifiques et de canaux $K^+$ dépendant du $Ca^{2+}$ de type BK. Ces résultats étendent notre compréhension des réseaux et des mécanismes cellulaires par lesquels les neurones du CPR et du CEL peuvent contribuer à la formation et au contrôle des mémoires à court et à long terme.

# Acknowledgements

First and foremost, I would like to express my special thanks to my parents, who have really devoted spiritually and financially their life to my elder sister (Ladan), me, and my younger brother (Radin). All my achievements in my life belong to my parents, without them I could not reach to the point that I am standing right now.

Next, I wish to thank my initial thesis supervisor the late Dr. Angel Alonso and subsequent supervisors Drs. Charles Bourque and David Ragsdale for all the help and support they have given me throughout my PhD studies at the Montreal Neurological Institute. Specifically, special thanks to Dr. Bourque who stepped in after unexpected death of the late Dr. Alonso without any expectation, and took the responsibility of helping me to bring my research and PhD study to an end. The completion of this thesis would not have been possible without Dr. Bourque's support.

I would also like to thank Drs. Erik Fransen and Michael Hasselmo for all their help and intellectual support after the unexpected death of the later Dr. Alonso. I also want to thank the members of my advisory committee Drs. Pierre Drapeau and Philippe Séguéla for their help and support. In addition, thanks go to those who went through the late Dr. Alonso's laboratory while I was there: Drs. Ruby Klink, Etienne de Villers-Sidani, Antonio Reboreda, Motoharu Yoshida, and Mr. Farhan Khawaja who acted not only as work colleagues but also they are good friends of mine. I would also like to thank Ms. Naomi Takeda and Monique Ledermann for all the administration help they provided.

## Statement of originality and contributions of authors

The experimental results described in this thesis are presented in four studies and correspond to a novel understanding of the cellular and synaptic properties of the perirhinal-lateral entorhinal circuit, the main conduit between the neocortex and the hippocampus. These studies are presented in manuscript format and have been published, submitted or considered to be submitted for peer-reviewed journal articles. In addition, some of the results included here have been presented as posters at the 2003, 2004, 2005 and 2006 Society for Neuroscience Meetings.

The first study, which is presented in chapter two, describes the first strong excitatory mono-synaptic *in-vivo* and *in-vitro* electrophysiological evidence for reciprocal connection between the perirhinal and the entorhinal cortices. I and the late Dr. Alonso developed the new *in-vitro* slice preparation; I performed all the *in-vitro* experimentations, analyzed all the related data, and also helped my co-author, Dr. Etienne de Villers-Sidani, to develop the *in-vivo* preparation and data analysis. The manuscript was written by myself and Dr. Etienne de Villers-Sidani and co-edited by the late Dr. Angel Alonso.

The second study presented in chapter three, provides an original and comprehensive study of the electrophysiological in conjunction with the morphological properties of layers II and III lateral entorhinal principal neurons. I carried out all the experiments and subsequent analysis under the supervision of the late Dr. Angel Alonso. The manuscript was written by myself and co-edited by the late Dr. Angel Alonso.

The third study presented in chapter four deals with characterizing the cholinergic modulation of post-burst activity of layer III lateral entorhinal principal neurons. I performed all the experiments and subsequent data analysis, initially under supervision of the late Dr. Alosno, and after his unexpected death I continued and conduct my research related to that work by myself. The manuscript was written by myself and co-edited by external collaborators Drs. Michael Hasselmo and Erik Fransen.

Finally, the fourth study, presented here in chapter five, describes the potential ionic mechanisms for induction and termination of post-stimulus evoked persistent activity observed in layer III lateral entorhinal principal neurons following the cholinergic activation. I conduct this part of my research under supervision of Dr. Charles Bourque. I performed all the experiments subsequent analysis, and wrote the manuscript, and it was co-edited by Dr. Charles Bourque.

This is a manuscript-based thesis and the results chapters represent either already published or submitted or considered for publication, as follows:

**Chapter two:** Reprinted from Neuroscience, 2004, de Villers-Sidani E, Tahvildari B, Alonso A: "Synaptic Activation Patterns of the Perirhinal-Entorhinal Inter-Connections", 129(1): 255-65, Copyright (2004), with permission from Elsevier science.

**Chapter three:** Reprinted from Journal of Comparative Neurology, 2005, Tahvildari B and Alonso A: "Morphological and Electrophysiological Properties of Lateral Entorhinal Cortex Layers II and III Principal Neurons", 491(2):123-40, Copyright (2005), with permission from Wiley-Liss.

**Chapter four:** Reprinted from Hippocampus, 2007, Tahvildari B, Fransen E, Alonso A and Hasselmo M: "Switching between 'On' and 'Off States of Persistent Activity in Lateral Entorhinal Layer III Neurons", 17(4): 257-63, Copyright (2007), with permission from Wiley-Liss Inc. a subsidiary of John Wiley & Sons, Inc.

**Chapter five:** Considered as a manuscript to be submitted to Journal of Neurophysiology, 2007, Tahvildari B, Alonso A and Bourque CW "Ionic Basis of 'On' and 'Off' Persistent Activity in Layer III Lateral Entorhinal Cortical Principal Neurons".

# Abbreviations

ACh: Acetylcholine

CAN: Calcium-activated non-specific cation current

CSD: Current source density

DAP: Depolarizing after-potential

DMS: Delayed match to sample task

DMNS: delayed non-match to sample task

EC: Entorhinal cortex

EPSP: Excitatory post-synaptic potentials

FFA: Flufenamic acid

fMRI: Functional magnetic resonance imaging

HC: Hippocampus

IBTX: Iberiotoxin

IPSP: Inhibitory post-synaptic potential

LEC: Lateral entorhinal cortex

MTL: Medial temporal lobe

NaPB: Sodium phosphate buffer

NC: Neocortex

PAR: Parahippocampal cortex

POR: Post-rhinal cortex

PP: Plateau potentials

PRC: Perirhinal cortex

TEA : Tetraethyl amonium

# CHAPTER 1: General Introduction

## 1.1 Overview of the thesis

Memory is a physiological capacity of the central nervous system by which perceived information about the environment is encoded, stored, and later retrieved. Based on the time over which stored information persists, memory can be divided into two main forms: short-term memory and long-term memory (Goelet et al., 1986). Short-term memory has a limited storage capacity and lasts for just seconds to minutes. In contrast, long-term memory has an unlimited storage capacity, and lasts as long as the life span of an individual (Rosenzweig et al., 1993; McClelland et al., 1995). It is widely believed that long-term memories are formed by the "consolidation" of short-term memory (Nadel and Moscovitch, 1997). One of the most difficult challenges in neurobiology is to define where and how memory is encoded, consolidated and stored.

Long-term memory is divided into two different types: "declarative memory" which is the memory for facts and events, and "non-declarative" memory which is the memory for skills and habits (Squire and Zola-Morgan, 1988). Neurophysiological, psychological, imaging and lesion studies have indicated that there are different compartments in brain for encoding, consolidating and storing the two different types of long-term memory (reviewed in Mishkin, 1982). While the medial temporal lobe is a crucial compartment for "declarative memory", other brain regions such as the neocortex, striatum,

amygdala and cerebellum are required for "non-declarative" memory (Squire, 1998). Neuroanatomical studies have indicated that the medial temporal lobe comprises several highly interconnected components including the hippocampus, and the adjacent parahippocampal, perirhinal, medial entorhinal and lateral entorhinal cortices. Among these regions, the perirhinal cortex and lateral entorhinal cortex have been identified as key components of the medial temporal lobe memory system (Squire and Zola-Morgan, 1991). Moreover, it is widely believed that formation of new long-term declarative memories is dependent on active bidirectional communication between the neocortex and the medial temporal lobe (Buzsaki, 1996; Suzuki and Eichenbaum, 2000).

In contrast to long-term memory, short-term memory is the ability to retain information for a brief period of time (up to several minutes) following exposure to a sensory stimulus (Fuster, 1997). Neurophysiological studies suggest that neurons in the perirhinal cortex and lateral entorhinal cortex actively encode short-term memories by responding to specific sensory stimuli, and store such memories by generating persistent electrical activity until the sensory information needs to be recalled (Suzuki et al., 1997; Young et al., 1997). Interestingly, human imaging studies have shown that the post-sensory sustained activity of these neurons may also be involved in the subsequent encoding of long-term memory (Schon et al., 2004; Schon et al., 2005).

Neuroanatomical studies have shown that both the perirhinal cortex and the lateral entorhinal cortex are massively innervated by inputs from basal forebrain cholinergic neurons (Alonso and Kohler, 1984). This cholinergic input

appears to play a critical role in memory formation. Indeed, pharmacological blockade of cholinergic receptors appears to reduce the generation of post-sensory sustained activity in medial temporal lobe neurons while impairing memory performance in humans (Schon et al., 2005). Moreover, selective chemical destruction of the basal forebrain cholinergic neurons that innervate the entorhinal cortices has been found to impair short-term memory performance in rats (McGaughy et al., 2005) and monkeys (Turchi et al., 2005).

Although significant advances have been made in our general understanding of how the central nervous system is involved in memory function, much remains to be learned concerning the detailed mechanisms by which neurons in the medial temporal lobe contribute to this process. In particular, the cellular properties and synaptic relationships of neurons within the perirhinal cortex and the lateral entorhinal cortex are poorly understood. In addition, the mechanisms by which cholinergic inputs contribute to genesis of post-sensory persistent electrical activity in these neurons are unknown. The main objectives of my thesis, therefore, were to investigate and determine if perirhinal and lateral entorhinal cortices are synaptically interconnected, and to investigate if cholinergic modulation of these neurons could contribute to the genesis of persistent activity. In the remainder of the introduction, I will review elements of primary literature that have led to the specific hypotheses that are elaborated in section 1.7.

## 1.2 The medial temporal lobe (MTL) and memory

### 1.2.1 A classic case of human amnesia: H.M.

The involvement of the MTL in memory was revealed by systematic analysis by the seminal work of Scoville and Milner, who reported a human case (H.M.) showing a profound impairment in memory following bilateral surgical removal of this part of the brain (Scoville and Milner, 1957). In 1955, H.M. a patient who had been suffering from MTL seizures for almost ten years was referred to Scoville for possible neurosurgical intervention. In an attempt to control H.M.'s epileptic seizures, parts of the MTL including: the hippocampus, part of the amygdala, as well as the entorhinal, perirhinal and portions of the parahippocampal cortices were removed bilaterally. Following recovery from the surgery, H.M.'s seizure activity was significantly reduced. However; he showed a profound impairment in memory function. Specifically, H.M. had lost the ability to retain a sequence of three digit numbers (e.g. 5-8-4), even for a few minutes, in the presence of distractors. In addition to this loss of short-term memory, H.M. also failed to make new long-term memories. For example, he always failed to recognize Milner, even though he met with her on a monthly basis. In contrast to this profound and evident loss of short-term and long-term memory function, H.M.'s ability to perceive objects and to learn new motor tasks remained completely intact (Scoville and Milner, 1957, 2000).

These observations on H.M. provided the first documented evidence indicating that the MTL is involved in short-term memory and in the

consolidation process by which short-term memories are converted to the new long-term ones.

### 1.2.2 Development of animal models of amnesia

Although Milner and Scoville described H.M. in detail in 1957 (Scoville and Milner, 1957), it was only in 1978 that an animal model of amnesia was developed, when Mishkin (1978) showed that experimental ablations of the MTL in monkeys resulted in short- and long-term memory deficits which mimicked those of H.M. (Zola-Morgan and Squire, 1990).

Most studies of short-term memory deficits in lesioned animals have been done using variations of the delayed match to sample (DMS) or delayed non-match to sample (DMNS) tasks (reviewed in Goldman-Rakic, 1995). These memory recognition tasks consist of three phases. In the first phase, a "sample" to be remembered (e.g. of a visual stimulus) is presented. This first phase is then followed by a "delay" period (second phase), during which the animal is expected to remember the sample stimulus. During the third (or "test") phase, sensory stimuli are again presented, and animals are rewarded for responding to either the stimulus that matches the sample (DMS task), or the stimulus that does not match the sample (DMNS task) as evidence of successful short-term memory function (reviewed in Suzuki and Eichenbaum, 2000). Experiments showed that following a bilateral ablation of the MTL, trained monkeys display a significantly diminished ability to recognize the "test" stimulus in a DMS task protocol (Mishkin, 1978).

Experiments on monkeys also demonstrated the involvement of the MTL in long-term memory. For instance, the ability of an animal to learn a new task to be repeated over prolonged intervals requires the capacity to form new long-term memories. Monkeys with ablations of the MTL show severe deficits in the ability to learn new tasks, indicating that such lesions can impair long-term memory (Squire and Zola-Morgan, 1991). However, like humans with similar lesions (e.g. H.M.), MTL-lesioned monkeys show no deficits in perception or in the performance of motor tasks (Zola-Morgan and Squire, 1984, 1985).

### 1.2.3 The rhinal cortex: A key component of the MTL memory system

As explained above, lesion studies indicate that the MTL is involved in short-term and long-term declarative memory. However, the MTL is a complex neural structure and these studies did not reveal if all of the individual components of the MTL are equally important in this process. Further insight into MTL components that appear to be essential for memory has emerged from experiments involving more selective lesions. For example, a selective lesion limited to the hippocampus in a human case (know as R.B.) resulted in an impairment of short-term memory (Zola-Morgan et al., 1986). However, memory deficits in R.B. were significantly (i.e. quantitatively) milder than those observed in H.M. This finding indicated that MTL structures other than the hippocampus are also important for memory function. Circumscribed bilateral lesions of the amygdala alone in monkeys, failed to induce impairments of short-term memory (Mishkin, 1978). Moreover, selective bilateral lesions of the amygdala did not exacerbate the deficits in memory impairment produced by prior hippocampal

lesions (Zola-Morgan et al., 1989a). These observations indicate that amygdala is not required for short-term and long-term declarative memory. In contrast, bilateral lesions of cortical regions lying adjacent to the hippocampus, including the rhinal cortex (entorhinal and perirhinal cortices) and the parahippocampal cortex, caused more severe deficits in short-term memory than hippocampal lesions alone (Murray and Mishkin, 1986; Zola-Morgan et al., 1989b; Suzuki et al., 1993; Zola-Morgan et al., 1993). Additional studies involving even more restricted and selective lesions of these areas revealed further that the rhinal cortex alone represents one of the most important structures of the MTL for memory function in primates. Indeed, ablation of the perirhinal cortex (PRC) and the entorhinal cortex (EC), which together form the rhinal cortex, induced impairments in memory recognition tasks that were almost as severe as those observed following complete bilateral removal of the MTL in monkeys (Meunier et al., 1993; Meunier et al., 1996) or humans (e.g. H.M.). In agreement with this interpretation, bilateral selective ablation of the PRC and EC also caused severe deficits in short-term memory tasks in rodents (Otto and Eichenbaum, 1992; Mumby and Pinel, 1994). These deficits did not occur simply because the animals had forgotten tasks learned prior to the ablation, since post-lesion animals were able to execute the DMNS (or DMS) tasks for brief delays (4 to 8 seconds). Taken together these observations indicate that the rhinal cortex is an important component of the MTL that is required for memory function in mammals.

## 1.3 Neocortical-hippocampal interactions in long-term memory

### 1.3.1 Involvement of the MTL in memory consolidation

Despite severe impairments in short-term memory and the establishment of new long-term memories, H.M. was able to recall most of the memories that concerned his remote past (for example childhood events). However, he was not able to recall those events that had occurred up to 14 months prior to the surgery (Scoville and Milner, 1957; Milner, 1972; Milner et al., 1998). Indeed, H.M. was suffering from *temporally graded retrograde amnesia*, meaning that the degree of impairment increased for the memories of events that were temporally closer to the surgery. Similar temporally graded impairments were also observed in animals following selective ablation of different regions of the MTL (Zola-Morgan and Squire, 1990; Cho et al., 1993; Cho and Kesner, 1996). It was observed in monkeys and rats that MTL lesions provoke ~ eight and four weeks, respectively, of retrograde amnesia (Zola-Morgan and Squire, 1990; Cho et al., 1993). These findings suggested that the MTL is required to recall long-term memories for a finite period of time before an MTL-independent system can support memory storage. Taken together, these data suggest that the storage of the long-term memory for events initially depends on the MTL, but gradually becomes independent of this part of the brain in the process of consolidation. But *where* are long-term memories stored?

### 1.3.2 Long-term memory is stored in the associative neocortex

Penfield first observed that electrical stimulation of temporal lobe result in an imagery recall of events in humans (Penfield and Perot, 1963). Subsequent characterization of lesions induced by trauma or stroke in humans, as well as selective lesions in animals, shed more light on the mechanisms of long-term memory (McClelland et al., 1995). MTL structures are responsible for a gradual process of reorganization and stabilization of neuronal circuit by changing the organization of associational cortical structures (Bontempi et al., 1999; Maviel et al., 2004), and after a sufficient time has passed the MTL is not needed to support the storage of long-term declarative memory (Alvarez et al., 1995). These studies, together, indicate that associative neocortex is the final location where long-term memories are stored.

### 1.3.3 Role of neocortical-hippocampal dialogue in memory formation

Since the hippocampus represents the final target in MTL circuitry (see sections 1.4.1 below), Buzsaki proposed a theoretical model describing how bidirectional interactions between this structure and the neocortex might be important for converting a short-term memory to a long-term memory (Buzsaki, 1989, 1996, 1998). In this process, known as the "two-stage" model of memory, it is hypothesized that environmental information perceived during wakefulness is initially encoded in associative areas of the neocortex. Signals originating from these areas then converge upon the hippocampus where information is thought to be stored by the creation of an "assembly" of neurons whose activities become temporarily synchronized because of an increase in the strength of excitatory

transmission at synapses interconnecting neurons within the assembly (Buzsaki, 1996; Chrobak and Buzsaki, 1998; Hasselmo, 1999). Later, during slow wave sleep, synchronized discharges in the relevant assembly of hippocampal neurons would reactivate the neocortical neurons that had originally encoded specific details of the environmental information (Wilson and McNaughton, 1994; Siapas and Wilson, 1998). It is then proposed that such reactivation leads to long-term synaptic changes in the associative neocortical networks that store memories (Skaggs and McNaughton, 1996; Sutherland and McNaughton, 2000; Pennartz et al., 2002; Sirota et al., 2003; Wiltgen et al., 2004).

Thus, an active communication between the hippocampus (HC) and neocortex (NC) appears to be an essential process for the gradual consolidation and storage of new long-term memories for events. In the following sections, I review anatomical and physiological observations that provide insight into the involvement of various MTL structures in the reciprocal dialogue between the HC and NC.

## 1.4 MTL structures involved in the HC-NC dialogue

Neuroanatomical studies have shown that the HC-NC dialogue is mediated by an extensive cascade of reciprocal connections between principal neurons in the neocortex and in the hippocampus. Indeed, most of these connections are mediated through relay stations incorporated in the cortical tissue surrounding the rhinal fissure [i.e. perirhinal (PRC), parahippocampal (PAR), and entorhinal (EC) cortices] (Burwell, 2000). In rodents and cats, the PAR is termed

postrhinal cortex (POR) because the region is not as developed as an independent gyrus (Burwell and Amaral, 1998b). Therefore, in the text that follows both terms will be used to refer to this area when discussing studies involving primates (i.e. PAR) and non-primates (i.e. POR). Moreover, the PRC, PAR (POR) and EC are subdivided into several different sub-regions based on cytoarchitecture and connectivity (Insausti et al., 1997; Burwell, 2001). Although the details of this categorization lie outside the scope of this thesis, it is important to emphasize that the entorhinal cortex can be divided to two main components: the lateral entorhinal cortex (LEC) and the medial entorhinal cortex (MEC) (Ramón y Cajal, 1901; Blackstad, 1956; Witter et al., 1989; Lopes da Silva et al., 1990). Although some notable species differences exist in the fine details of the NC-HC connectivity, the general organization of this circuitry is highly conserved (reviewed in Suzuki and Eichenbaum, 2000) (figure 1.1). In the sections that follow I review anatomical (section 1.4.1) and electrophysiological (section 1.4.2) data that reveal the functional organization of MTL structures that supports the NC-HC dialogue.

### 1.4.1 Hierarchical organization of NC-HC-NC connections: Anatomical studies

The majority of connections from NC are first relayed to the PRC or the PAR (POR). Most neurons in these areas then project, respectively, to the LEC or MEC, which act as the second relay. Principal EC neurons then send axonal projections to different regions of the hippocampus, where information is processed through unidirectional circuits that terminate in the subiculum. Neurons

in the subiculum then send return projections to the EC, which subsequently connects with the PRC or PAR (POR). Finally, neurons in these areas project to the NC. The NC-HC dialogue is therefore supported via reciprocal projections with two relay stations within the MTL (figure 1.1). We now review the individual components of this circuitry.

### *1.4.1a) NC-PRC and NC-PAR (POR) connections*

Neuroanatomical studies have shown that principal neurons in superficial layers (layers II and III) of primary sensory cortex, as well as in uni- and poly-modal association neocortex, project axons that terminate directly in the superficial layers (layers II and III) of the PRC or PAR (POR) (Suzuki and Amaral, 1994b; Burwell et al., 1995; Burwell and Amaral, 1998a; Burwell, 2000; Lavenex et al., 2002). In all species that have been examined, more than two thirds of the neocortical neurons targeting the MTL terminate primarily in the superficial layers of the PRC or PAR (POR) (Suzuki and Eichenbaum, 2000; Suzuki and Amaral, 2004). Anatomical studies have also revealed that the PRC and PAR (POR) receive different inputs from the NC. For instance, different sensory modalities appear to favor different targets. In rodents, information from the olfactory system mainly innervates the PRC, whereas visual information primarily targets the POR (Burwell and Amaral, 1998a). Additionally, information content within the modalities may also follow different pathways. In primates for example, an NC-PRC conduit conveys mainly visual signals relating to non-spatial information (i.e. the "what" pathway), whereas an NC-PAR conduit carries mainly visual signals relating spatial information (i.e. the "where"

pathway) (Suzuki and Amaral, 2004). Regardless of modality or content these observations indicate that the PRC and PAR (POR) together represent the first order relay for information transfer within the MTL (figure 1.1).

### *1.4.1b) PRC-LEC and PAR (POR)-MEC connections*

Principal neurons within layers II and III of the PRC and PAR (POR) also project axons that form essentially distinct and parallel conduits which terminate in distinct parts of the entorhinal cortex (EC). PRC neurons project mainly to the superficial layers of the lateral entorhinal cortex (LEC), whereas those of the PAR (POR) project mainly to the medial entorhinal cortex (MEC) (Suzuki and Amaral, 1994a; Burwell and Amaral, 1998b; Burwell and Witter, 2002). Thus the LEC and MEC together represent the second order relay for information transfer within the MTL (figure 1.1).

### *1.4.1c) EC-HC connections*

Generally speaking the two parallel pathways originally initiated in the NC are also relayed in a segregated fashion from the EC to the HC (Ruth et al., 1982, 1988; Dolorfo and Amaral, 1998b). Principal neurons in superficial layers of the LEC project mainly to the dorsal part of the HC, whereas those of the MEC project mainly into the ventral part of this structure. These projections are also relayed through separate pathways into different regions of the HC. A major source of inputs is the perforant pathway, which comprises the axons of LEC and MEC layer II principal neurons that terminate in the dentate gyrus and area CA3 (Steward, 1976; Steward and Scoville, 1976). A second source of inputs is the

temporo-amonic pathway, which comprises the axons of LEC, and MEC layer III principal neurons that terminate in area CA1 and the subiculum (Witter et al., 1988; Witter et al., 1989) (figure1.1).

### *1.4.1d) Intra- HC connections*

As mentioned above, information flow through the HC is unidirectional. Although afferents of EC origin can enter HC in different areas, intra-HC connectivity proceeds from the dentate gyrus (DG) to area CA3 to area CA1 to the subiculum, thus forming a trisynaptic unidirectional loop (Suzuki and Eichenbaum, 2000). Functionally, therefore, EC projections contacting the neurons in the DG will initiate a cascade of information transfer that will flow through all components of the HC. In contrast, information reaching area CA1 via the temporo-amonic pathway will only proceed to the subiculum (Lopes da Silva et al., 1990) (figure 1.1).

### *1.4.1e) HC-EC Connections*

Projections from the ventral HC to the MEC and from the dorsal HC to the LEC arise from principal neurons in both the subiculum and area CA1. These return projections terminate exclusively in the deep layers (layers V and VI) of the LEC and MEC (Swanson and Cowan, 1977; Sorensen and Shipley, 1979; Naber et al., 2001; Kloosterman et al., 2003a).

### *1.4.1f) LEC-PRC and MEC-PAR (POR) connections*

Principal neurons in the deep layers (V and VI) of the LEC and MEC project to the PRC and the PAR (POR), respectively (Swanson and Kohler, 1986;

Insausti et al., 1987; Suzuki and Amaral, 1994b; Insausti et al., 1997; Burwell and Amaral, 1998b). In both cases, projections from the EC terminate predominantly in layers I and V of the PRC and PAR (POR). Thus, intra-MTL connections that are initiated in PRC or PAR are reciprocated from the HC back onto their original sites within the PRC and PAR.

#### *1.4.1g) PRC-NC and PAR (POR)-NC connections*

In order to complete NC-HC-NC dialogue, principal neurons in the deep layers of the PRC and PAR (POR) send return projections to sensory and associative parts of the NC that originally targeted the PRC and PAR (POR) (see section 1.4.1a and figure 1.1) (Suzuki and Amaral, 1994b; Burwell and Amaral, 1998a).

### 1.4.2 Hierarchical organization of NC-HC-NC connections: Electrophysiological studies

The neuroanatomical studies cited above indicated how neocortical neurons are connected bidirectionally, and hierarchically, with principal neurons in the HC. It is widely believed that NC-HC-NC connections form the basis of a network that is required for the formation of declarative memories. Although anatomical studies have revealed potential inputs and output structures within these circuits, they have not provided any evidence concerning the specific functional nature of these pathways. Fortunately, extracellular and intracellular electrophysiological investigations have provided important functional data concerning some, but not all, of the NC-HC-NC circuitry. Indeed, although we

know some elements of the circuit related to formation of non-spatial memories (e.g. object recognition; i.e. NC-PRC-LEC-HC circuit), we understand little of the circuitry related to spatial memory (i.e. NC-PAR/POR-MEC-HC circuit) (Suzuki and Eichenbaum, 2000). In the remainder of this section, therefore, I will review the electrophysiological data related to the functional aspects of the NC-PRC-LEC-HC circuit.

#### *1.4.2a) Bi-directional electrophysiological interactions between NC and PRC*

Intracellular recordings along with extracellular field potential recordings, in combination with current source density (CSD) analysis, on *in-vitro* preparations have revealed evidence for functional connectivity between the temporal associational NC and the PRC. In these preparations, stimulation of the NC evoked a monosynaptic excitatory post-synaptic potential (EPSP) associated with a current sink in layers II and III of the PRC (Biella et al., 2001; Martina et al., 2001; Biella et al., 2002). These data have been supported by multi-site extracellular single unit recordings in anaesthetized cats showing that the spontaneous action potential firing in PRC neurons is correlated to that of temporal NC neurons (Pelletier et al., 2004). Less data are available to support the existence of functional connections from the PRC to NC. However, in freely moving rats field EPSPs, and long-term potentiation can be induced in the frontal NC by tetanic electrical stimulation of the PRC. Although this observation suggests that a functional excitatory connection also exists between the PRC and NC, direct evidence that such connections are monosynaptic remain to be

obtained (Ivanco and Racine, 2000). These data suggest that neurons in the PRC reciprocally communicate with those in the NC via excitatory synapses.

### *1.4.2b) Bi-directional electrophysiological interactions between PRC and LEC*

Evidence for bi-directional connectivity between the PRC and the LEC was first provided by extracellular field potential recordings performed in freely moving rats (Ivanco and Racine, 2000). This study showed that field EPSPs can be recorded in the PRC following stimulation of the LEC. Moreover, field EPSPs can also be recorded in the LEC following electrical stimulation of the PRC. Based on latency analysis the authors proposed that the early components of these responses might be due to mono-synaptic connections, but this was not confirmed. Additional evidence for direct projections from the PRC to the LEC was obtained using *in-vitro* guinea pig whole brain preparations (Biella et al., 2002; Biella et al., 2003). In these studies, electrical stimulation of the PRC induced mono-synaptic EPSPs during intracellular recordings from about 40% of principal neurons in layer II of the EC (including both LEC and MEC). These data provided strong evidence for the existence of a direct excitatory pathway from the PRC to the LEC. Surprisingly, current source density analysis of field profiles performed by these authors failed to reveal a clearly demarcated sink in LEC following stimulation of the PRC. The authors speculated that propagation of information from the NC to the LEC might be influenced by the simultaneous activation of the inhibitory pathways to the LEC originating within the PRC. In agreement with this hypothesis, recent axonal labeling studies combined with

immuno-histochemistry in guinea pigs showed that a substantial fraction (~25%) of PRC axons projecting to the LEC express the inhibitory neurotransmitter γ-aminobutyric acid (GABA) (Pinto et al., 2006). Taken together, these data suggest that co-activation of excitatory and inhibitory pathways originating in the PRC might suppress the functional excitation of LEC neurons. If this is the case, then it suggests that the transmission of information along the NC-PRC-LEC-HC pathway might fail at the second relay of this cascade (i.e. PRC-LEC). Indeed, multi-site extracellular single unit recordings in anaesthetized cats have shown that the spontaneous action potential firing in LEC neurons is not correlated to that of PRC neurons (Pelletier et al., 2004). Therefore, the existence of strong excitatory projections from the PRC to the LEC is controversial. This is the first issue that was addressed in my research project (see hypothesis section 1.7).

#### *1.4.2c) Bi-directional electrophysiological interactions between LEC and HC*

An extensive series of electrophysiological experiments combined with pharmacological approaches have provided strong evidence for the existence of direct reciprocal interactions between the LEC and HC. For example, electrical stimulation of layers II and III of the LEC evokes monosynaptic EPSPs in intracellularly recorded neurons of the dentate gyrus (Lomo, 1971a, b), area CA3, and area CA1 (Biscoe and Duchen, 1985; Yeckel and Berger, 1990). These responses are typically associated with clearly demarcated current sinks in the parts of these areas that contain the apical dendrites of resident principal neurons (Charpak et al., 1995; Canning et al., 2000). In terms of reverse projections from

the HC toward the LEC, it has been shown that electrical stimulation of either the subiculum or area CA1, the main outputs of the HC (see section 1.4.1), generates field EPSPs associated with clearly demarcated current sink in the deep layers of the EC (both layers V and VI) (Bartesaghi et al., 1989; Bartesaghi, 1994; Kloosterman et al., 2003b). Moreover, a recent study also showed that short-term and long-term plasticity occurs in the subiculum-LEC circuit (Craig and Commins, 2006). Taken together, these data indicate that neurons in the LEC and HC are connected bi-directionally, and that these connections are made via excitatory synapses.

### 1.4.3 LEC neurons as ultimate relays of non-spatial information to the HC

In the preceding sections, we reviewed evidence indicating that forward projections from associative NC to HC are required for formation of long-term memory, and that information flow in this circuit proceeds through a series of MTL regions. We also saw that the EC represents the final relay station of this cascade, and therefore provides most of the NC information entering the HC. Whereas neurons in the MEC are believed to provide most of the spatial information relayed to the HC, little functional information is available concerning the NC-PAR(POR)-MEC-HC circuit as a whole (section 1.4.2). In contrast, neurons in the LEC are known to receive non-spatial information from well characterized inputs from the NC and PRC. The output neurons of the LEC (i.e. principal neurons in layers II and III), therefore, provide the essential signals that are sent to the HC during the encoding of short–term and long-term memories

related to object recognition. In the next section, we highlight neuro-physiological studies that have provided information concerning how the electrical activity of LEC neurons may participate in this process.

## 1.5 Physiology of the PRC and the LEC neurons related to short-term memory

Studies reviewed in sections 1.2 and 1.3 revealed that the rhinal cortex (i.e. the PRC and EC) is necessary for short-term memory. However, anatomical and lesion studies can not alone provide insights into the mechanisms by which neural activity may allow the brain to perform short-term memory tasks. Indeed, memory function is a dynamic process that can presumably only be studied using real time experimental approaches. Accordingly, the characterization of memory-related electrical activity in different parts of the rhinal cortex have provided the most direct insights into the neural processes that may be associated with the performance of short-term memory (Suzuki and Eichenbaum, 2000).

### 1.5.1 Memory representation in PRC and LEC neurons

As mentioned in section 1.2, the most extensive work on lesion-dependant memory deficits has been performed using variants of the DMS or DMNS tasks (Goldman-Rakic, 1995; Fuster, 1997). In these tasks, animals are trained to indicate whether a test stimulus is recognized as either a match, or a non-match, shortly after the presentation of a sample sensory stimulus (e.g. presentation of an object on a computer video screen). The percentage of correct responses observed following a variety of delay intervals generally declines as a function of

interval length. The percentage of correct responses observed following any particular delay is taken as a measure of memory performance. In order to perform such tasks correctly, animals must first be able to identify the sample stimulus. This process presumably occurs in associative NC areas, where the electrical activity of subsets of neurons encodes the identity of the sample. In order to remember the nature of the sample during a delay interval, information arising from the NC is relayed to the LEC where neural signals somehow allow subsequent recognition of the sample during the test phase. What is the nature of this signal?

Recent, functional magnetic resonance imaging (fMRI) studies in humans have revealed that part of the MTL may be actively involved in the encoding of sensory stimuli (Stern et al., 1996). More importantly, fMRI analysis during the performance of DMS tasks has revealed that this area shows sustained activation (oxygen consumption) during the delay phase of the protocol (Stern et al., 2001). This observation suggests that neurons in this area may fire in a sustained manner during the delay phase, and in this way participate in the maintenance of a short-term memory. Indeed, *in-vivo* single unit recordings in rats (Young et al., 1997) and monkeys (Suzuki et al., 1997) have revealed that some PRC and LEC neurons generate a persistent increase in electrical activity during the delay phase of short-term memory tasks. In rats, performing an odor-guided DNMS task featuring a 500 ms sample period and delay intervals lasting either 3 or 30s, many PRC and LEC neurons show an excitatory response during the "sample" period. Specificity for particular stimuli was shown further by the fact that different neurons could

consistently respond to some, but not all, odorants. Moreover, a substantial proportion of cells showed odor selective persistent activity through out the memory delay period (Young et al., 1997). Similarly, a proportion of PRC (Miller et al., 1996) and LEC neurons (Suzuki et al., 1997) recorded in monkeys performing a DMS task (500 ms sample, 1000 ms delay) displayed stimulus-selective changes in activity during sample presentation. Moreover, many of these neurons also exhibited a persistent increase in electrical activity during the delay interval.

Although these data suggest that PRC and LEC neurons may store short-term memory for identified samples by generating a maintained increase in activity during a delay interval, additional studies indicate that this task is best performed by LEC neurons. Indeed, Miller and colleagues (Miller et al., 1996) showed that stimuli other than the "sample" can interfere with the ability of PRC neurons to maintain persistent firing prior to the presentation of a matching (i.e. test) stimulus, whereas LEC neurons are not subject to such interference (Suzuki et al., 1997). Taken together, these observations suggest that short-term memory may be accomplished specifically as a result of post-stimulus (i.e. post-sampling) persistent firing in LEC neurons. Indeed, post-excitation persistent firing displayed by these neurons is now commonly recognized as a putative mnemonic signal (Goldman-Rakic, 1995).

### 1.5.2 Acetylcholine and short-term memory in the rhinal cortex

It is well known that perception (e.g. object recognition), and therefore short-term memory tasks, can only be performed during the awake state.

Accordingly, it is presumed that the genesis of memory related neuronal activity is state-dependent and might therefore be conditionally regulated by neurotransmitters involved in the control of arousal (McCormick et al., 1993). Interestingly, acetylcholine (ACh) is well-known for its involvement in the sleep-wake cycle and for promoting wakefulness in particular (Hasselmo and Bower, 1993; Hasselmo, 1999). Indeed, ACh produced and released by basal forebrain neurons contributes to various physiological processes including learning, attention, and arousal states in different animal species (Celesia and Jasper, 1966; Krnjevic, 1993; Hasselmo, 1999; Himmelheber et al., 2000).

Evidence indicating that ACh contributes to the performance of short-term memory tasks was first obtained in studies showing that memory function in monkeys is enhanced or impaired by systemic administration of cholinergic agonists or antagonists, respectively (Aigner and Mishkin, 1986; Aigner et al., 1991). Evidence that the rhinal cortex is a critical site for the cholinergic modulation of memory performance was provided by the observation that there is an increase in extracellular ACh concentration in the PRC (Tang and Aigner, 1996), and that memory task performance is impaired following micro-infusion of an ACh antagonist into this area (Tang et al., 1997). Moreover, selective deafferentation of the basal forebrain cholinergic input to the rhinal cortex of monkeys (including PRC and EC) also impaired short-term memory function (Turchi et al., 2005). Similarly, ACh-dependent memory function has also been demonstrated by systemic pharmacological studies in rats (Warburton et al., 2003; Abe et al., 2004). Moreover, in agreement with the monkey studies cited above,

selective deafferentation of cholinergic inputs to the EC of rats induced substantial short-term memory deficits (McGaughy et al., 2005).

Taken together, these observations suggest that neurons in the rhinal cortex, and EC neurons in particular (section 1.5.1), contribute to the performance of short-term memory tasks by generating persistent and sustained activity during the delay period, and that this process is somehow modulated by ACh. Interestingly, it has been observed that systemic administration of scopolamine, a blocker of muscarinic cholinergic receptors, inhibits the persistent activation of the MTL observed by fMRI during the delay period of a DMS task in humans (Schon et al., 2005). It is therefore tempting to speculate that ACh somehow promotes the ability of EC neurons to generate a post-stimulus persistent increase in electrical activity. Important information concerning the basis for such an effect has been derived from intracellular recordings obtained in *in-vitro* slices of rat MEC.

## 1.6 Role of intrinsic cellular properties in the control of LEC neurons

So far, our review of the neurophysiology of the MTL memory circuit, and of LEC neurons in particular, has emphasized data obtained during imaging, anatomical, and extracellular recording studies in intact animals. Although the information provided by these experiments has helped define the neural circuitry involved in memory formation, and the changes in electrical activity that are associated in this process, the basic mechanisms underlying these changes in electrical activity have not been defined. The existence of well-defined

connections in the NC-HC-NC loop implies that network synaptic interactions participate in memory processing. However, an increasing body of evidence indicates that the intrinsic properties of the neurons in this loop may also play a crucial role in the function of the MTL memory circuit.

### 1.6.1 Role of intrinsic cellular properties in the genesis of delay-firing

As mentioned above, many LEC neurons show a persistent increase in firing rate during the delay-period of DMS tasks that is hypothesized to play an important role in short-term memory. A similar type of response has also been observed in neurons of the prefrontal cortex, where it was proposed to result from synaptic reverberation in reciprocal connections between these cells and thalamic neurons (Wang, 2001). It is therefore possible that reciprocal excitatory connections with local neurons, or via the feed-forward LEC-HC-LEC excitatory network (figure1.1), might underlie or contribute to the genesis of delay-firing in these neurons. However, it is also possible that the intrinsic cellular properties of the neurons may also participate in the genesis of such activity (Marder et al., 1996). As mentioned in section 1.5.1, many LEC neurons that show delay-firing during a DMS task are first excited upon presentation of the sample stimulus, and a variety of cortical neurons have been shown to display self-sustained after-discharges following a brief excitatory stimulus (e.g. Major and Tank, 2004). Interestingly, previous studies have shown that principal neurons in the MEC can generate after-discharges following bursts of action potentials in presence of the cholinergic agonists (Klink and Alonso, 1997c). Moreover, such responses are mediated by the intrinsic properties of these cells, and are preserved in the

absence of synaptic transmission (Egorov et al., 2002; Magistretti et al., 2004). Studies in MEC neurons (Egorov et al., 2002; Shalinsky et al., 2002), and other types of neurons (e.g. Fraser and MacVicar, 1996; Haj-Dahmane and Andrade, 1997), have shown that self-sustained after-discharges can be mediated via the activation of calcium activated non-selective cationic (CAN) channels. Indeed, the activation of such channels in response to calcium influx during a brief train of action potentials causes an inward membrane current that depolarizes the neuron and thus promotes continued spiking activity. Whether principal neurons in the LEC display CAN currents or self-sustained after-discharges in the absence or presence of cholinergic agonist is unknown, and determining if such is the case represents a primary objective of this thesis (see section 1.7).

### 1.6.2 Basic morphology and electrophysiological properties of LEC neurons

In addition to the potential role of after-discharge mechanisms in delay-firing, a number of other important intrinsic features could play significant roles in the physiology of the LEC neurons. For example, although the major inputs from this area to the HC are known to arise from principal neurons located in layers II and III (section 1.4.1c), up to three distinct morphological sub-types of neurons projecting to the HC are present in layer II (Schwartz and Coleman, 1981). However, it is not know if the basic electrophysiological characteristics of the different principal neurons in the superficial layers of the LEC are similar or heterogeneous. A major objective of this study, therefore, will be to examine the

characteristics of morphologically defined subtypes of neurons in layers II and III of the rat LEC (see section 1.7).

## 1.7 Objectives of this study

As reviewed in sections 1.2.3 and 1.4.1, the PRC and LEC hold a critical position within the MTL memory system. Specifically, these structures serve as conduit for the bidirectional transfer of non-spatial information between the NC and HC. Moreover, the functional contribution of electrical activity in the PRC-LEC circuit is known to require cholinergic modulation. To increase our understanding of how the PRC and LEC participate in memory function, it is crucial: (i) to increase our understanding of the functional interaction between these two structures, (ii) to investigate the properties of the distinct subtypes of principal neurons in the superficial layers of the LEC and, (iii) to examine how cholinergic modulation can regulate the firing patterns of LEC neurons. Therefore the experiments presented in this thesis will address the following:

- Investigate PRC-LEC connectivity, using novel *in-vivo* and *in-vitro* approaches (Chapter 2)
- Investigate the basic electrophysiological properties of morphologically defined neurons in layers II and III of the LEC (Chapter 3)
- Determine if muscarinic receptor activation can cause the emergence of post depolarization delay-firing in layer III LEC principal neurons (Chapter 4)
- Characterize intrinsic ionic mechanism(s) that may play a role in the genesis of after-discharges in principal neurons in layer III of the LEC (Chapter 5)

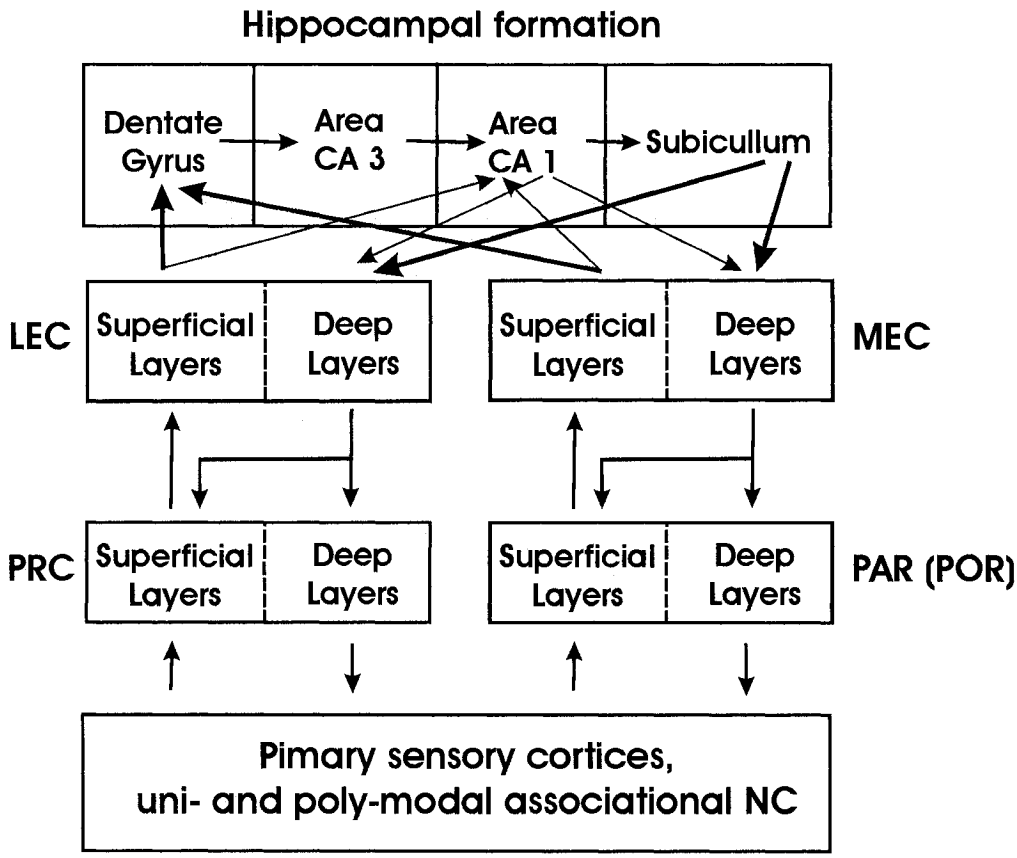


**Figure 1.1.**

**Schematic diagram of bi-directional connections between the neocortex and the hippocampus.** See text for detail explanation (section 1.4.1).

# CHAPTER 2: Synaptic Activation Patterns of the Perirhinal-Entorhinal Inter-Connections

## 2.1 Preface

As explained in sections 1.2 and 1.3, accurate operation of the MTL memory circuit requires a bidirectional transfer of information between the HC and the NC. In this respect, neuroanatomical studies have provided evidence that non-spatial information is specifically relayed through the PRC and the LEC. However, as explained in section 1.4.2b, the existence of functional excitatory connections between these structures has been a matter of controversy. In this study, therefore, we performed an extensive analysis of these circuits using intracellular recording and extracellular field potential recordings in combination with current source density analysis in novel *in-vivo* and *in-vitro* approaches.

## 2.2 Abstract

Ample neuropsychological evidence supports the role of rhinal cortices in memory. The perirhinal cortex (PRC) represents one of the main conduits for the bi-directional flow of information between the entorhinal–hippocampal network and the cortical mantle, a process essential in memory formation. However, despite anatomical evidence for a robust reciprocal connectivity between the PRC and entorhinal cortex (EC), neurophysiological understanding of this circuitry is lacking. We now present the results of a series of electrophysiological

experiments in rats that demonstrate robust synaptic activation patterns of the perirhinal–entorhinal inter-connections. First, using silicon multi-electrode arrays placed under visual guidance *in-vivo* we performed current source density (CSD) analysis of lateral EC (LEC) responses to PRC stimulation, which demonstrated a current sink in layers II–III of the LEC with a latency consistent with monosynaptic activation. To further substantiate and extend this conclusion, we developed a PRC-LEC slice preparation where CSD analysis also revealed a current sink in superficial LEC layers in response to PRC stimulation. Importantly, intracellular recording of superficial LEC layer neurons confirmed that they receive a major monosynaptic excitatory input from the PRC. Finally, CSD analysis of the LEC to PRC projection *in-vivo* also allowed us to document robust feedback synaptic activation of PRC neurons to deep LEC layer activation. We conclude that a clear bidirectional pattern of synaptic interactions exists between the PRC and LEC that would support a dynamic flow of information subserving memory function in the temporal lobe.

## 2.3 Introduction

During the past two decades, an increasing amount of attention has been drawn to the contribution of the rhinal cortices in memory function. Studies in primates and rodents indicate that lesions in selective parts of the rhinal cortices can produce distinct memory deficits to those resulting from hippocampal lesions thus suggesting a differential role for the hippocampus and adjacent parahippocampal areas in memory (Zola-Morgan et al., 1989b; Zola-Morgan et

al., 1993; Mumby and Pinel, 1994; Wiig and Bilkey, 1995; Nemanic et al., 2004). The function of the rhinal cortices in memory is nevertheless dependent on a convergent cascade of cortico-cortical projections and a reciprocal feedback that presumably allows long-term memories to be stored in as yet undisclosed distributed manner throughout the cortical mantle.

Since pioneering work of Van Hoesen and Pandya in the 1970s (Van Hoesen and Pandya, 1975a; Van Hoesen et al., 1975; Van Hoesen and Pandya, 1975b) a plethora of anatomical studies detailed the series of steps by which sensory information reaches the parahippocampal region (Burwell and Witter, 2002). Anatomically, it has been established that within the parahippocampal region, there is a hierarchical organization with the PRC providing a profuse input to the LEC and the post-rhinal cortex (POR) to the medial EC (MEC) (Van Essen et al., 1992; Suzuki, 1996; Burwell and Amaral, 1998b; Lavenex and Amaral, 2000). In turn, the superficial layers of the EC project to all subfields of the hippocampal formation, which feeds back in a topographically organized manner, primarily to the deep layers of the EC (Naber et al., 2001). Then, the EC can distribute information back to the cortical mantle in a step sequence through the PRC and POR (Swanson and Kohler, 1986; Witter and Groenewegen, 1986; Suzuki and Amaral, 1994a; Burwell and Amaral, 1998b).

The physiological importance of the neocortical-hippocampal-neocortical circuitry has been very well established by a vast number of neuropsychological, lesioning and imaging investigations (Scoville and Milner, 1957; Mishkin, 1982; Squire, 1998), and the electrophysiology of the entorhinal-hippocampal

interactions has been extensively characterized as well (Deadwyler et al., 1975; Charpak et al., 1995; Chrobak and Buzsaki, 1996; Kloosterman et al., 2003b). However, a different issue has been the interconnectivity between the parahippocampal areas. In fact, recent investigations have questioned the efficacy of the perirhinal to entorhinal pathway to transmit sensory information with fidelity and suggested that there is a lack of correspondence between the anatomical data and the physiology of the perirhinal to entorhinal pathway (Pelletier et al., 2004). In the *in-vitro* guinea-pig whole brain no local field potential responses could be evoked in the EC after PRC stimulation and intracellular recordings found only late polysynaptic responses in EC neurons after PRC stimulation (Biella et al., 2002; Biella et al., 2003). This is somewhat surprising since the PRC to EC projection is one of the main paths into the hippocampal system (Burwell et al., 1995; Burwell and Amaral, 1998a, b; Witter et al., 2000) and one would expect information to flow with relative ease in this system in order to actively participate in generating and maintaining sensory representations (O'Keefe and Nadel, 1978; Eichenbaum, 2000; Naya et al., 2001). It has, however, been shown that amygdala input promotes the spread of excitatory neural activity from the PRC to the EC (Kajiwara et al., 2003).

Determining whether PRC activation leads to a well-defined pattern of synaptic activation in the EC, and vice versa, is thus of fundamental importance for understanding the synaptic and cellular mechanisms that contribute to memory function of the temporal lobe. For this reason, we decided to re-visit the issue of the PRC–EC connections in the rat by performing laminar profiles of field

potential recordings *in-vivo* under visual guidance, as well as field profiles and intracellular recordings *in-vitro* in a slice preparation that was developed in order to preserve the PRC–EC connectivity.

## 2.4 Materials and methods

All experimental protocols were approved by the McGill University Animal Care Committee and were in compliance with the guidelines of the Canadian Council on Animal Care. All efforts were made to minimize the number of animals used and their suffering.

### 2.4.1 Surgical approach for *in-vivo* recordings

Our recordings were obtained from 14 Long-Evans male rats (125–150 g; Charles River of Canada) using the following method. Under urethane anesthesia (1.5 g/kg, i.p.), the animals were placed in a stereotaxic instrument, the skull was exposed and two screws were cemented to it. These screws were then fastened to a vertically placed custom-made holding bar attached to a manipulator in the stereotaxic. This allowed removal of the ear bars and tilting of the head to gain a lateral access to the brain. The skull and soft tissues overlying the brain area of interest was then exposed and removed surgically (figure 2.1). Placement of the stimulating and recording electrodes was done under direct visualization of the rhinal sulcus and by using micromanipulators. Typically, the trephine window obtained for recordings and stimulation spanned from 3.5-4.8 mm posterior to bregma. For the experiments where field potentials were recorded in the LEC

after PRC stimulation, the stimulating and recording electrodes were placed 4.1 mm and 4.2-4.6 mm posterior to bregma, respectively. Dorso-ventrally, the stimulating and recording electrodes were located 0.5 mm dorsal and 1 mm ventral to the rhinal fissure, respectively. When the reverse pathway was tested (stimulation in the LEC and recording in the PRC), the position of the recording and stimulating electrodes was inverted. Recordings in the LEC posterior to 4.8 mm from bregma could not be obtained because of the surgical technical difficulties. The temperature of the animal was continuously monitored with a rectal probe and maintained at 37 °C using a heating blanket.

### 2.4.2 Slice preparation

Brain slices were obtained from Long-Evan Hooded rats (150–250 g) following standard procedures (Hamam et al., 2000). In brief, under halothane anesthesia the animals were quickly decapitated, and brain was rapidly removed from the cranium and placed in an ice-cold (4 °C) Ringer solution containing (in mM): 124 NaCl, 3 KCl, 1.6 $CaCl_2$,1.8 $MgSO_4$,26 $NaHCO_3$,1.25 $NaH_2PO_4$ and 10 glucose (pH maintained at 7.4 by saturation with 95% $O_2$/5% $CO_2$). Then, a block of tissue containing the parahippocampal region was dissected out by removing the rostral half of the brain with a dorso-ventral cut at a 20° angle with respect to the coronal plane in the anterior–posterior direction (figure 2.4 A, B). Slices (400 μm thick) that maintained the cytoarchitectonic integrity of the PRC and LEC, and the connectivity between both structures as described by others (Burwell and Amaral, 1998a; Burwell, 2001; Burwell and Witter, 2002), were then obtained with the help of a vibratome (Pelco 101, Redding, CA, USA) and

by sectioning parallel to the frontal face of the block. These PRC-LEC slices that corresponded to stereotaxic coordinates of approximately 4.8 mm to 6 mm posterior to bregma were transferred to an interface holding chamber where they were maintained at room temperature for at least 1 h prior to recording. Then individual slices were transferred one by one to the interface recording chamber (Fine Science Tools, North Vancouver, BC, Canada), and perfused with Ringer solution for recording at 34 °C±1 °C.

### 2.4.3 Electrophysiological recording

*In-vivo*. Electrical stimuli were applied using a concentric bipolar electrode (Frederick Haer Co., Bowdoinham, ME, USA) positioned at a depth of 200 μm in the PRC or 800 μm in the LEC. The stimuli applied had an intensity ranging from 200 to 600 μA, a duration of 100 μs and were delivered at 3-10 s intervals. Laminar depth field profiles used for CSD analysis were recorded using silicon probes bearing 16 recording sites (1–2 MΩ) spaced by 100 μm. The silicon probes were kindly provided by the Center of Neural Communication and Technology (University of Michigan, Ann Arbor, MI, USA). Field signals were amplified and recorded using a Cheetah32 acquisition system (Neuralynx, Tucson, AZ, USA) and digitized on a PC computer for off-line analysis. The signals were acquired at a sampling frequency of 2.5 kHz and filtered between 0.1 Hz and 1 kHz. At the end of the recording session, a current of 500 μA for 250 ms was passed through one of the silicon probe active sites and the stimulating electrode for posterior histological electrode placement verification. After sacrificing the animal with an overdose of anesthetic, the brain was quickly

removed and fixed in 4% paraformaldehyde in 0.1 M sodium phosphate buffer (PBS; pH 7.5).

*In-vitro*. Recording electrodes were pulled from borosilicate glass capillaries (World Precision Instruments Inc., Sarasota, FL, USA) on a P87 Sutter Instruments puller (Novato, CA, USA). Extracellular field electrodes were filled with Ringer's solution (tip resistance 3–7 MΩ), and intracellular electrodes were filled with 1.5 M potassium acetate and 2% biocytin (tip resistance of 90–120 MΩ). Signals were recorded with an Axoclamp 2A amplifier (Axon Instruments, Union City, CA, USA), viewed on-line with an oscilloscope, digitized (Digidata 1320; Axon Instruments) and acquired with Axoscope in a computer for later analysis. Field signals were preconditioned with a CyberAmp amplifier (Axon Instruments) to a final gain of 1000 and bandpass filtered at 0.1 Hz-1.0 kHz. Intracellular current-clamp recordings were obtained from neurons in layers II and III of the LEC and PRC. During the experiments, the cortical layers were readily identified with the help of a dissecting microscope (World Precision Instruments Inc., Sarasota, FL, USA) and transillumination. Once the neurons were electrophysiologically characterized they were injected with biocytin by applying negative current pulses of 0.3 nA and 0.3 s (50% duty cycle) for at least 5 min. At the end of the recording session the electrodes was pulled out from the cell and the slice was kept for another 15-20 min in the recording chamber before being fixed with 4% paraformaldehyde in 0.1 M PBS for at least 48 h at 4 °C.

In the slice, field potential profiles were constructed by moving one electrode orthogonally to the lamination of LEC at 50 μm steps from layer I to the

angular bundle. A bipolar stimulating electrode was positioned on the superficial layers of the PRC in order to activate orthodromically the LEC. The PRC was stimulated at low frequency (0.1 Hz, 100 μs duration) at 100–500 μA. Six sweeps taken at each recording site were averaged.

### 2.4.4 Field data analysis

Data were analyzed with Matlab (Mathworks, Natick, MA, USA) and graphs were made with IGOR Pro (Wavemetrics, Lake Oswego, OR, USA). The stimulation artifacts were subtracted from the traces using matching exponential functions. Current source density (CSD) analysis is the second derivative of the field potential with respect to position and it can be calculated using the following equation (Freeman and Nicholson, 1975):

$$CSD(h,t) = \frac{\sigma_h(\Phi(h-n\Delta h,t) - 2\Phi(h,t) + \Phi(h+n\Delta h,t))}{(n\Delta h)^2}$$

CSD($h,t$) is the CSD at a fixed time $t$ and depth $h$, $\Phi(h,t)$ is the average field potential at time $t$ and depth $h$. For this study, $\Delta_h$ was 100 μm and 50 μm in the *in-vivo* and *in-vitro* studies, respectively. The parameter $n$ defines the amount of spatial smoothing. N=2 was used here. Since $\sigma_h$ (tissue conductivity) was not measured, the CSD value is presented in arbitrary units.

### 2.4.5 Histology

In *in-vivo* studies 50 μm thick coronal sections through the recording region were cut with a vibrotome and stained with Cresyl Violet (figure 2.1 B–E). In *in-vitro* studies histochemical processing and biocytin revealing were

performed as previously described (Hamam et al., 2000). Three dimensional reconstructions of the biocytin injected cells in the PRC were made with the neurolucida system (MicroBrightField Inc., Colchester, VT, USA).

## 2.5 Results

### 2.5.1 PRC to LEC projection *in-vivo*

In order to test whether activation of the PRC elicits a well-defined pattern of synaptic activation in the LEC, we first examined in 10 animals the laminar distribution of field potential responses in the LEC following PRC stimulation. To facilitate the proper placement of electrodes in the target areas, and to enable the conduction of laminar profiles with a normal orientation to the cortical layers, a visual approach was developed (figure 2.1A). Making use of this approach, the stimulating electrode was always placed in the PRC at a location approximately 4.1 mm posterior to bregma and at a depth of 200–300 μm (figure 2.2A). This allowed activation of the PRC superficial cell layers which are known to be the main origin of projections to the LEC (Burwell and Amaral, 1998b; Burwell, 2000). In each animal, from one and up to five field potential profiles were conducted at five different LEC entry points located 100 μm apart, 500–1000 μm ventral to the rhinal sulcus and oriented in parallel to the sulcus. The most rostral entry point was always aimed at approximately 4.2 mm posterior to bregma. In all laminar profiles conducted we noted that PRC stimulation led to an apparent field potential negativity at a depth of 200–500 μm (corresponding to layers II–III) and a positivity at deeper locations (see below). CSD analysis (figure 2.2B)

demonstrated that the superficial field negativity corresponded to a current sink centered over layers II–III. At deeper levels, we consistently observed a current source that spread from the deepest aspect of layer III down to middle layer V–VI and a more modest current sink over the deepest section of layers V–VI. At the most rostral entry point (approximately 4.2 mm posterior to bregma) the latency at the peak of the layer II–III field negativity (and current sink) was 6.4±0.4 ms (mean ± S.D.; n=9) for stimulus intensities of 250 μA. The latency decreased to 4.8±0.8 ms (n=3) for a stimulus intensity of 500 μA. Interestingly, at the higher stimulus intensities (400–500 μA), a late current sink consistently emerged toward the superficial aspect of LEC layer V with a latency of 14.6±2.8 ms (n=3; figure 2.3B). As expected, the latency of the field responses at a particular recording depth also increased with the distance from the stimulating electrode increased (figure 2.2A). At approximately 4.6 mm posterior to bregma the latency of the layer II–III field negativity was 12±1.4 ms (n=3).

### 2.5.2 PRC to LEC projection *in-vitro*

The well-defined current sink that we observed over the superficial LEC layers at a latency of approximately 5ms is consistent with a monosynaptic activation of LEC superficial cell layer neurons by afferent PRC fibers. From the published anatomical descriptions of PRC to LEC projections (Burwell and Amaral, 1998b; Burwell, 2001), and the above-described electrophysiological findings, we reasoned that it should be possible to develop a slice preparation that contained the essential components of the projection which would therefore allow us to confirm through combined field profile analysis and intracellular recording

the excitatory nature of the synaptic input to the superficial LEC neurons. The approach used to develop such PRC-EC slice preparation is described in detail in the materials and methods and illustrated in figure 2.4A and B. In order to test the validity of the preparation we first attempted to confirm the preservation of the axons of PRC layer II–III neurons within the plane of the slice. For this purpose we recorded intracellularly and labeled with biocytin eight neurons from layers II–III of the PRC and found that, as in the case illustrated in figure 2.4C-E, in 50% of the cases the main axon gave off collaterals that could be followed up to and branched within the superficial cell layers of the LEC. Next, and in a parallel analysis to the *in-vivo* work described above, we proceeded to examine in the PRC-EC slice the laminar distribution of field potential responses in the LEC following stimulation of superficial PRC layers. As illustrated in figure 2.5A, in all cases tested (n=6) we noted that PRC stimulation led to a field potential negativity centered in layer III of the LEC at a latency of 6.2±0.6 ms (range 5.2-6.9 ms). CSD analysis (figure 2.5A) demonstrated that this negativity was correlated to a robust current sink centered over layers III-II with associated current sources at more superficial (layers II-I) and deeper levels (deep layer III). The elicitation *in-vitro* of a robust current sink on the superficial LEC layers by PRC stimulation (figure 2.5) is consistent with the *in-vivo* observations described above (figures 2.2 and 2.3), and point to prominent excitation of superficial LEC neurons by PRC terminals.

In order to confirm the monosynaptic excitation of superficial LEC neurons following PRC activation, we performed intracellular recordings of LEC

layer II-III neurons and analyzed their synaptic responses to PRC stimulation. All neurons examined were intracellularly labeled with biocytin which allowed their exact cell layer localization as well as analysis of their somato-dendritic and local axonal structure. As in the case illustrated in figure 2.5, all neurons tested in layer III (n=14) were pyramidal cells and invariably responded to PRC stimulation with an excitatory post-synaptic potential (EPSP) at a latency at onset of 3.2±0.2 ms (range 2.9–3.6 ms). The amplitude of the EPSP increased with stimulus intensity but its latency remained constant (figure 2.5B). Significantly, we did not observe in layer III cells any evidence of an inhibitory component in the synaptic response to PRC stimulation. With respect to the layer II neurons (n=16) they were multipolar and, similarly to the layer III pyramidal cells, all responded to PRC stimulation with an early EPSPs (latency at onset: 3.5±0.7 ms; range 2.8 ms-4.6 ms). However, as in the case illustrated in figure 2.5E, in some LEC layer II neurons (n=5; 30%) the EPSP was cut short by an inhibitory post-synaptic potential (IPSP; i.e. the cells responded with an EPSP–IPSP sequence) that displayed an early component which reversed at rather depolarized levels and a late slower component which did not reverse with hyperpolarizations down to −80 mV.

### 2.5.3 LEC to PRC projection *in-vivo*

Anatomical data demonstrate the presence of a feedback projection from the deep layers of the LEC to the PRC (Deacon et al., 1983; Kohler, 1988; Burwell and Amaral, 1998b). In order to determine whether the LEC to PRC projection gives rise to a well-organized pattern of synaptic activation, we

undertook four experiments where we examined the laminar field potential profile responses in the PRC after stimulation of the deep layers of the LEC (800 μm, layer V). As in the experiment illustrated in figure 2.6, in all cases, stimulation of the deep LEC layers elicited a CSD pattern at short latency consisting of a deep and a superficial current sink centered over layers V and I–II, respectively, which were accompanied in time by a current source that spread over layer III. The latency at the peak of the deep and superficial sinks were 10±1.1 ms and 7.0±0.8 ms (n=6), respectively. Occasionally (n=2), a weak polysynaptic response (sink) could be seen with a latency of approximately 19ms in layer II, as seen in figure 2.6. In essence, the pattern of synaptic activation in the PRC following LEC stimulation appears like a mirror image of that observed in the LEC following PRC stimulation. The deep and superficial current sinks elicited in the PRC following LEC stimulation coincide with the main terminal fields of the LEC to PRC projection (Burwell and Amaral, 1998b) and are thus likely to be active sinks representing synaptic excitation of PRC deep and superficial layer neurons in response to LEC activation.

## 2.6 Discussion

A large amount of anatomical literature has shown a massive bi-directional connectivity between the neocortex and the parahippocampal region which for the most part appears organized as a hierarchical system (Rosene and Van Hoesen, 1977; Burwell and Amaral, 1998a; Lavenex and Amaral, 2000). Key in this system is the connectivity between the PRC and the EC and, again, anatomical studies have shown a robust afferent system to the LEC from the PRC

(Burwell and Amaral, 1998b). The EC plays a very important role in memory function in conjunction with but also independently from the hippocampus (Zola-Morgan et al., 1989b; Zola-Morgan et al., 1993; Leonard et al., 1995). One would expect that information must be able to flow with relatively ease in and out of this system to facilitate the neocortical-hippocampal-neocortical dialogue (Buzsaki, 1996). Indeed, neurophysiological investigations in primates have shown clear functional interactions in the activity of EC/hippocampal and neocortical neurons (Higuchi and Miyashita, 1996; Siapas and Wilson, 1998; Sirota et al., 2003), and human brain imaging studies support the co-activation of hippocampal and neocortical areas (Gottfried et al., 2004). In the rat, stimulation of primary sensory areas has also been shown to elicit unit responses in the PRC (Naber et al., 2000). However, there is considerable controversy on the issue and recent electrophysiological investigations by Biella et al. (2002, 2003) in the *in-vitro* guinea-pig brain reported no local field potential responses in the LEC following activation of either area 36 or 35 of the PRC and an apparent lack of mono-synaptic excitation. This is surprising in view of our data and may be related to species differences, or the use of the whole brain preparation. Similar conclusions were also reached by Kajiwara et al. (2003), who explored the spread of PRC activation into the LEC in rat brain slices with the use of the voltage-sensitive dye RH-795. In this case, however, the authors stimulated distally in the PRC while in our slice work we stimulated at more proximal locations to the LEC (at the transition between area 35 and 36). Slight differences in the angle of slice sectioning and/or the use of voltage-sensitive dyes could also explain the

differences between studies. The work by Kajiwara et al. (2003) shows nicely, however, that the amygdala can deeply influence the transfer of information between the PRC and EC. Nevertheless, our combined CSD analysis *in-vivo* and *in-vitro* in combination with intracellular recordings *in-vitro* clearly demonstrate, however, that activation of the PRC can also efficiently and monosynaptically excite the target neuronal populations in the EC. Similarly, our CSD analysis *in-vivo* also indicates that the EC can efficiently excite the target neuronal populations in the PRC as previously predicted by the anatomical data (Burwell and Amaral, 1998b) and in agreement with other electrophysiological studies in slices (Ziakopoulos et al., 1999). There is, therefore, a well-organized pattern of synaptic activation in the LEC following discharge of the PRC and, in turn, there is also a well-organized pattern of synaptic activation in the PRC following discharge of the LEC.

As indicated, the apparent lack of efficient communication between PRC and EC reported in the above mentioned studies may reflect species differences, differences in connectivity among different subdivisions of the PRC, or decreased excitability because of the experimental approaches utilized. In a recent study in the cat, Pelletier et al. (2004) have also concluded that there is a low probability of transmission of neocortical and entorhinal impulses through the PRC. In this study, the PRC-LEC interconnectivity was examined indirectly by recording in the PRC and LEC after temporal cortex stimulation and recording in the PRC and LEC after ventro-LEC stimulation. Unfortunately, these authors did not directly address the issue of the PRC to EC pathway and did not examine the laminar

distribution of evoked field potential responses in the PRC and EC following neocortical stimulation.

The laminar field profiles that we obtained *in-vivo* in the LEC after PRC stimulation showed consistently negative potentials in layers II and III and field positivity at deeper locations. CSD analysis of these field profiles translate in the presence of a current sink in the superficial layers with an apparently corresponding source at deeper levels. The latency of the response in the LEC after PRC stimulation increased with distance from the stimulating electrode but remained in a range consistent with a monosynaptic response. Our CSD findings *in-vivo* are perfectly consistent with previous anatomical data (Burwell and Amaral, 1998b; Burwell, 2000) suggesting that there is a feed-forward transfer of information between the PRC and LEC.

The laminar profiles that we obtained *in-vitro* in the PRC-LEC slice were consistent with the *in-vivo* observation of a current sink located over layers III-II and suggestive of monosynaptic excitation of layer III-II cells. In conformity with this, intracellular recordings demonstrated that PRC stimulation elicited a monosynaptic EPSP in all LEC layer III and layer II investigated though in some layer II cells the early EPSP was cut short by an IPSP. Intriguingly, our CSD analysis revealed a robust current source over layers V-VI *in-vivo* but not (only apparent in two cases) *in-vitro*. The basal dendrites of layer III-II cells do not extend into layer V (Tahvildari and Alonso, unpublished observations), so this source cannot result from a synaptic effect on layer II/III cells. It could, however, reflect to some extent a PRC excitatory input at the apical dendritic level of the

layer V pyramidal cells. This could explain the massive sink observed over layers II-III *in-vivo* and the robust source over layer V. A similar situation happens with the presubicular input over layer III of the MEC which synapses both on the apical dendrites of the layer III and layer V pyramidal cells (van Haeften et al., 2000). Yet, the LEC layer V current source *in-vivo* was very prominent. It may also be that the PRC input leads to feed-forward inhibition on LEC layer V pyramidal cells.

Interestingly, we noted that when the PRC was stimulated at high stimulus intensities a late current sink developed over the deep LEC layers at a latency of approximately 15ms. There are several potential explanations for this late sink. The deep LEC layers are the target of the hippocampal feedback and the superficial LEC layer activation could have led to reverberation through the hippocampal loop (figure 2.7). However, the latency of the deep sink is inconsistent with the long looping around the hippocampus. It could also be that the deep late sink represents a rebound phenomenon of the layer V network. Alternatively, the late sink could also represent propagation of activity from superficial to deep cell layers (Iijima et al., 1996; Buckmaster et al., 2004). Since lesioning and imaging studies have shown that the EC can play a role in memory independent of the hippocampus (Leonard et al., 1995), one would expect that information must be able to flow from superficial (input layers) to deep layers (output layers) without looping around the hippocampus (figure 2.7).

We also investigated the bidirectional flow of information between the PRC and LEC *in-vivo* by constructing the laminar profile of field potential

responses in the PRC following LEC stimulation. Importantly, the pattern of synaptic activation was very different (almost a mirror image) to that of the PRC to LEC projection. Essentially, LEC stimulation led to two well-defined current sinks, one located deep over layer V-VI the other very superficially located over layer I. This is again perfectly consistent with the anatomically described pattern of connections between the LEC and the PRC. LEC to PRC projections originate in the deep LEC layers and innervate primarily layers V and I (Burwell and Amaral, 1998a, b), the exact locations were we observe current sinks indicative of cellular excitation.

In summary, our electrophysiological data *in-vivo* and *in-vitro* involving CSD analysis and investigation of intracellular synaptic responses clearly demonstrates a well organized spatio-temporal pattern of synaptic activation in the LEC following discharge of the PRC and, conversely, a well-organized pattern of synaptic activation in the PRC following discharge of the LEC. These data are consistent with previous anatomical knowledge and provide further support for the hypothesis that hippocampal and neocortical signals in the form of synchronized discharges of activity can transfer information in relation to memory encoding along the neocortical-hippocampal axis (Buzsaki, 1996; Higuchi and Miyashita, 1996; Siapas and Wilson, 1998; Sirota et al., 2003). The data are also consistent with previous neurophysiological investigations in lower mammals and primates, including humans, indicating the importance of a fluent dynamical trafficking of information between the neocortex and the parahippocampal/hippocampal region to subserve memory function (including

working memory) and spatio-visual recognition tasks (Squire, 1998; Eichenbaum, 2000; Naya et al., 2001; Frey and Petrides, 2002; Gottfried et al., 2004).

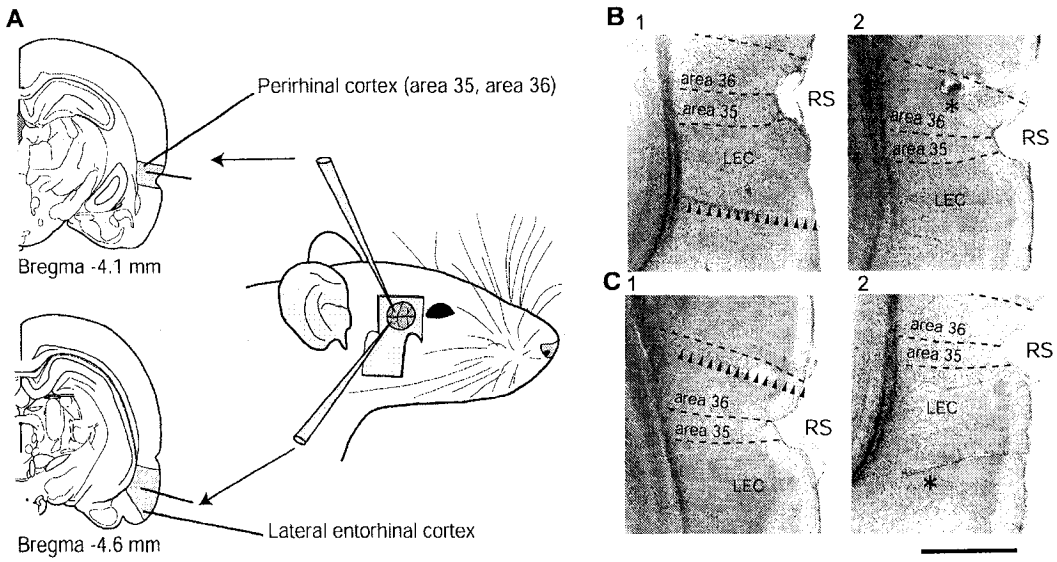


**Figure 2. 1.**

**Surgical technique and electrode positioning.** *In-vivo* experiments: (A) The stimulating and recording electrodes were positioned in the perirhinal cortex (PRC) and lateral entorhinal cortex (LEC) by direct visualization of the rhinal sulcus. (B) and (C) coronal sections from two different cases, respectively, demonstrating the position of the silicon probe recording site (1) and stimulating electrode (2, asterisk). Scale bar: 1mm. (RS, rhinal sulcus).

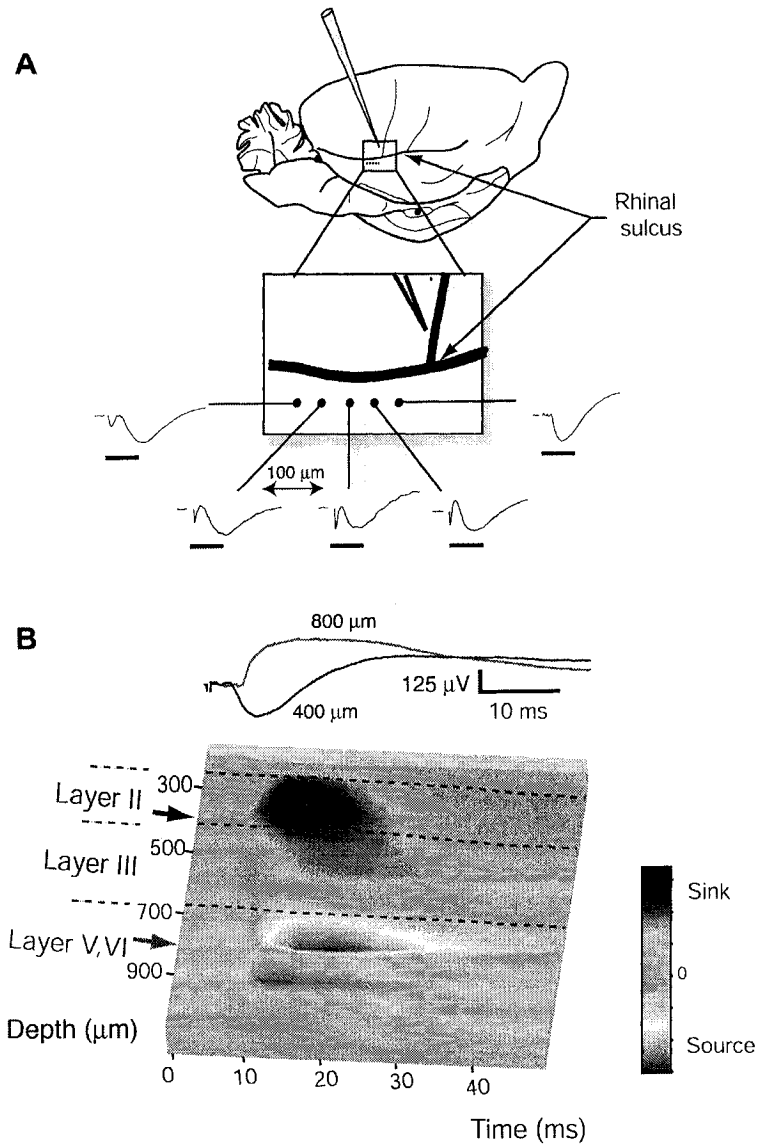


**Figure 2. 2.**

**LEC field responses to PRC stimulation *in-vivo*.** (A). Lateral schematic view of the rat brain showing the positioning of the stimulation electrode above the RS and five sequential recording sites separated by 100 µm below the RS. The inset shows a magnified view of the area, and the field potentials recorded at 400 µm beneath the surface of the cortex. Scale bar: 10 ms. Note the increase in the response latency as the distance between the stimulating and recording electrodes

increases. (B). Typical field responses (top) and corresponding current source density (CSD) profile (bottom; pseudo-color surface contour plot) obtained in the LEC following PRC stimulation. The data corresponds to the rostral entry point in A. The distance between the stimulating electrode and the silicon probe was ~ 2 mm and the stimulius intensity used to construct the profile was 250 μA. In this and the following figures, the colored arrows to the left of the CSD plot point to the depth at which the represented, equally colored, field potential traces were recorded. The dotted lines mark the border between cell layers and are curved for perspective only. Note that the CSD profile demonstrates a robust current sink (blue) centered on layers II-III, and a current source (red) and minor sink over the deep cell layers.

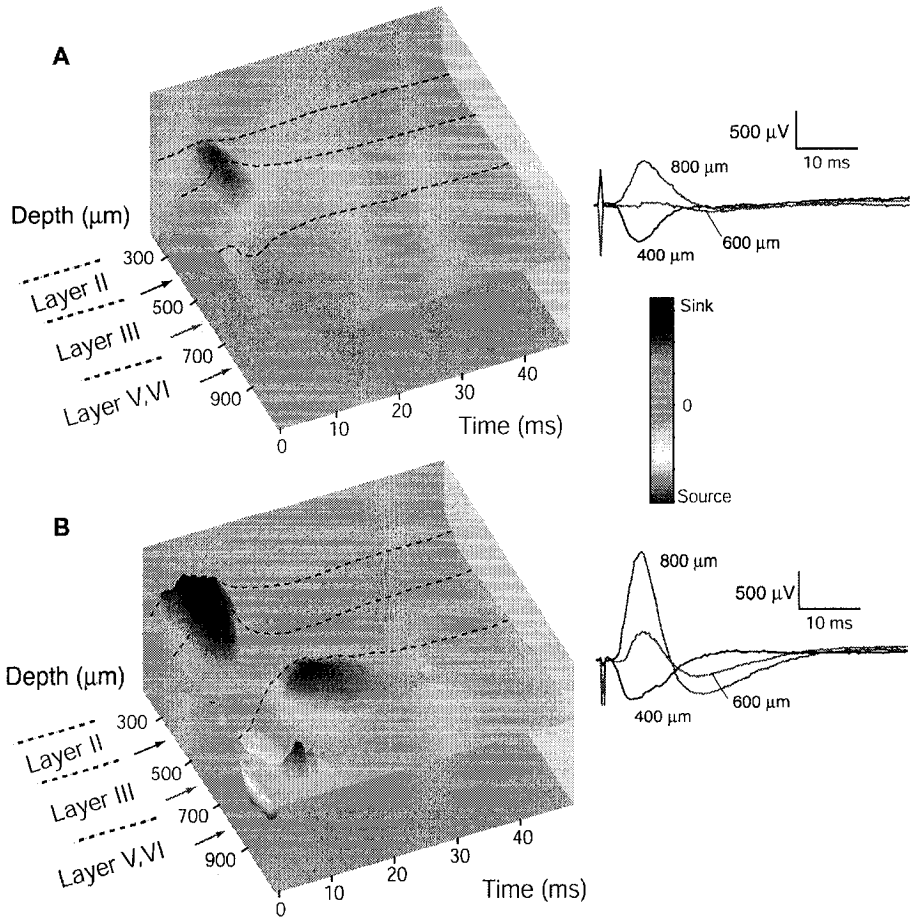


**Figure 2. 3.**

**Effect of stimulation intensity on the CSD profile of the LEC to PRC stimulation *in-vivo*.** (A). Left, CSD plot showing the presence of a short latency current sink (blue) in the superficial layers of the LEC after low intensity stimulation (200 μA for 100 μsec) of the PRC. Right, exemplary field responses used to construct the CSD plot. (B). Left, CSD plot demonstrating the emergence of a relatively long latency current sink on the superficial aspect of layer V following high intensity stimulation (500 μA for 100 μsec) of the PRC. Right,

exemplary field responses used to construct the CSD plot and obtained at the same recording sites as in A.

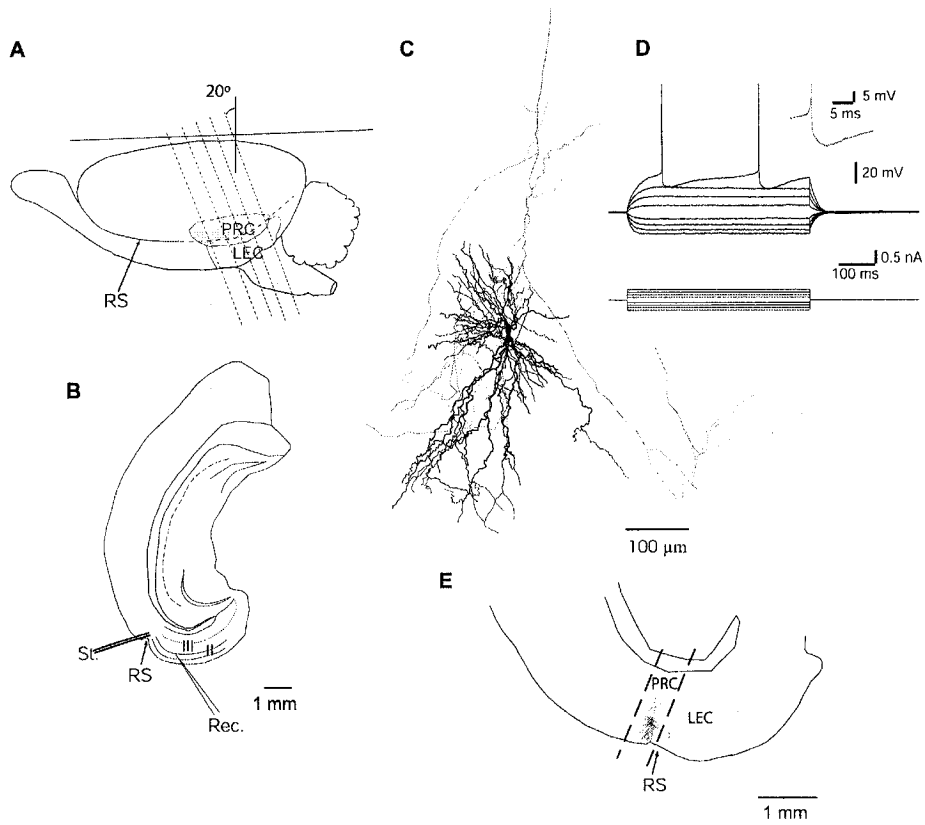


**Figure 2. 4.**

**Preservation of axonal projections in a PRC-EC slice preparation.** (A). Oblique brain slices preserving the integrity of the PRC to LEC connectivity were obtained by cutting the brain (dotted lines) at a 20° angle with respect to the coronal plane. (B). Schematic diagram showing the position of the stimulating (St.) and recording (Rec.) electrodes in the slice (II and III represent the second and third cortical layers, respectively). (C). Computer-aided three-dimensional reconstruction of a biocytin filled neuron in superficial cell layers of the PRC. The axon is in red. (D). Voltage/current relation of the same neuron. Inset, action potential at an expanded time and voltage base. (E). The location of the neuron represented in C in the slice.

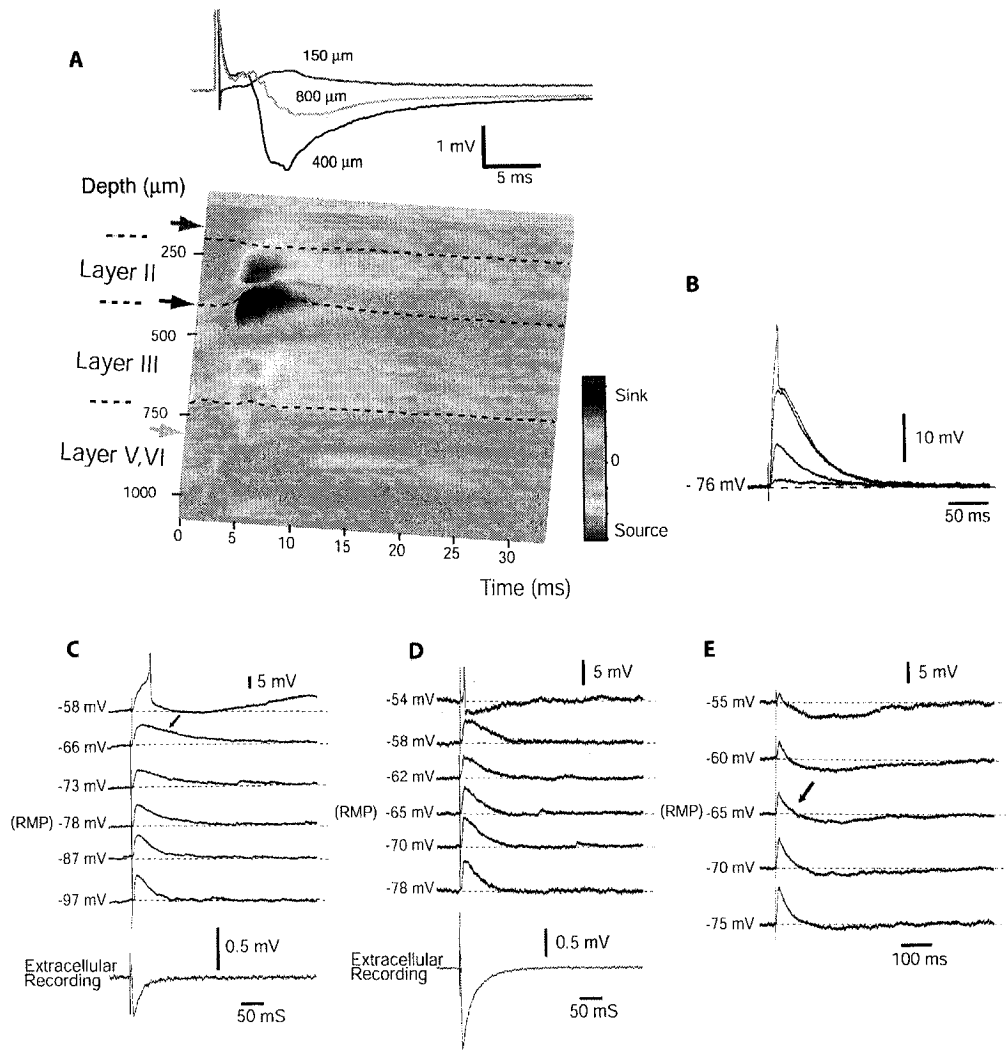


**Figure 2. 5.**

**Activation of the LEC after PRC stimulation *in-vitro*.** (A). Typical field responses (top) and corresponding CSD profile (bottom) in the LEC after PRC stimulation. Note in the CSD plot the robust current sink centered over layers II-III. (B) Graded intracellular synaptic responses (top) in a LEC layer III neuron to PRC stimulation at increasing intensities (200, 300, 400 and 450 µA) that eventually triggered a spike. (C). Pure EPSP in a representative LEC layer III neuron to PRC stimulation. The arrow shows the appearance of a slow EPSP component as the membrane potential is held at a more depolarized state.

Simultaneous extracellular recording in layer II (bottom trace). (D), (E). Synaptic responses to PRC stimulation in two different layer II neurons. Note that while one cell responded with an EPSP only (D) the other manifested an EPSP-IPSP sequence (E). The arrow in E points to the approximate level of reversal of the faster component of the IPSP. The bottom trace in D corresponds to a simultaneously recorded field response in layer III. Stimulus intensity was 300 μA in all cases. RMP, resting membrane potential. Action potentials in B, C and D have been truncated.

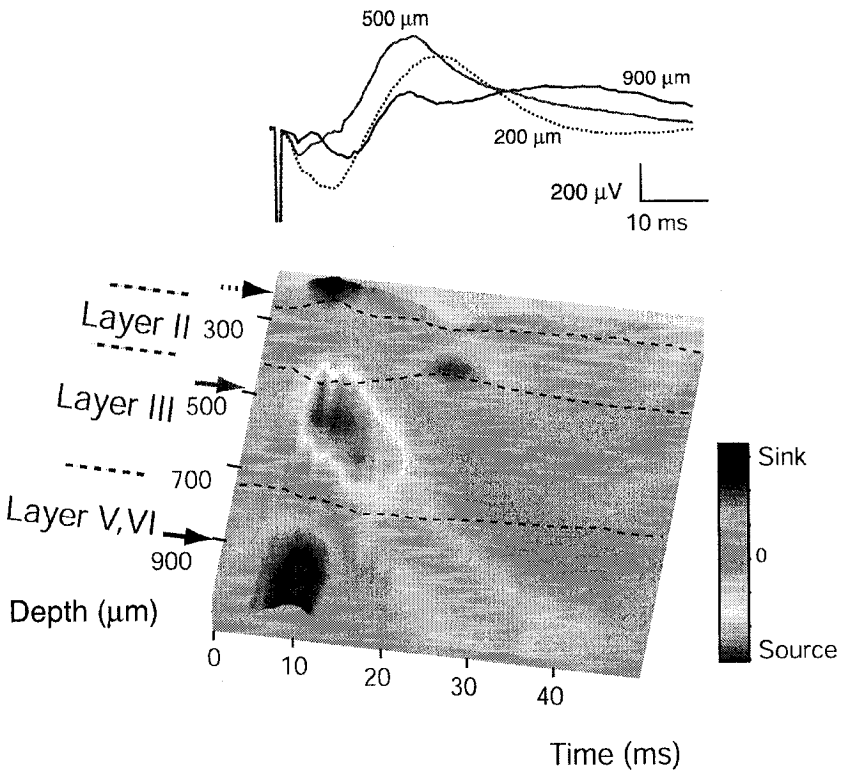


**Figure 2. 6.**

**CSD profile in the PRC in response to LEC stimulation *in-vivo*.** Representative field responses (top) and corresponding CSD plot (bottom). Note the early current sinks in layers I-II and V-VI accompanied in time by a current source over layer III.

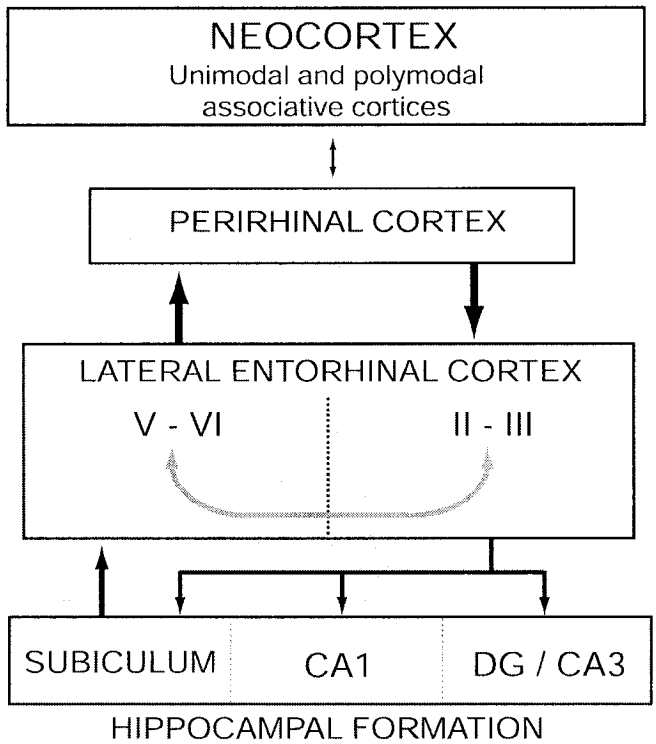


**Figure 2. 7.**

Simplified representation of the interconnectivity between the neocortex, the perirhinal cortex, the lateral entorhinal cortex and the hippocampal formation comprising the subiculum area CA1, area CA3 and the dentate gyrus (DG). The concept of possible transmission of information within the LEC is emphasized.

# CHAPTER 3: Morphological and Electrophysiological Properties of Lateral Entorhinal Cortex Layers II and III Principal Neurons

## 3.1 Preface

In chapter two, several different approaches were used to provide the first demonstration of functional and bidirectional mono-synaptic excitatory connections between the PRC and the LEC. However, a more complete understanding of the PRC-LEC circuit also requires a characterization of the morphological and electrophysiological properties of principal neurons in these structures. Previous studies have revealed some of the properties of PRC principal neurons [layers II and III (Beggs and Kairiss, 1994; D'Antuono et al., 2001); layer V (Moyer et al., 2002); layer VI (McGann et al., 2001)]. In contrast, the electrophysiological properties of morphological identified LEC principal neurons have only been investigated in layer V (Hamam et al., 2002). Since principal neurons in layers II and III of the LEC are the main recipients of neocortical input via the PRC (section 1.4.1b), and provide one of the most prominent inputs to the hippocampus (section 1.4.1c), it is essential to gain information concerning the properties of these cells. In this chapter, therefore, I performed intracellular recordings from these neurons and revealed the passive and active electrophysiological properties of morphologically identified principal neurons.

## 3.2 Abstract

The intrinsic electrophysiology and morphology of neurons from layers II and III of the lateral entorhinal cortex (LEC) was investigated in a rat brain slice preparation by intracellular recording and biocytin labeling. Morphologically, we distinguished three groups of layer II principal neurons. The most numerous group included cells with multiple radiating dendrites that spread over layers II and I in a fan-like fashion. While morphologically "fan" neurons were similar to the "stellate" cells of the MEC, electrophysiologically the fan cells lacked the persistent rhythmic subthreshold oscillations and the very pronounced time-dependent inward rectification typical of the stellate cells. The second group consisted of pyramidal cells that manifested regular spike firing and had a more negative resting potential and longer spike duration than the fan cells. In the third group we included all those neurons that had diverse multipolar appearances distinct from the fan cells. Neurons in this group had electrophysiological profiles intermediate between those of the fan and pyramidal cells. All neurons recorded in layer III were pyramidal in shape with a basal dendritic tree that could extend into layer V and an axon that could also give off collaterals into layer V. Electrophysiologically, layer III pyramidal cells were very similar to those of layer II. On the basis of these and other data we suggest that in different EC regions layer II neurons may be conducting more input-dependent specialized processing, while cells from layer III may perform a more global or generalized function.

## 3.3 Introduction

Over the last few years there has been a growing interest in understanding the functional organization of the entorhinal cortex (EC) (Witter et al., 1989; Insausti et al., 1997; Dolorfo and Amaral, 1998a, b; Fyhn et al., 2004; Suzuki and Amaral, 2004; Uva et al., 2004; Steffenach et al., 2005). Anatomically, Ramón y Cajal (1901) pointed out over 100 years ago that since the major input to the hippocampus comes from the EC via the perforant path, understanding hippocampal function would require investigating the EC. He wrote: "*Such connections are so notable that they necessarily imply a functional unity of the two centers, in such a way that it can be said without fear of error that if the angular ganglion is olfactory then Ammon's horn must be olfactory, if optic then optic, etc*".

Neuroanatomical tracing studies over the last few decades have demonstrated that via a cascade of cortico-cortical connections the superficial cell layers of the EC receive converging sensory input from the entire cortical mantle, which is then funneled toward the hippocampus via the perforant and temporo-amonic pathways (PP and TAP, respectively) (Steward and Scoville, 1976; Burwell and Amaral, 1998a; Burwell, 2000). Principal neurons from layer II project to the dentate gyrus and CA3 (Steward and Scoville, 1976; Ruth et al., 1982, 1988), while principal neurons from layer III project to CA1 and subiculum (Steward, 1976; Witter et al., 1988; Naber et al., 2001). In turn, the subiculum feeds back mainly to the deep layers of the EC, from which the information is distributed back to the cortex in a remarkable system that reciprocates the input

channels (Swanson and Kohler, 1986; Suzuki and Amaral, 1994a; van Haeften et al., 1995; Insausti et al., 1997; Burwell and Amaral, 1998b; Naber et al., 2001). Neuropsychological, lesion, imaging, and behavioral neurophysiological investigations in animals and humans have demonstrated that this system of cortical-hippocampal-cortical connections forms the basis of a network that allows the coding, storage, and recall of declarative memories (i.e., memories for facts and events) (Scoville and Milner, 1957; Mishkin, 1982; Squire and Zola-Morgan, 1991; Buzsaki, 1996; Squire and Zola, 1998; Eichenbaum, 2000).

On cytoarchitectural grounds the EC classically has been subdivided into a medial and a lateral subregion (Blackstad, 1956; Insausti et al., 1997). In Nissl staining the medial EC (MEC) is characterized by a densely packed layer II and a clear "*lamina dissecans*" which is poorly defined in the lateral EC (LEC). MEC and LEC also give rise to distinct components of the PP and TAP that terminate on distinct fields along the dendrites of the dentate granule cells and CA3 pyramidal cells and on distinct pools of CA1 and subicular pyramidal cells, respectively (Steward, 1976; Ruth et al., 1988; Dolorfo and Amaral, 1998b). The MEC and LEC components of the PP also differ with regard to the peptide content of their cells of origin and their physiology (McNaughton, 1980; Gauthier et al., 1983; Neumaier and Chavkin, 1989; Bramham et al., 1991).

In recent years it has also been recognized that, in addition to the classical medial and lateral subdivisions of the EC, there are also three dorsoventral bands in the EC that cut across the cytoarchitectonic subdivisions (Ruth et al., 1982, 1988; Witter et al., 1988; Dolorfo and Amaral, 1998a, b). While these bands were

initially defined on the basis of connectivity (Witter et al., 1988), recent neurophysiological investigations *in-vivo*, as well as lesion studies, have suggested distinct functional correlates of the dorsoventral bands. The superficial layers of the of the MEC corresponding to the caudal portion of the lateral band contain numerous "place cells" and lesions of this region of the EC result in spatial memory deficits (Fyhn et al., 2004; Steffenach et al., 2005). On the other hand, the superficial cell layers of the MEC at the level of the ventromedial band do not contain cells with precise positional modulation and lesions in this region result in reduced defensive behavior (Steffenach et al., 2005).

We and others have previously characterized the electrophysiology and morphology of neurons in the MEC (Schwartz and Coleman, 1981; Germroth et al., 1989, 1991; Alonso and Klink, 1993; Tamamaki and Nojyo, 1993; Jones, 1994; Empson et al., 1995; Dickson et al., 1997; Gloveli et al., 1997; Schmitz et al., 1998; van der Linden and Lopes da Silva, 1998; Hamam et al., 2000). In our studies recordings were obtained mainly at a MEC level corresponding to the caudal aspect of the dorsolateral band (Alonso and Llinas, 1989; Alonso and Klink, 1993; Dickson et al., 1997; Dickson et al., 2000). Those analyses revealed that MEC layer II is composed primarily of "stellate" cells that have a rather unique electroresponsiveness characterized by a very prominent hyperpolarization-activated current (h current), a persistent $Na^+$ current, and persistent rhythmic subthreshold oscillations in the theta frequency range (Alonso and Llinas, 1989; Agrawal et al., 2001). MEC layer III pyramidal cells were found to be regularly spiking neurons that lacked subthreshold oscillations

(Dickson et al., 1997; Gloveli et al., 1997). Our present goal was to explore whether the morphological attributes and basic intrinsic electrophysiological properties of neurons from the superficial cell layers of the LEC (rostral level of the dorsolateral band) were distinct from those of the MEC, as previously published. We were interested to understand the basis for the functional differentiation between the different regions of the EC, particularly since a recent characterization of cells in the deep layers of the MEC and LEC did not reveal profound differences between the two areas (Hamam et al., 2000; Hamam et al., 2002). Our data shows that, in fact, neurons in layer II of the LEC are very distinct in terms of their morphology and electrophysiology from those of the MEC. Cells in the LEC layer III, however, were found to be quite similar to those of the MEC. Some of the results have been previously presented in abstract form (Tahvildari and Alonso, 2003).

## 3.4 Materials and methods

All experimental protocols were approved by the McGill University Animal Care Committee and were in compliance with the guidelines of the Canadian Council on Animal Care.

### 3.4.1 Slice preparation

Semicoronal brain slices were obtained from male Long-Evans Hooded rats (150-250 g; Charles River, Canada) following procedures described previously (de Villers-Sidani et al., 2004). In brief, under halothane anesthesia the animals were decapitated and the brain was quickly removed from the skull and

placed in ice-cold (4°C) Ringer's solution containing (in mM): 124 NaCl, 3 KCl, 1.6 $CaCl_2$, 1.8 $MgSO_4$, 26 $NaHCO_3$, 1.25 $NaH_2PO_4$, and 10 glucose (pH maintained at 7.4 by saturation with 95% $O_2$/5% $CO_2$). A block of tissue containing the parahippocampal region was dissected out by removing the rostral half of the brain with a dorsoventral cut at a 20° angle with respect to the coronal plane in the anterior-posterior direction (figure 3.1, upper panel). Slices (400 μm thick) that maintained the cytoarchitectonic of the LEC (Burwell and Amaral, 1998b; Burwell, 2000; Burwell and Witter, 2002) were then obtained using a vibratome (Pelco 101, Redding, CA) and by sectioning parallel to the frontal face of the block. The slices that corresponded to stereotaxic coordinates of ~ 4.8mm to 6.1mm posterior to bregma were selected and then transferred to an interface holding chamber where they were maintained at room temperature for at least 1 hour prior to recording. Then individual slices were transferred one-by-one to the interface recording chamber (Fine Science Tools, North Vancouver, BC) and perfused for recording with Ringer's solution at the rate of 1-2 ml/min at 34°C ± 1°C.

### 3.4.2 Electrophysiological recording

Recording electrodes were pulled from borosilicate glass capillaries (World Precision Instruments, Sarasota, FL) with a P-97 Sutter Instruments puller (Novato, CA). Intracellular electrodes were filled with 1.5 M potassium acetate and 2% biocytin (tip resistance of 80-120 MΩ). Signals were recorded with an Axoclamp 2B amplifier (Axon Instruments, Union City, CA), low-pass filtered at 5 kHz, viewed on-line with a digital storage oscilloscope (Tektronix 2201,

Heerenveen, The Netherlands), digitized (Digidata 1320, Axon Instruments) at a sampling rate of 10 kHz, and acquired with Axoscope (Axon Instruments) in a computer for later analysis. Intracellular current-clamp recordings were obtained from neurons in layers II and III of the LEC at a level corresponding to the rostral dorsolateral band. During the experiments the cortical layers were identified with the help of a dissecting microscope (World Precision Instruments) and a video camera (Sony XC-75) that allowed easily noticing distinct densities of cellular packaging when the slice was transilluminated. Once the recorded neurons were electrophysiologically characterized they were injected with biocytin (Sigma, St. Louis, MO) by applying negative current pulses of 0.3 nA and 0.3 seconds (50% duty cycle) for at least 5 minutes. At the end of the recording session the electrode was pulled out from the cell and the slice was kept for another 15-20 minutes in the recording chamber before being fixed with 4% paraformaldehyde in 0.1 M sodium phosphate buffer (NaPB) for at least 48 hours at 4°C.

### 3.4.3 Histochemical processing

Histochemical processing for biocytin was performed using procedures similar to those described by Hamam et al. (2002). Fixed tissue slices were removed from paraformaldehyde solution, washed in 0.1 M NaPB (3 × 5 minutes), and processed without further sectioning. Endogenous peroxidase activity was suppressed by incubating slices in 2% $H_2O_2$ in 0.1 M NaPB for 30 minutes, followed by washing in 0.1 M NaPB (3 × 5 minutes). Nonspecific binding sites were blocked by incubating the slices in PHT (0.1 M NaPB; 0.2% gelatin, 0.25% Triton X-100) for another 30 minutes. Then the slices were labeled

with an avidin-biotin-horseradish-peroxidase complex (Vector Laboratories, Burlingame, CA) in 0.1 M NaPB and 0.3% Triton X-100 overnight. The next day the slices were washed extensively in PHT: first, brief washes (5 × 3 minutes), followed by a longer wash (1 × 30 minutes), then a series of long washes (6 × 1 hour), and finally a wash overnight. The final day, slices were washed with 0.1 M Tris-buffered saline (TBS; pH 7.6; 3 × 10 minutes) and then transferred to 3, 3'-diaminobenzidine solution (DAB substrate solution; Vector Laboratories). The DAB reaction was stopped when the desired staining was reached by washing the slices in TBS (3 × 10 minutes). Finally, the slices were mounted on glass slides, left to air-dry for 5 minutes, and cover-slipped with moviol (Calbiochem, La Jolla, CA).

### 3.4.4 Data analysis

For morphological analysis neurons were first reconstructed using the Neurolucida system (MicroBrightField, Colchester, VT) on a Nikon microscope (Eclipse E800) at 63x magnifications and the quantitative data was obtained using the Neuroexplorer software (MicroBrightField). Photomicrographs were taken using the same set-up at 20x magnification. In the dendritic stick histograms, bars oriented between 0-180° were regarded as ascending dendrites and those between 180-360° were regarded as descending dendrites. The ascending-descending dendritic index was estimated as the ratio between the cumulative dendritic length of ascending and descending dendrites.

The data for the analysis of the input/output relations were taken from the Axoscope program and plotted and quantified using Origin software (Microcal,

Northampton, MA) or Clampfit (Axon Instruments). The apparent input resistance was estimated from the voltage deflection after injection of a 0.1 nA/100 ms hyperpolarizing pulse from the resting membrane potential, and the time constant was taken as the time it took the corresponding voltage deflection to reach 63% of its maximal value. Action potential duration was measured at threshold and action potential amplitude was measured from threshold to peak. The amplitude of the depolarizing after-potential (DAP) for the action potential was measured from the peak of the fast after-hyperpolarization to the depolarizing peak. The degree of time-dependent inward rectification was estimated by calculating the "sag" percentage (sag%), which consisted of the percentage change in membrane potential from peak to steady state during a hyperpolarizing current pulse that caused a peak voltage deflection of ~25 mV. Neurons that had a sag ratio of less than 5% were not considered to have time-dependent rectification. To characterize the regularity of firing, the coefficient of variation (CV) of the instantaneous frequency for the last 3 seconds of a 4-second step depolarization was calculated. Average values were expressed as means ± SE. Statistical significance was evaluated by means of the two-tail Student's *t*-test for unpaired data.

## 3.5 Results

In order to examine the electroresponsiveness and somatodendritic architecture of LEC layer II-III neurons, we made use of a semicoronal slice preparation (figure 3.1) that maintains the integrity of LEC neurons and their

main cortical input (de Villers-Sidani et al., 2004). Using this preparation, we recorded and labeled intracellularly with biocytin 31 neurons from layer II and 25 neurons from layer III in a region that extended from ~4.8-6.5 mm posterior to bregma (figure 3.1, lower panel). Within the LEC slice, the soma of the recorded neurons was located at a depth of ~120-240 μm from the slice surface. All neurons presented extensive dendritic arbors the ascending portions of which always extended up to the pia and an axon which could frequently be traced down to the angular bundle. All neurons were recorded for at least 20 minutes and had a minimum resting potential of -60 mV, an input resistance larger than 30 MΩ, and an overshooting action potential. In what follows, we first describe the characteristics of neurons in layer II and then those of layer III.

### 3.5.1 Layer II

We (Alonso and Klink, 1993; Klink and Alonso, 1997a) and others (Jones, 1994; van der Linden and Lopes da Silva, 1998; Wang and Lambert, 2003; Erchova et al., 2004) have previously described the morphological and electrophysiological characteristics of neurons from layer II of the MEC and found two main electrophysiological and morphological categories: the classical "stellate" cells of Cajal and another group that we referred to as the "non-stellate" (or pyramidal-like) cells. A recent study addressed the electrophysiological properties of LEC layer II neurons and found some differences with respect to those of the MEC, but all lateral EC neurons were lumped into one group (Wang and Lambert, 2003). In the present study we subdivided LEC layer II neurons into three categories according to anatomical criteria (figure 3.2). In the next sections

we will describe first the morphological characteristics of these cellular groups and then their electrophysiology.

***Layer II morphology***

The most numerous group (n = 15) consisted of cells that had a large (329.9±29.3 $\mu m^2$) polygonal body and whose most distinctive morphological feature was the presence of multiple thick primary dendrites (see table 3.1) that fanned out from the soma mostly in the ascending and horizontal direction (figures 3.2A, 3.5A). These dendrites branched repeatedly, thus covering an area that approximated the shape of a semicircle with the base oriented parallel to layer II (figure 3.2A). Because of the fanning out of their dendrites, we refer to these cells as the "fan" cells. While the presence of multiple ascending dendrites radiating out from a polygonal soma is also a characteristic of the MEC layer II stellate cells, the fan cells did not have the prominent descending dendritic arbor that gives MEC stellate cells their characteristic "star" appearance. Descending dendrites were present in some (n = 3) of the fan cells; however, these were typically thin and short and did not cover a wide area or extend into layer III, as the descending dendrites of the stellate cells typically do (Klink and Alonso, 1997a). The ascending/descending dendritic ratio (see materials and methods) of the fan cells was 3.18 (n = 10), and the total dendritic length of the ascending dendrites far exceeded that of the descending dendrites ($P < 0.001$) (figure 3.3A, table 3.1). All primary and higher-order dendrites of the fan cells were sparsely covered with spines. The axon was always seen leaving the soma in the

descending direction and, frequently, it could be followed down to the angular bundle (n = 8).

The second clearly distinctive morphological group of LEC neurons was pyramidal cells (n = 9) (figure 3.2B). We included in this group all those neurons that had a pyramidal-shaped soma (253.5 ± 17.5 $\mu m^2$), which was smaller (although not significantly) than that of the fan cells and from which a distinct thick apical dendrite emerged (table 3.1). In all cases the apical dendrite bifurcated within layer II, each secondary dendrite branching repeatedly within layers II and I until reaching the pia. As a group, the apical dendritic arbor of the pyramidal cells had the appearance of a rectangle (figure 3.2B, right-most column) rather than a semicircle, as in the fan cells. The pyramidal cells also had numerous basal primary dendrites that were thinner than the apical dendrite (table 3.1) and branched repeatedly within layer II and the upper half of layer III. The basal dendritic tree of the pyramidal cells was therefore quite profuse. In fact, the total dendritic length of the basal dendrites was not significantly different than that of the apical dendritic tree (table 3.1, figure 3.3B). As in the fan cells, the dendrites of the pyramidal cells were also sparsely covered with spines. The axon could be followed down to layer III in five cases and up to the angular bundle in one case. Recurrent collaterals could be clearly distinguished in one case spreading over layers III and II.

We also identified a third group of cells that included all those layer II neurons (n = 7) whose morphological characteristics did not correspond to the fan or pyramidal cell category. We refer to this group of cells as the "multiform"

cells. The multiform cells had a large cell body (346.1 ± 44.2 $\mu m^2$; table 3.1) similar in size to that of the fan cells and pyramidal cells, which could be polygonal, fusiform, or round (figure 3.2C). Similar to the fan cells, the multiform cells also had multiple primary dendrites, but these tended to be oriented in all directions and, thus, the overall dendritic arbor did not exhibit a "fanning" appearance forming a semicircle as in the fan cells (figure 3.2C). All the multiform cells had dendrites that extended over layers I, II, and deep into layer III. The aspect of one of the multiform cells was very similar to that of the stellate cells from MEC layer II, with an ascending and a descending arbor that extended widely over layers I-II and II-III, respectively (figure 3.10). The physiology of this cell, however, was very different from that of the stellate cells in that it lacked time-dependent rectification (see below), which is a salient characteristic of the MEC stellate cells. The dendrites of all multiform cells were also sparsely covered with spines. The axon could be traced down to the white matter in two cases.

***Layer II electrophysiology***

The basic electrophysiological characteristics of the three morphologically categorized groups of LEC layer II neurons are summarized in table 3.2. We found that, according to a series of passive and active membrane properties, there were significant differences between the group of fan cells and pyramidal cells (figure 3.4). From the electrophysiological point of view, the multiform group represented more of a mixed pool with some cells manifesting characteristics typical of fan cells and others exhibiting characteristics more typical of the

pyramidal cells. None of the multiform cells had a unique electrophysiological profile.

The fan cells had the most depolarized resting potential (~-66 mV) of the three cell groups and this difference was highly significant (table 3.2, figure 3.4A). Their input resistance was also larger and the membrane time constant longer than in the other cell groups, but this difference was only significantly different between the fan cells and the pyramidal cells ($P < 0.05$ and $P < 0.01$, respectively) (table 3.2, figure 3.4B,D). In addition, the action potential of the fan cells was significantly shorter (~1.2 ms) than that of the pyramidal cells (~1.8 ms) ($P < 0.001$) or multiform cells (~1.7 ms) ($P < 0.001$) (figure 3.4C), but the spike threshold and spike amplitude was the same for the fan cells as for the other cell groups (table 3.2). With respect to other spike characteristics, the action potential of the fan cells was followed in most cases (n = 10) by a depolarizing after-potential (figure 3.5B, inset) which was, however, of very small amplitude (table 3.2).

Analysis of the current/voltage (I/V) relationships demonstrated that all fan cells, without exception, manifested time-dependent inward rectification (figure 3.5B,C) quantified as a "sag"% (see materials and methods) of ~11% (table 3.2). In contrast, none of the pyramidal cells demonstrated time-dependent inward rectification (figure 3.5E,F and table 3.2), although all pyramidal cells did display "instantaneous" inward-rectification as reflected by the upward bending of the instantaneous I/V curve toward the negative end (figure 3.5F). Both fan cells and pyramidal cells also demonstrated inward rectification in the

depolarizing direction manifested by the upward bending of the I/V relation towards the positive end (figure 3.5C,F).

The input-output relation was also characterized by analyzing the firing behavior of the cells in response to long-lasting (4 seconds) depolarizing current steps from rest to a level slightly above threshold and another 0.2-0.4 nA stronger than that. This analysis revealed some differences between the fan cells and pyramidal cells (figure 3.6). The pyramidal cells were more homogeneous with respect to their firing pattern and, thus, we will describe them first. In response to the low-intensity pulse, the pyramidal cells typically reacted with an initial spike doublet (figure 3.6D, upper trace, asterisk) followed by a highly regular tonic discharge (figure 3.6D,E). In response to the high-intensity pulse (figure 3.6D, lower trace), the same cells reacted with a very fast-adapting discharge followed by a highly regular tonic phase (figure 3.6F). The coefficient of variation (CV; an index of regularity) of the instantaneous firing frequency for the tonic phase of the discharges was 0.062 ± 0.007 (figure 3.7A) for the low-intensity pulse and 0.043 ± 0.006 (n = 8) for the higher-intensity pulse.

In contrast to the tonic discharge of the pyramidal cells, most of the fan cells (~65%) displayed a phasic behavior (figure 3.6A-C). In response to the low-intensity pulse (figure 3.6A, upper trace), these neurons displayed a discharge initiated by a single spike (not spike doublet) that was followed by phasic firing consisting of single spikes or groups of few spikes (spike clusters) interspersed by silent periods in which some membrane potential oscillations could be observed (figure 3.6A,B; note the serrated nature of the frequency *vs.* time plot in B). In the

same cells the stronger pulse (figure 3.6A, lower trace) evoked an initial fast-adapting response followed by a maintained discharge in spike clusters that repeated over time (figure 3.6C). For this group of "phasic" fan cells the CV of the instantaneous firing frequency yielded a value of 0.47 ± 0.04 for the low-intensity pulse (figure 3.7A) and 0.30 ± 0.07 (n = 9) for the high-intensity pulse. A small group of fan cells (35%) behaved similarly to the pyramidal cells in that their discharges to step depolarizations were similarly tonic and regular. In these "tonic" fan cells the CV of the instantaneous firing frequency for the tonic phase of the discharges was 0.06 ± 0.007 for the low-intensity pulse (figure 3.7A) and 0.046 ± 0.005 (n = 5) for the higher-intensity pulse.

As mentioned above, pyramidal cells typically reacted to depolarization with an initial spike doublet (figure 3.6D, asterisk) that was not characteristic of the fan cells. Reflecting this initial response, during the high-intensity pulse the firing frequency corresponding to the first inter-spike interval was significantly higher in the pyramidal cells than in the fan cells (table 3.2, figure 3.7B). In all pyramidal and fan cells the instantaneous frequency *vs.* time plots could be well fitted by a double exponential decay function (figure 3.6C,F), which yielded fast and slow time constants of adaptation that were faster, although not significantly, in the pyramidal cells than in the fan cells (figure 3.7C,D). The irregular discharge with spike clusters present in most fan cells (figure 3.6A) is reminiscent of that of the MEC layer II stellate cells (see figure 5 in Alonso and Klink, 1993). Similar to the fan cells, the stellate cells also manifest time-dependent inward rectification, although in a much more robust manner (as reported by Alonso and Klink (1993)

the "sag" percentage of the stellate cells is ~35% vs 11% for the fan cells ). The electrophysiological signature of the stellate cells, however, is the expression of persistent rhythmic subthreshold membrane potential oscillations (Alonso and Llinas, 1989; Alonso and Klink, 1993). Because of the parallels between fan cells and stellate cells we explored whether the fan cells would also express rhythmic subthreshold membrane potential oscillations. We did notice that in all cases for a rheobase DC depolarizing level (corresponding to ~-50 mV) the membrane potential displayed clear fluctuations. However, power spectral analysis of these fluctuations displayed significant power in a broad range of low frequencies (1-10 Hz) without a unique distinctive peak indicative of high rhythmicity. In fact, in no case was the autocorrelation function of prolonged (5-10 seconds) subthreshold periods found to be rhythmic (not shown). To illustrate these data, the fan cell that manifested the most salient fluctuations is shown in figure 3.8. Note that only at the level of -52 mV are clear fluctuations apparent. Nevertheless, brief periods (2-6 cycles) of apparently constant frequency oscillations can be seen, particularly during the intercluster periods. These fluctuations were likely nonsynaptic in origin since, in this case, recordings were performed during glutamatergic and GABAergic synaptic transmission block with kynurenic acid (2 mM) and picrotoxin (100 μM).

As mentioned above, with respect to the electrophysiology, the multiform cells represented a mixed group. None of these neurons manifested an electrophysiological profile distinct from the ones described above for the fan cells and pyramidal cells. Similar to the fan cells, some of the multiform cells (n =

3) displayed a clustering discharge (figure 3.9) but, in contrast to the fan cells, only one of these cluster firing cells demonstrated time-dependent inward rectification. Similar to the pyramidal cells, the rest of the multiform cells (n = 3, in one neuron the recording is not conclusive about being clustering or regular firing) displayed a tonic discharge and no-rectification (figure 3.10). The series of electrophysiological parameters that were quantified in these neurons are presented in table 3.2 and figures 3.4 and 3.7.

### 3.5.2 Layer III

All recorded neurons from layer III were identified morphologically as pyramidal cells. The neurons had a large soma (250 ± 21.1 $\mu m^2$), on average almost identical in size to that of the layer II pyramidal cells (table 3.1), from which a characteristic thick (5.88 ± 0.36 μm) apical dendrite and a profuse basal dendritic arborization emerged. As in the neuron illustrated in figure 3.11, in all cases the apical dendrite was found to bifurcate prior to entering or at the border with layer II and then typically to ramify very profusely over layers II and I. The basal dendritic arborization was typically very extensive, spreading over a large area of layer III and, frequently (n = 8), also extending well into layer V (figures 3.12 and 3.13). In fact, the total length of the basal dendrites was significantly longer than that of the apical dendritic tree ($P < 0.05$) and this was a distinctive feature with respect to the layer II pyramidal cells (figures 3.2B, 3.11B and table 3.1). In all cases the basal and apical dendrites were sparsely covered with spines (not shown). The axon was seen in most cases reaching the angular bundle. In four cases the axon was seen giving off collaterals that spread over layer III and in

one case reaching layer II (figure 3.12). Interestingly, descending collaterals were also seen reaching layer V in three cases (figures 3.12 and 3.13).

The electrophysiological profile of the layer III pyramidal cells was very similar to that described above for the layer II pyramids. Layer III pyramids had a resting membrane potential of ~-74 mV, an input resistance of ~50 MΩ, and membrane time constant of ~23 ms (table 3.1). Similar to the layer II pyramidal cells, none of the layer III pyramidal cells demonstrated time-dependent inward rectification (figure 3.11C and table 3.2), but all neurons showed instantaneous inward rectification as well as inward rectification in the depolarizing direction (figure 3.11D). With respect to their firing pattern, all but one of the cells studied responded both to low-intensity and high-intensity step depolarizations with an initially adapting response followed by a regular tonic discharge (figure 3.11E,F). As for the layer II cells, quantification of the degree of adaptation was obtained by fitting a double exponential function to the frequency *vs.* time response for the high-intensity pulse. This analysis yielded fast- and slow-time constants of adaptation of 10.25 ± 1.13 ms and 273.5 ± 29.04 ms, respectively. The fast time constant was similar to the layer II pyramidal cells, but the slow time constant was significantly shorter in the layer III pyramidal cells than in the layer II pyramidal cells ($P < 0.001$) (figure 3.7D). As in the layer II pyramidal cells, the initial response to the depolarizing steps was typically a spike doublet (figure 3.11E, asterisk). Only one of the pyramidal cells we recorded differed from the rest in that it discharged in a "cluster" mode (Figure 3.14) as that typical of the fan cells.

## 3.6 Discussion

We studied the basic morphological and intrinsic electrophysiological characteristics of principal neurons in layers II and III of the LEC. From the morphological point of view, our data shows that there are at least three categories of principal neurons in layer II: fan cells, pyramidal cells, and a third multiform group. Layer III principal cells constituted a homogeneous group of pyramidal cells. Layer II fan cells and layer II pyramidal cells could also be distinguished by their electrophysiological characteristics, whereas neurons from the layer II multiform group displayed electrophysiological properties similar to those of the fan and/or pyramidal cells. Morphologically, layer II pyramidal cells and layer III pyramidal cells differed in that the basal dendritic arborization of the layer III pyramids was much more profuse than that of the layer II pyramids; however, electrophysiologically, layer II and layer III pyramidal cells appeared very similar. In addition to the diversity of neurons in LEC layer II, perhaps the most significant observation of this study was that both the morphological and electrophysiological profiles observed in LEC layer II neurons were quite distinct from those previously characterized in the MEC (Alonso and Klink, 1993; Klink and Alonso, 1997a). This aspect adds to the functional differentiation between the medial and lateral components of the EC and it will be further treated below. We should point out, however, that most of our recordings were obtained in the most lateral aspect of the EC (figure 3.1), and it is possible that the most medially located cells within layer II of the LEC are more similar to those of the MEC. In contrast to the layer II neurons, the intrinsic electrophysiology of LEC layer III

pyramidal cells appeared quite similar to that previously described for the MEC layer III pyramidal cells (Dickson et al., 1997; Gloveli et al., 1997). The electrophysiological and morphological differentiation of neuronal cell types in layer II suggest a differentiation of perforant path processing channels of information.

The most common cellular type in LEC layer II were the cells we referred to as "fan" cells. Morphologically, these neurons are similar to MEC layer II stellate cells in that they displayed multiple primary dendrites and in that the ascending dendrites diverged widely and branched repeatedly over layers II and I. However, MEC stellate cells also have a prominent basal dendritic arbor, which was minimal in the fan cells and rarely reached layer III, as it frequently does in the stellate cells (Klink and Alonso, 1997a). The dendritic arrangement of the fan cells indicates that these neurons are targets for inputs distributed over layers II and I. The axon of the fan cells could be followed toward the angular bundle. We observed in a few cases that toward the transition between layer II and III this axon gave off ascending recurrent collaterals, but these were too faint to be traced. This observation suggests that the fan cells may form part of an associative network over layer II similar to that which the stellate cells seem to form in the MEC (Klink and Alonso, 1997a). Electrophysiologically, both fan cells and stellate cells express time-dependent inward rectification indicative of a prominent h current ($I_h$); however, this time-dependent inward rectification is much more robust in stellate cells than in fan cells (Alonso and Klink, 1993; Klink and Alonso, 1993). The fan cells (and all the neuronal types we studied)

also expressed inward rectification in the depolarizing direction, which is typically indicative of a "persistent" $Na^+$ current ($I_{NaP}$). In the stellates, $I_h$ and $I_{NaP}$ allow the cells to develop very prominent rhythmic subthreshold oscillations thought to be of importance in the pacing of theta rhythmicity (Dickson et al., 2000; Agrawal et al., 2001). However, rhythmic subthreshold oscillatory dynamics were almost entirely absent in the fan cells. Interestingly, theta rhythmicity *in-vivo* appears to be much less prominent in the LEC than in the MEC (Boeijinga and Lopes da Silva, 1988). We did not study the resonant behavior of the membrane in the fan cells, but this is likely to be significant since the cells did display some degree of time-dependent inward rectification (Erchova et al., 2004). This clustering discharge may be important in generating phasic activities or mixed frequency oscillatory behaviors defined by the intracluster and intercluster intervals.

Layer II pyramidal cells had a prominent dendritic tree that extended over layer II and, primarily, layer I, and a basal dendritic arbor that extended mostly over layer II and the superficial aspect (~1/3) of layer III. These neurons, therefore, could be a target for afferent fibers to layers I, II, and the superficial layer III. The axons of the pyramidal cells were also seen giving off recurrent collaterals that branched out from the main axon, typically at around the transition between layers II and III. A population of non-stellate cells is present in the MEC, and many of these neurons have a pyramidal-looking appearance (Klink and Alonso, 1997a). However, in the MEC the apical dendrite is frequently tilted, which was not the case for the more typical-looking pyramidal cells of the LEC.

Again, this points to important differentiation between the two regions, at least with respect to layer II. Electrophysiologically, LEC layer II pyramidal cells and MEC pyramidal-like cells are similar in that both populations are formed by regular spiking cells that maintain a tonic discharge upon membrane depolarization (Alonso and Klink, 1993). However, MEC pyramidal-like cells manifest time-dependent inward rectification (Alonso and Klink, 1993) which is absent in the LEC pyramidal cells. As mentioned above, time-dependent inward rectification is indicative of $I_h$. It is likely, however, that this voltage-dependent conductance, while not appreciable by sharp electrode recordings at the somatic level, might be present at the dendritic level (Shah et al., 2004).

The multiform cell group was rather heterogeneous but, interestingly, none of the multiform cells we recorded from were electrophysiologically distinct from either fan or pyramidal cells. Since the dendrites of these neurons were sparsely covered with spines and their axon could be followed down to the angular bundle, it seems reasonable to assume that multiform neurons also give rise to perforant path fibers. Indeed, retrograde tracing studies have shown quite diverse morphological types from LEC layer II projecting to the dentate gyrus (Schwartz and Coleman, 1981).

We found that layer III pyramidal cells were very homogenous both with respect to their morphology and intrinsic electrophysiology. Morphologically, their only apparent difference from the layer II pyramidal cells was the much more prominent basal dendritic tree. This basal dendritic arbor covered a wide area of layer III and also extended in a significant number of neurons (~35%) well

into layer V. The apical dendrite of the layer III pyramidal cells also branched quite profusely over layers II and I. LEC layer III pyramidal cells are therefore potential targets for inputs to layers III, II, and I, and to layer V as well.

There is a tendency to functionally subdivide the cell layers of the EC into superficial (II and III) and deep (V and VI) since layers II-III give rise to the perforant path and layers V-VI receive the main hippocampal feedback. However, while it is true that the entorhinal-hippocampal projection originates in the superficial cell layers, there seem to be also deep layer cells that project to the hippocampus (Gloveli et al., 2001). Conversely, there are also some hippocampal feedback fibers that terminate over layer III (Witter et al., 2000; Kloosterman et al., 2003a). In addition, our dendritic data suggests that those hippocampal-subicular feedback fibers innervating LEC layer V may also make synaptic contact with basal dendrites of LEC layer III pyramidal cells. LEC layer III neurons thus appear capable of monitoring afferent information reaching all cell layers of the EC (with the exception of layer VI). Importantly, we also found that, in addition to the main axonal branch directed towards the hippocampus, the axon of the LEC layer III pyramidal cells gave off collaterals that branched within layer III and which could either ascend or descend to innervate layer V as well (figure 3.12). Thus, LEC layer III neurons appear capable not only of spreading information towards the hippocampus, but also probably of influencing the hippocampal/subicular feedback to layer V as well (van Haeften et al., 1995). Our anatomical observation of layer III axonal branching within layer V is also consistent with our recent CSD analysis on the spread of synaptic activity in the

LEC following perirhinal stimulation (de Villers-Sidani et al., 2004). A recent study has also shown that in the primate EC the axon of pyramidal cells from layer III also gives off collaterals that innervate layer V (Buckmaster et al., 2004). Electrophysiologically, LEC layer III pyramidal cells were indistinguishable from layer II pyramidal cells and, perhaps more significantly, they also appeared very similar to previous descriptions of MEC layer III pyramidal cells (Dickson et al., 1997; Gloveli et al., 1997). We recently made a similar observation with regard to EC layer V neurons; MEC and LEC neurons share similar electrophysiological and morphological profiles (Hamam et al., 2000; Hamam et al., 2002). These observations suggest that further clarifying the physiological organization of EC layer II might be key to understanding the differential functional role(s) of distinct EC subregions (see below). We believe this is an issue on which further research should be intensified, particularly in view of the recent behavioral neurophysiological data on MEC superficial layer neurons (Fyhn et al., 2004). This being said, a more exhaustive electrophysiological characterization of LEC layer III neurons intrinsic excitability (dendritic, for example) or synaptic physiology is likely to yield different categories of layer III pyramidal cells and, perhaps, more fine differences between the MEC and LEC neurons. In fact, MEC layer III neurons are known to degenerate in temporal lobe epilepsy, but LEC layer III neurons are spared (Du et al., 1995).

## 3.7 Concluding remarks

Our data show that neurons from layer II of the LEC are morphologically and electrophysiologically distinct from those previously described for the MEC. This suggests an important compartmentalization of functions between both subdivisions and points that afferent cortical sensory signals are processed very differently by those neurons that give rise to either the medial or the lateral component of the perforant path. This is consistent with previous observations indicating important physiological differences between the medial and lateral components of the perforant path. It is also important to note that the neurons we recorded were located in the rostral aspect of the dorsolateral band and that their intrinsic properties are very different from those previously recorded in the caudal aspect of the dorsolateral band (corresponding to medial EC). It may be that the bands reflect primarily an associative system between distinct EC subregions rather than defining functional subdivisions *per se*. If this were the case, one would expect similar cellular physiology along the bands independently of whether the cells fall in the lateral or medial subdivisions of the EC. It would be important to test whether neurons in the rostral aspect of the dorsolateral band display precise positional modulation (i.e., are they place cells?), as recently reported for neurons in the caudal aspect of the dorsolateral band (Fyhn et al., 2004), or to explore which are the spatial navigation deficits resulting from selective lesions of rostral versus caudal regions of the dorsolateral band.

Interestingly, pyramidal cells from layer III, which project to CA1 and subiculum, appear very similar between the MEC and LEC, suggesting that this cell layer

performs similar operations throughout the entorhinal cortex. As discussed above, this does not appear to be the case for layer II. Layer II cells may be conducting more input-dependent specialized processing, while cells from layer III may perform a more global or generalized function, perhaps, comparing the hippocampal input to the output.

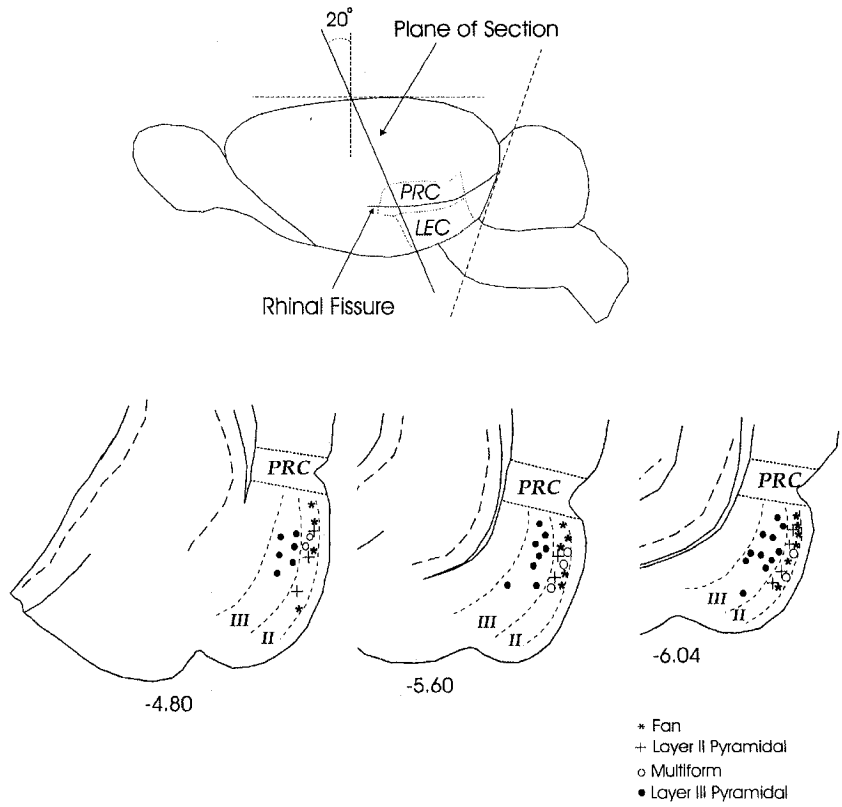


**Figure 3. 1.**

**Slice procedures and distribution of labeled neurons.** Top: Schematic representation of the procedure used to obtain semi-coronal slices. The brain was cut (dotted lines) at a 20° angle with respect to the coronal plane after removing the cerebellum and brainstem. Bottom: location of labeled neurons in layer II and III of the lateral entorhinal cortex at three different rostro-caudal levels. Different morphological groups are represented with different symbols. The numbers below each section indicate the antero-posterior coordinates in millimeters relative to the bregma. PRC: Perirhinal cortex. LEC: Lateral entorhinal cortex.

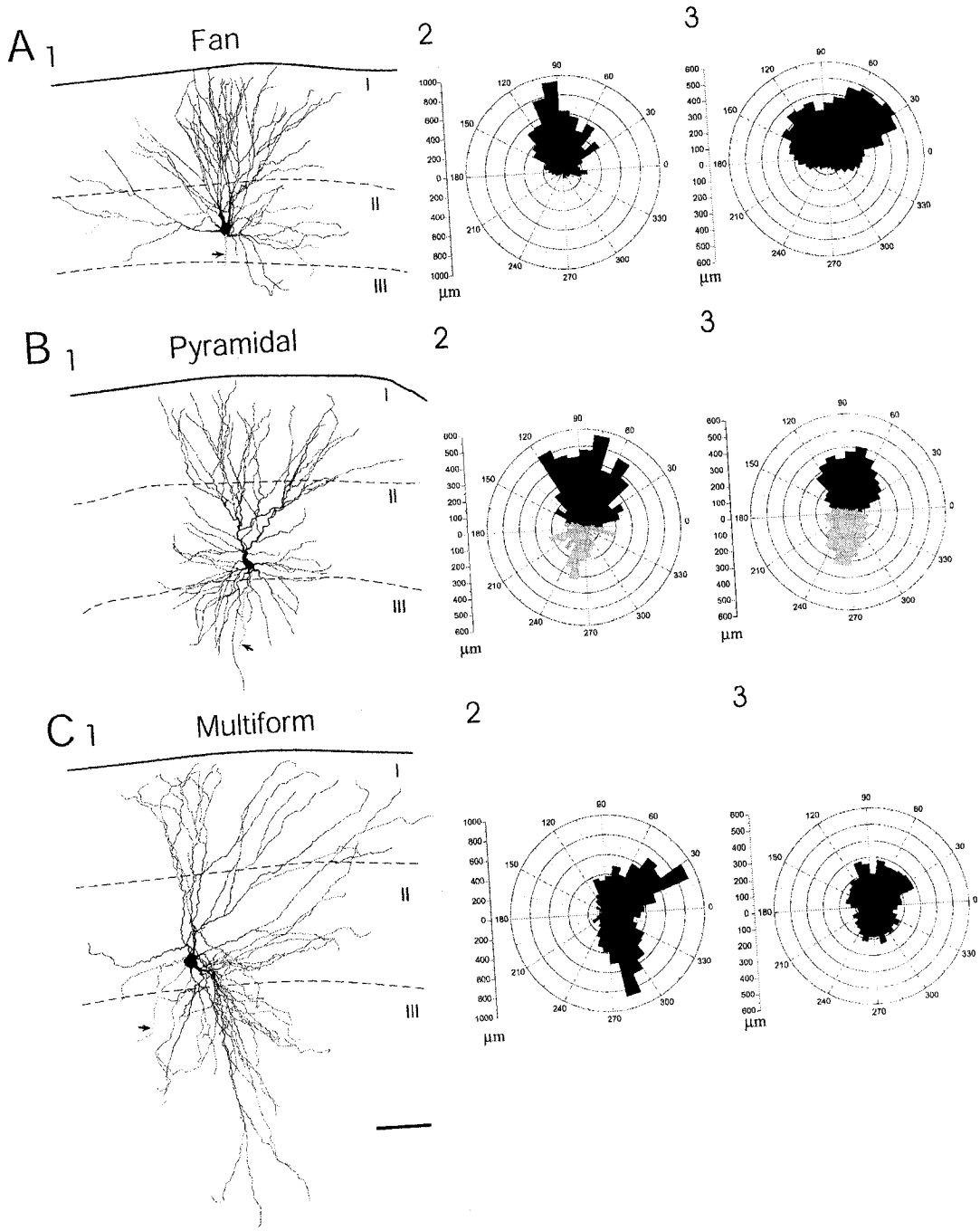
A 1
Fan
I
II
III
2
3
µm
B 1
Pyramidal
I
II
III
2
3
µm
C 1
Multiform
I
II
III
2
3
µm

**Figure 3. 2.**

**Lateral EC layer II morphological subtypes.** A1, B1 and C1: Computer-aided reconstruction of a representative fan cell, pyramidal cell and multiform cell, respectively. Axons are indicated by arrows. A2-C2: Dendritic polar histograms corresponding to the representative neurons. A3-C3: average dendritic polar histograms for the three different populations of neurons (n = 10 fan cells, 7 pyramidal cells and 6 multipolar cells). The sticks corresponding to the basal dendrites of pyramidal cells in B are in grey. Scale bar: 100 μm.

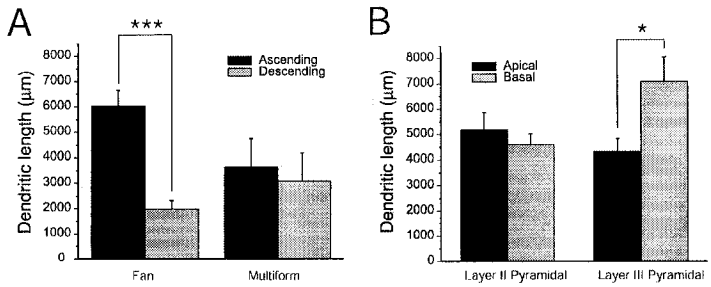


**Figure 3. 3.**

**Dendritic length in lateral EC layer II and III neurons.** A: Dendritic length histogram for ascending *vs.* descending dendritic branches in layer II fan cells and multiform cells. B: Dendritic length histogram for apical vs basal dendrites in layer II and III pyramidal neurons. In this and the following plots, for statistical significance: three asterisks = $p < 0.001$; two asterisks = $p < 0.01$ and one asterisk = $p < 0.05$.

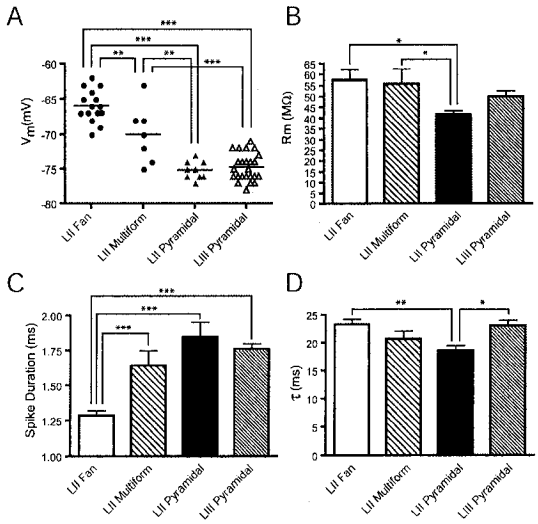


**Figure 3. 4.**

**Distribution of basic electrophysiological parameters of morphologically identified lateral EC superficial layer neurons.** A: resting membrane potential ($V_m$); B: input resistance (Rm) at rest. C: spike duration. D: membrane time constant ($\tau_m$).

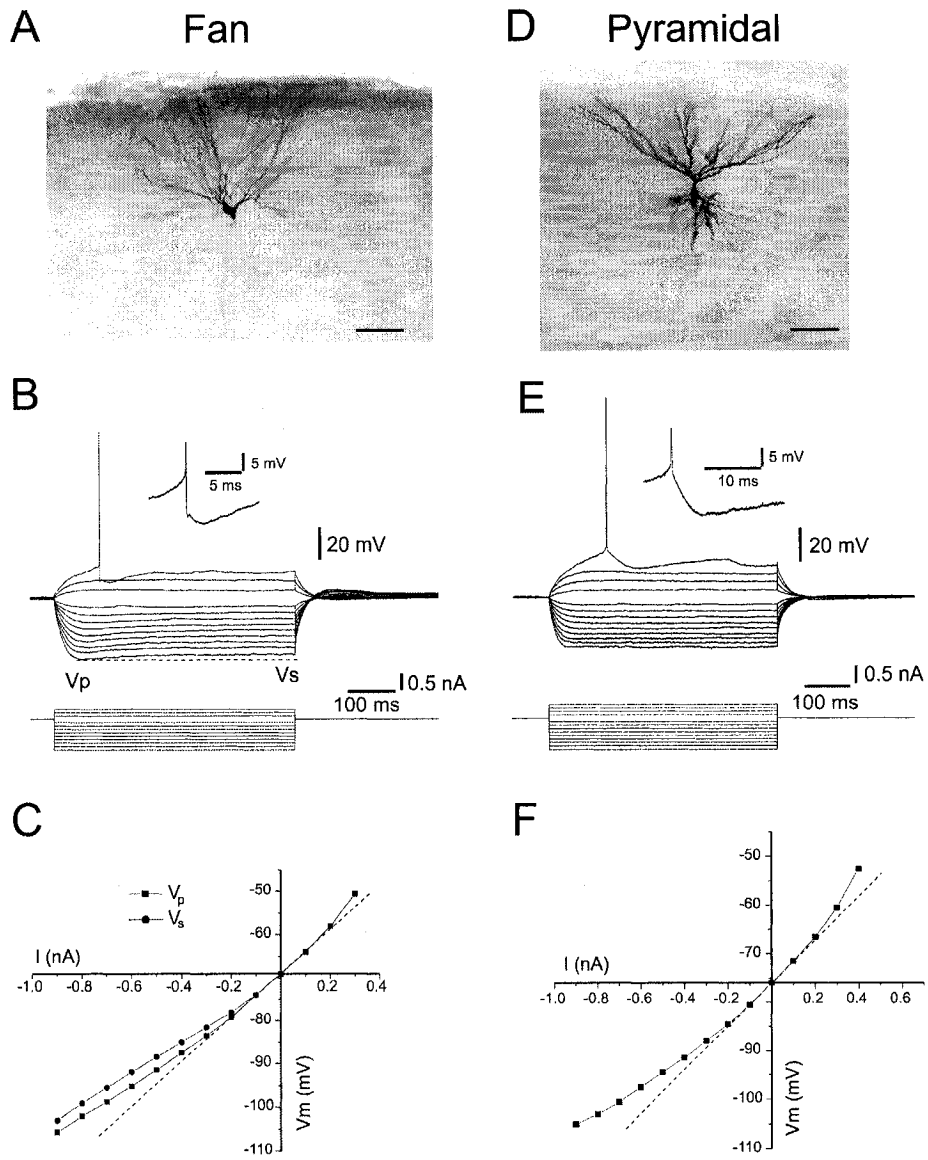


**Figure 3. 5.**

**Electrophysiological profile of fan and pyramidal cells from lateral EC layer II.** A and D: photomicrograph of a typical fan cell and a typical pyramidal cell, respectively. B and E: voltage responses to a series of current steps in the same neurons as in A and D, respectively. The inset in each case displays the spike afterpotentials at larger time and voltage scales. C and F: I/V relations for the

responses in B and D, respectively. The dotted line represents the linear fit for a region of ~ 10 mV centered at rest. Note that the fan cells displayed time-dependent inward rectification (compare $V_p$ and $V_s$ in B and C). Both fan cells and pyramidal cells also displayed inward rectification in the depolarizing direction (upward bending of the I/V relation at the positive end). $V_p$, voltage measured at the peak. $V_s$, voltage measured at steady state. Scale bar for A and D: 100 μm.

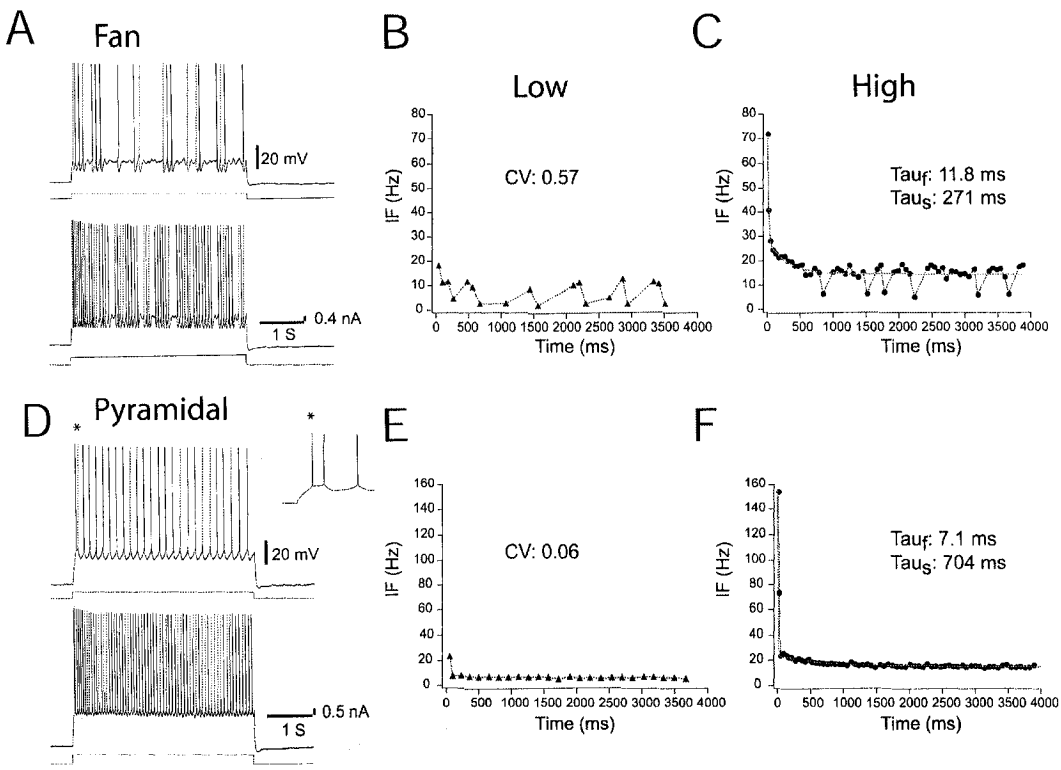


**Figure 3. 6.**

**Differential firing pattern profile of lateral EC layer II fan and pyramidal cells.** A and D: firing response for a typical fan cell (A) and a typical pyramidal cell (D) in response to a low intensity (upper trace) and a high intensity (lower trace) step depolarization from rest. The asterisk in D marks an initial spike doublet represented at a larger time and voltage scale in the inset to the right. B,C and E, F: plots of instantaneous frequency (IF) versus time from pulse onset for the corresponding low and high intensity pulses in A and D. CV, coefficient of variation of IF. Tauf and Taus, fast and slow time constant, respectively, for the double exponential fitting (grey line) to the IF *vs.* time plot.

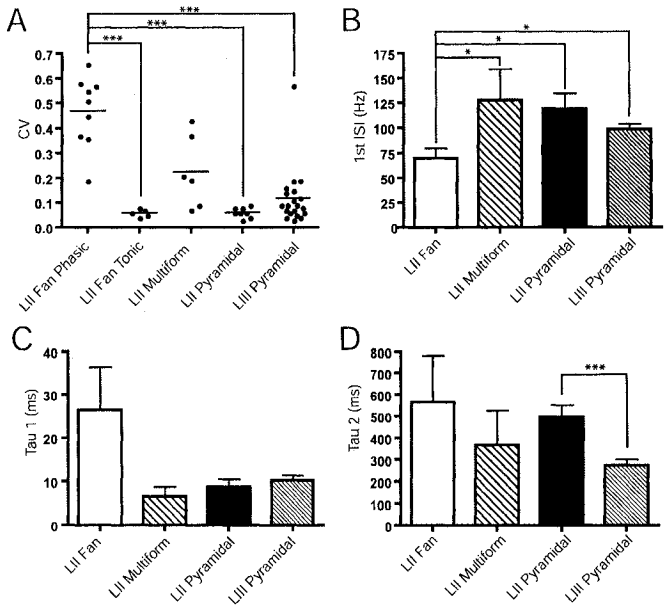


**Figure 3. 7.**

**Firing parameters for superficial lateral EC morphological neuronal subtypes.** A: coefficient of variation of IF corresponding to a 4 second-long, low intensity step depolarization from rest (as in Fig. 6A and D) for all neurons in each cellular category. B: bar histogram of first inter-spike interval (ISI) frequency corresponding to high intensity current steps (as in Fig. 6C and F) for each morphological category. C and D: bar histograms for the fast (tau 1; C) and slow (tau 2; D) time constants of adaptation, derived from double exponential fittings of the IF vs time plots corresponding high intensity current steps (as in Fig. 6C and F) for each morphological category.

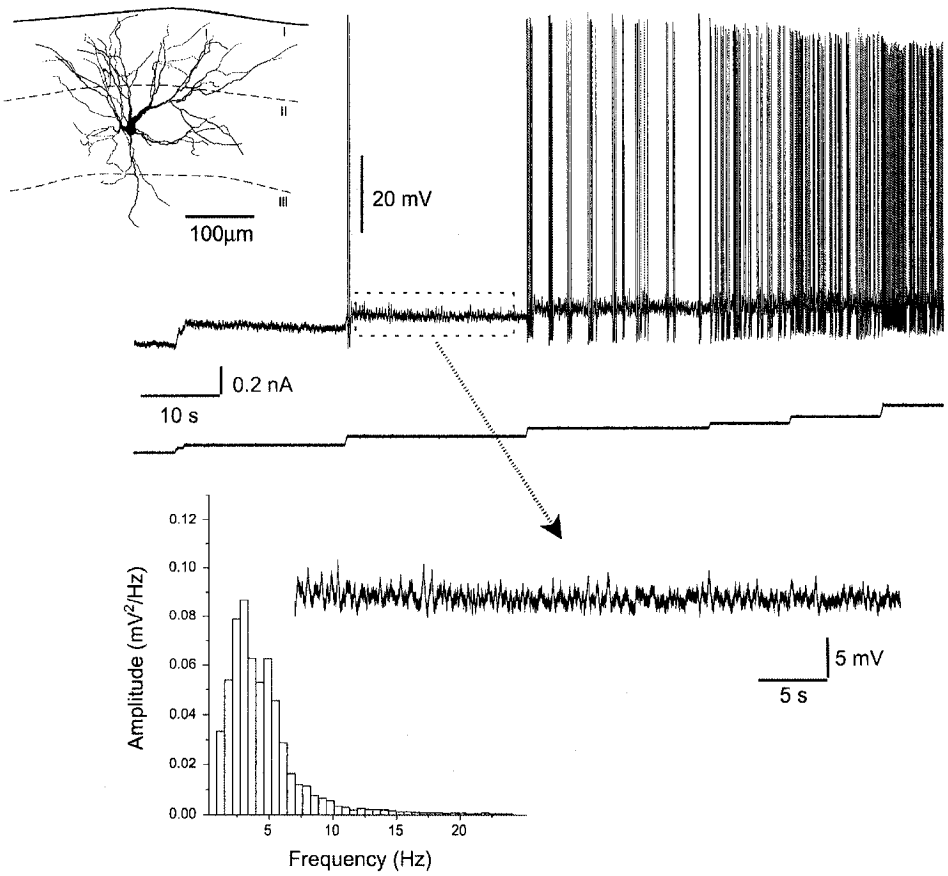


**Figure 3. 8.**

**Subthreshold membrane potential fluctuations in lateral EC layer II fan cells.** Upper pannel: voltage response (upper trace) to a series of long-lasting dc depolarizations (lower trace) for a typical fan cell (morphologically reconstruction on the upper left). Note the emergence of membrane fluctuations at a voltage level of ~ -52 mV (boxed area expanded at the bottom). Fourier analysis of these fluctuations (lower left power spectrum histogram) reveals the significant low frequency content of the fluctuations without a distinctive peak characteristic of high rhythmicity.

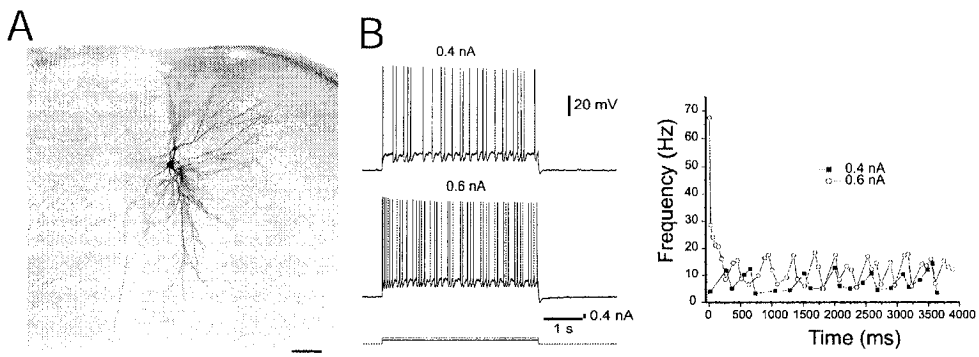


**Figure 3. 9.**

**Cluster firing behavior in a multipolar neuron.** A: photomicrograph of a characteristic multipolar cell. B: firing behavior of the same cell in response to a low (upper trace) and a high (lower trace) intensity current step. C: instantaneous frequency versus time plots corresponding to the traces in B. Note the high irregularity of the firing discharge. Scale bar in A: 100μm.

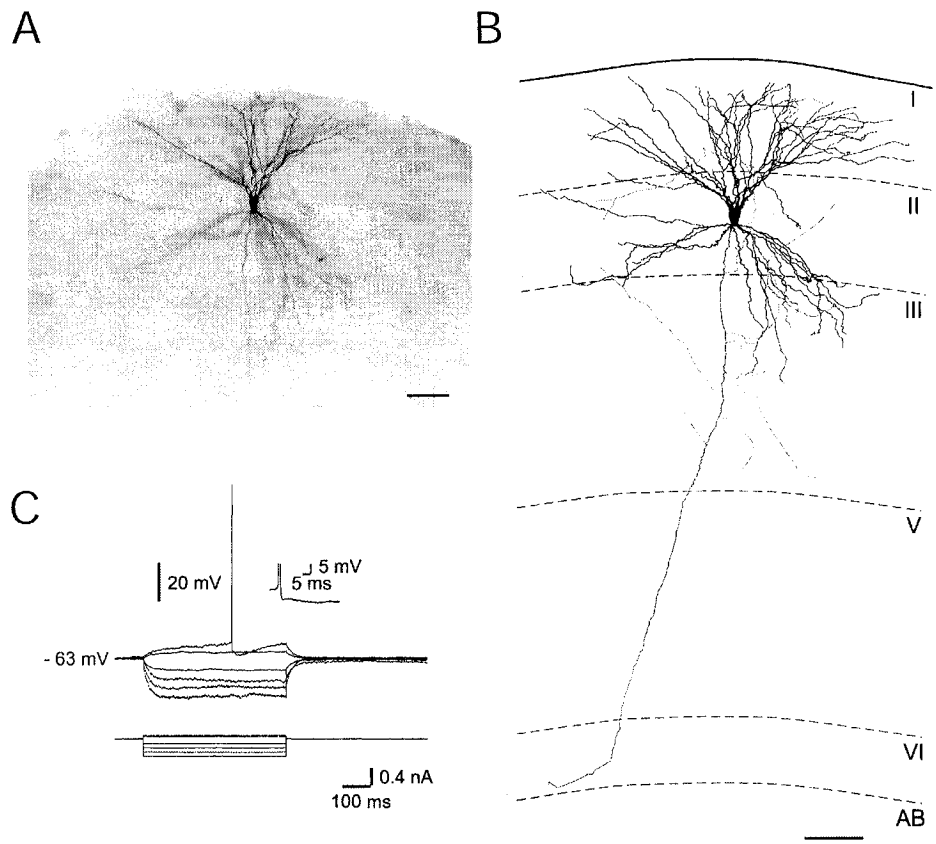


**Figure 3. 10.**

**Multipolar cell with a morphological "stellate cell" -like appearance.** A and B: low magnification photomicrograph and neuralucida reconstrunction of the neuron. Note the presence of multiple, radiating ascending and descending dendrites. The axon (in red) of this neuron could be followed down to the angular bundle (AB) and gave of numerous collaterals at the level of layer III. C: voltage responses to a series of step depolarizations in the same neuron. Note the absence of "sag" responses to the hypedrpolaerizing pulses. The inset shows the spike afterpotentials at a larger scale. Scale bar in A and B: 100μm.

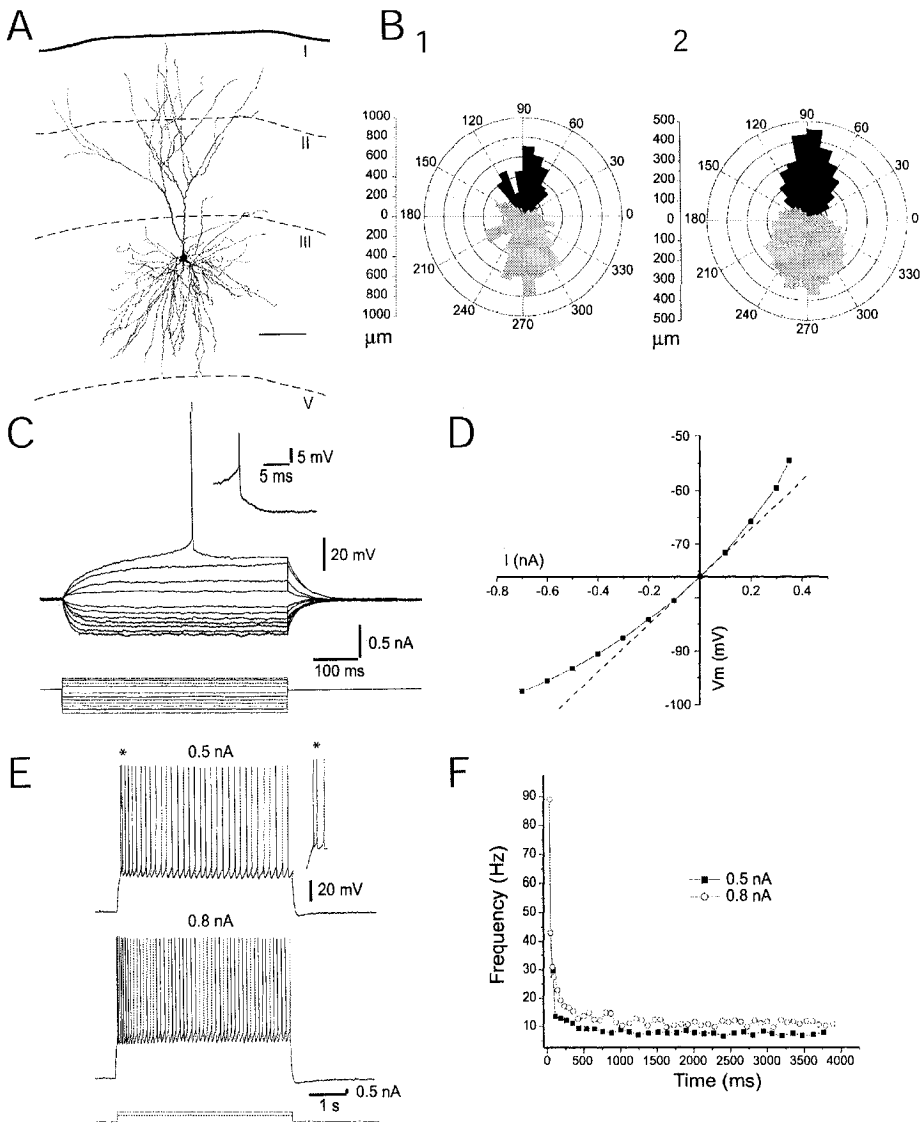


**Figure 3. 11.**

**Morphological and electrophysiological profile of lateral EC layer III pyramidal neurons.** A: computer-aided reconstruction of a typical layer III pyramidal cell. B1 and 2: dendritic polar histogram of the representative neuron in A (B1) and average dendritic polar histogram of the layer III pyramidal cell population (B2). C: voltage responses to a series of current steps in the same

neuron as in A. The inset to the upper right shows the spike afterpotentials at an expanded scale. D: I/V relation for the responses in C. The dotted line represents a linear fit for a region of ~ 10 mV centered at rest. E: for the same neuron, firing pattern in response to a low intensity (upper trace) and a high intensity (lower trace) long (4 s) current step. F: plot of IF *vs.* time for the corresponding responses in E. Scale bar in A: 100μm.

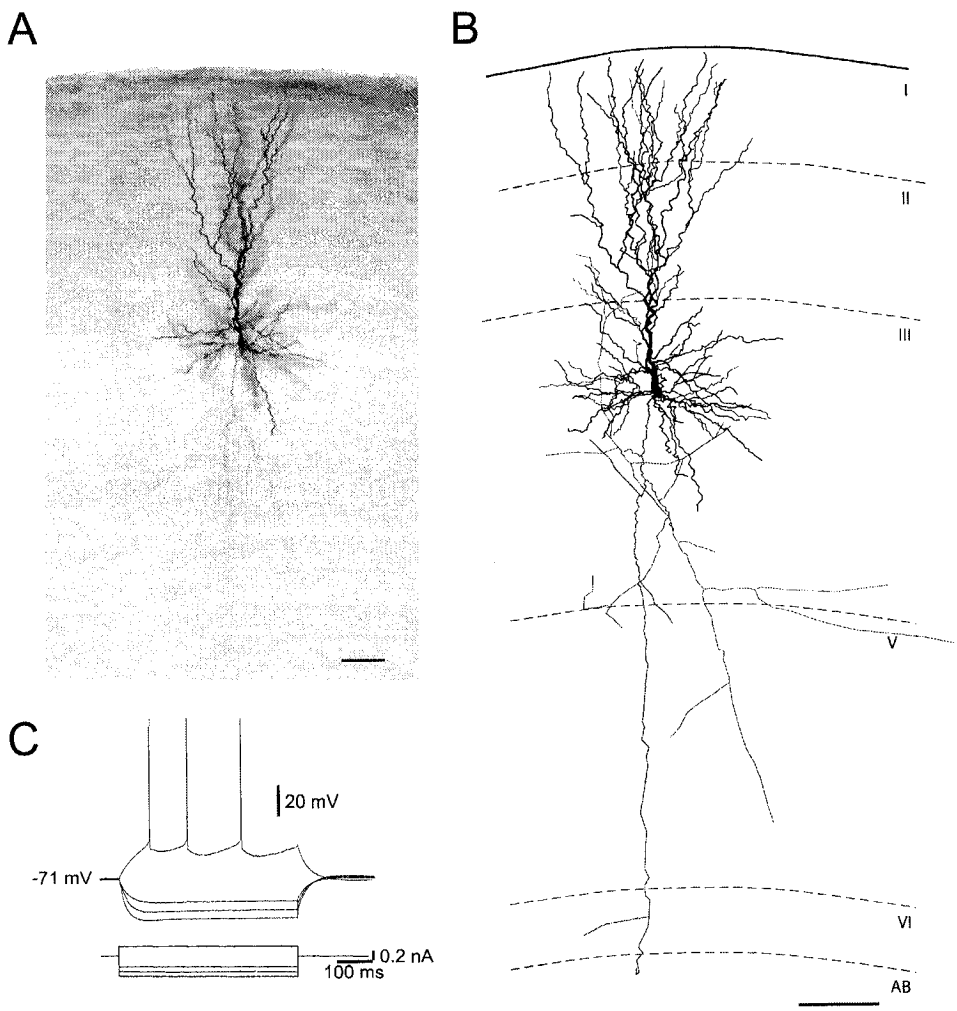


**Figure 3. 12.**

**Layer III pyramidal cell with axonal collaterals that descend to layer V.** A and B: photomicrograph and computer-aided reconstruction of a layer III pyramidal cell. The axon is shown in red. Note the axonal collaterals that branch at the level of layer III and that some ascend towards layer II while other descend reaching layer V. C: Current-voltage relation for the same cell. Scale bar in A and B: 100μm.

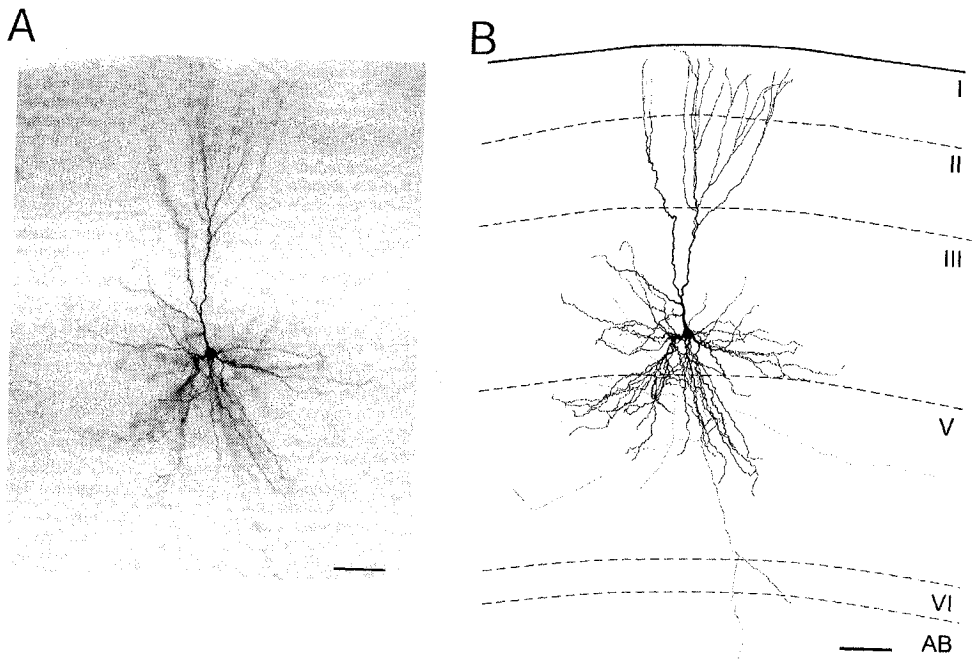


**Figure 3. 13.**

**Layer III pyramidal cells can have dendrites extending into layer V.** A and B: photomicrograph and computer-aided reconstruction of a layer III pyramidal cell, respectively. The axon is shown in red. Note that the basal dendrites extend widely within layer V. Scale bar in A and B: 100μm.

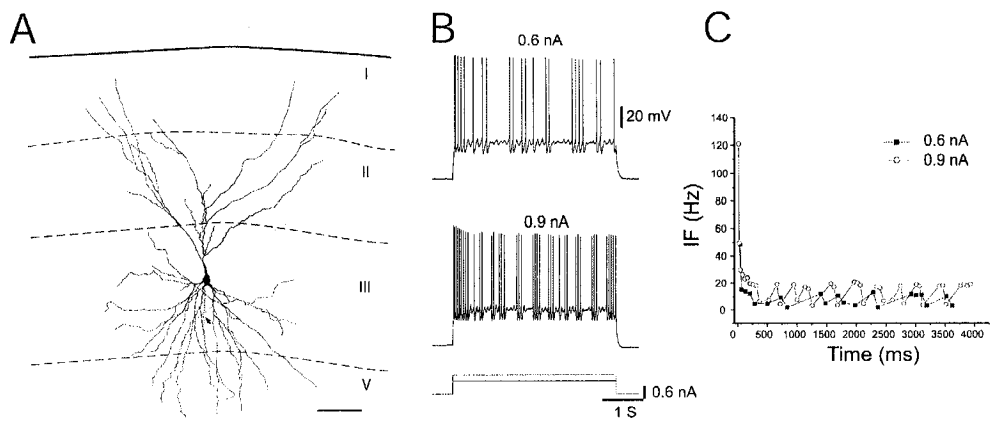


**Figure 3. 14.**

**Layer III pyramidal neuron that displayed cluster firing.** A: computer aided reconstruction of the neuron. Note that the basal dendritic tree extends into layer V. Axon labeled in red. B: for the same neuron, firing pattern in response to a low intensity (upper trace) and a high intensity (lower trace) long (4 s) current step. C: plot of IF *vs.* time for the corresponding responses in B. Scale bar in A: 100μm.

| Cell type | Soma area ($\mu m^2$) | Number of primary dendrites | Diameter of primary dendrites ($\mu m$) | Total Dendritic length ($\mu m$) | Ascending Dendritic Length ($\mu m$) | Descending Dendritic length ($\mu m$) | Apical dendrite diameter ($\mu m$) | Number of basal dendrites | Basal dendrites diameter ($\mu m$) |
|---|---|---|---|---|---|---|---|---|---|
| **Fan** | 329.9 ± 29.3 | 5.3 ± 0.5 | 3.6 ± 0.26 | 9252.5 ± 997.1 | 6305.9 ± 618.8 * | 1980.2 ± 344.9 * | N/A | N/A | N/A |
| **Multiform** | 346.1 ± 44.2 | 5.33 ± 0.84 | 2.95 ± 0.29 | 7530.1 ± 2076.8 | 3929.4 ± 948.3 | 2912.3 ± 811.2 | N/A | N/A | N/A |
| **Pyramidal L II** | 253.5 ± 17.5 | N/A | N/A | 9786.5 ± 812 | **Apical Dendritic Length ($\mu m$)** 5176.8 ± 686.5 | **Basal Dendritic Length($\mu m$)** 4605.8 ± 412.2 | 6.35 ± 0.35 | 4.57 ± 0.48 | 2.52 ± 0.23 |
| **Pyramidal L III** | 250 ± 21.1 | N/A | N/A | 11404.2 ± 1219.8 | 4513.2 ± 513.8* | 7089.2 ± 960.1* | 5.88 ± 0.36 | 4.26 ± 0.24 | 2.84 ± 0.18 |

**Table 3.1.**

**Summary of Morphological Parameters.** Values are means ± SE. For the fan and multiform cells, ascending and descending dendritic lengths were derived from the stick polar histograms. * $P < 0.001$ for fan cells and $P < 0.05$ for layer III pyramidal cells. N = 10 fan cells, 6 multiform cells, 7 layer II pyramidal cells, and 11 layer III pyramidal cells.

| Cell type | RMP (mV) | Time constant (ms) | Input resistance (MΩ) | Action potential threshold (mV) | Action potential duration (ms) | Action potential amplitude (mV) | Sag % (n/nT) | DAP (mV) (n/nT) |
|---|---|---|---|---|---|---|---|---|
| Fan | -65.9 ± 0.58 | 23.2 ± 0.94 | 57.3 ± 4.9 | -45.4 ± 0.48 | 1.28 ± 0.03 | 77.2 ± 0.86 | 11.5 ± 0.70 (15/15) | 0.98 ± 0.25 (10/15) |
| Pyramidal L II | -75.1 ± 0.42 | 18.6 ± 0.87 | 41.6 ± 1.6 | -44.6 ± 0.7 | 1.85 ± 0.1 | 80.1 ± 2.1 | 0 | 0.96 ± 0.18 (5/9) |
| Multiform | -70.0 ± 1.55 | 20.7 ± 1.32 | 55.7 ± 6.85 | -45.8 ± 0.5 | 1.64 ± 0.10 | 78.0 ± 1.13 | 25 (1/7) | 1.2 ± 0.8 (2/7) |
| Pyramidal L III | -74.7 ± 0.39 | 23.1 ± 0.94 | 50.0 ± 2.6 | -45.9 ± 0.41 | 1.76 ± 0.03 | 78.2 ± 1.04 | 0 | 1.09 ± 0.2 (12/25) |

**Table 3.2.**

**Summary of Electrophysiological Parameters.** Values are means ± SE. n = 15 fan cells, 9 layer II pyramidal cells, 7 multiform cells, and 25 layer III pyramidal cells. RMP, resting membrane potential; Sag %, sag percentage; DAP, depolarizing after potential. See materials and methods for details on data analysis procedures.

# CHAPTER 4: Switching between "On" and "Off" States of Persistent Activity in Lateral Entorhinal Layer III Neurons

## 4.1 Preface

In section 1.5.1, I indicated that LEC neurons may contribute to short-term memory by generating persistent activity following exposure to a sensory stimulus. Moreover, *in-vivo* experiments have shown that the generation of post-stimulus sustained activity may require an elevation of extracellular acetylcholine concentration (see section 1.5.2). Since neurons in layers II and III of the LEC relay most of the NC inputs in to the HC, it is important to establish if acetylcholine can modify the excitability of principal neurons in these layers in a manner that facilitates the generation of persistent firing. Since it was found that layer II of the LEC comprises three distinct subtypes of principal neurons, whereas a single subtype was identified in layer III, I initiated an analysis of the effects of cholinergic modulation on superficial LEC principal neurons by investigating its effect on those in layer III.

## 4.2 Abstract

Persistent neural spiking maintains information during a working memory task when a stimulus is no longer present. During retention, this activity needs to be stable to distractors. More importantly, when retention is no longer relevant, cessation of the activity is necessary to enable processing and retention of

subsequent information. Here by means of intracellular recording with sharp microelectrode in *in-vitro* rat brain slices, we demonstrate that single principal layer III neurons of the lateral entorhinal cortex generate persistent spiking activity with a novel ability to reliably toggle between spiking activity and a silent state. Our data indicates that in the presence of muscarinic receptor activation, persistent activity following an excitatory input may be induced and that a subsequent excitatory input can terminate this activity and cause the neuron to return to a silent state. Moreover, application of inhibitory hyperpolarizing stimuli is neither able to decrease the frequency of the persistent activity nor terminate it. The persistent activity can also be initiated and terminated by synchronized synaptic stimuli of layer II/III of the perirhinal cortex. The neuronal ability to switch "On" and "Off" persistent activity may facilitate the concurrent representation of temporally segregated information arriving in the entorhinal cortex and being directed toward the hippocampus.

## 4.3 Introduction

Persistent activity occurs in different regions of the central nervous system (Andrade, 1991; Fraser and MacVicar, 1996; Klink and Alonso, 1997c; Egorov et al., 2002; Shu et al., 2003; Loewenstein et al., 2005), and such activity in the cortex presumably enables neurons to encode and maintain information for short-term memory (e.g. working memory) (Goldman-Rakic, 1995; Miller and Cohen, 2001). While several studies have focused on how this activity may persist in the presence of distractors (Egorov et al., 2002; Koulakov et al., 2002; Fransen

et al., 2006), cessation of this robust firing has received little attention (Fransen et al., 2002, Soc. Neurosci., abstract). For instance, in a discrete trial delayed match to sample task of object recognition, animals are presented with a sample stimulus during the sample period, and then the animal must ignore different non-match distractors stimuli during a delay period, and finally it must respond if a match stimulus is presented again (Suzuki et al., 1997). Importantly, after the second matching presentation, the sample stimulus must be forgotten in order not to interfere with subsequent inputs. Thus, robust delay activity must be generated and terminated reliably following sensory inputs.

The lateral entorhinal cortex (LEC) is a crucial component of the medial temporal lobe memory system, based on its neuronal connections (Witter et al., 1989), and neural activity (Higuchi and Miyashita, 1996; Suzuki et al., 1997; Young et al., 1997). Neuroanatomical tracing studies showed that superficial cell layers of the LEC are one of the targets of association cortices (Burwell and Amaral, 1998a), and that the LEC mainly receives non-spatial information (e.g. information necessary for object recognition) (Knierim et al., 2006). Moreover, principal neurons of layers II and III of LEC are one of the main inputs to the hippocampus (Steward, 1976). In this respect, layer III of the LEC provides direct associational inputs to region CA1, which is a primary focus of research on memory related neural activity and cellular mechanisms of memory. Neurophysiological studies demonstrate that LEC neurons are able to generate persistent activity during the delay period of different working memory tasks (Suzuki et al., 1997; Young et al., 1997). Moreover, *in-vivo* investigations

indicate that the maintenance and encoding of memories is associated with elevation of acetylcholine concentration (Tang and Aigner, 1996), and pharmacological studies confirm that muscarinic receptor blockade reduces persistent activity, and impairs the formation of long-term memory (Schon et al., 2005; Hasselmo and Stern, 2006). Since cholinergic activation is crucial for a correct performance of a memory task, and layer III LEC principal neurons are also important in gating the flow of information to the hippocampus, we decided to investigate if muscarinic receptor activation induces a mnemonic signature in these neurons.

## 4.4 Materials and methods

All experimental procedures were approved by the McGill University Animal Care Committee and were in compliance with the guidelines of the Canadian Council on Animal Care. Conventional sharp micro-electrode intracellular recordings were performed on brain slices obtained from male adult Long-Evans rats (150-250 gr., Charles River Canada, Saint-Constant, QC, Canada). Semi-coronal *in-vitro* slices (450μm thick) were prepared following the protocol explained in detail previously (de Villers-Sidani et al., 2004; Tahvildari and Alonso, 2005). All drugs and chemicals were purchased from Sigma Chemical Co. (Oakville, ON, Canada). Normal Ringer solution was prepared for daily requirements and contained (mM): 124 NaCl, 3 KCl, 1.6 $CaCl_2$, 1.8 $MgSO_4$, 26 $NaHCO_3$, 1.25 $NaH_2PO_4$ and 10 glucose [pH was adjusted at 7.4 by continuous application of $O_2/CO_2$ (95/5%)].

Recordings were performed in an interface recording chamber (Fine Science Tools Inc., North Vancouver, BC, Canada) at 34 ± 1 °C. Borosilicate glass electrodes (World Precision Instruments Inc., Sarasota, FL, USA) were pulled on a Brown Flaming puller (Model P-97, Sutter Instruments Co., Novato, CA, USA), and backfilled with 2 M $K^+$-acetate and 2% biocytin (tip resistance of 80-120 MΩ). Electrical signals were amplified using an Axoclamp 2B amplifier (Axon Instruments Inc., Union City, CA, USA), low-pass filtered at 5kHz, digitized at 10 kHz by Digidata 1320 (Axon Instruments Inc.) and stored on a Pentium computer using Axoscope software (Axon Instruments Inc.) for subsequent and further analysis. Cortical layers were identified during experiments by the help of a dissecting microscope (World Precision Instruments Inc.). However, locations of recordings were also verified later with biocytin staining according to the protocol explained previously (Tahvildari and Alonso, 2005). Since the muscarinic phenomenon studied did not desensitize, most of the neurons were directly impaled in the presence of carbachol (CCh) (n=40 out of 60). Electrophysiological data were analyzed using Clampfit 9.0 (Axon Instruments Inc.), Origin 6.0 (Microcal Software Inc., North Hampton, MA, USA) software packages. Average values were expressed as means ± SE. Statistical significance was evaluated by means of the two-tail Student's *t*-test for paired data.

## 4.5 Results

In this study, 60 principal neurons of layer III of the LEC were recorded and labeled intracellularly with the sharp micro-electrode technique. All recorded neurons were identified as pyramidal in shape and they had regular firing patterns as previously reported (Tahvildari and Alonso, 2005). To investigate the effect of cholinergic modulation solely on the neuronal intrinsic properties and to avoid synaptic interference, the majority of recordings (n=50) were performed during glutamatergic and GABA-mediated neurotransmitter block with kynurenic acid (2 mM) and picrotoxin (100 μM), respectively.

We observed that bath application of CCh (10 μM), a non-hydrolyzable cholinergic agonist, changed neither the resting membrane potential (RMP) of layer III LEC neurons (RMP=-72.14±0.43 and -71.88±0.39 mV before and after application of CCh, respectively; n=20; P>0.4) nor their input resistance (IR) (IR=56.11±2.26 and 56.85±2.33 MΩ before and after application of CCh, respectively; n=20; P>0.1). It was reported previously that these neurons generate adapting regular firing discharges during application of a supra-threshold depolarizing current pulse which is followed by slow hyperpolarizing after-potentials (Tahvildari and Alonso, 2005). In this study, we observed that bath application of CCh suppressed the slow hyperpolarizing after-potentials appearing after a depolarizing current injection.

We found that depolarizing current injection pulses in the presence of CCh were able to trigger the development of a plateau potential that could be accompanied by post-stimulus spikes if the supra-threshold pulses were triggered

from a holding membrane potential more depolarized than -70 mV (figure 4.1A). Moreover, it was observed that from more depolarized levels (between about -65 to -60 mV) these post-stimulus spikes can generate persistent spiking activity with a stable frequency which might last for several minutes (range from 8 to 12 minutes; n=5). In the following analysis we always considered activity as persistent when we observed sustained spiking activity at a stable frequency for a duration of 40 to 60 seconds.

In the next step, we investigated the relation between the duration of the plateau potential (or post-stimulus spikes) and that of the injected current pulse. We chose injection duration as the changeable parameter, which allowed us to apply step depolarizing current pulses with a broad range of duration values. We observed that from holding membrane potentials around -65 mV in all tested neurons (n=6), application of short pulses (0.5 to 1 s) was not sufficient to trigger a plateau potential which could generate accompanying post-stimulus spikes. In addition, application of prolonged current pulses above 8 seconds induced self-terminating post-stimulus spikes (figure 4.1B). However, a 4-second supra-threshold current pulse that trigged firing frequency at 20-30 Hz was always sufficient to induce persistent activity in all tested neurons (figure 4.1B). Shorter or longer duration pulses were usually not able to induce persistent activity, but in some cases either 2-second (2 out of 6) or 8-second (1 out of 6) pulses were also able to trigger persistent activity (figure 4.1B). Thus, in further experiments presented here we always used 4-second pulses for inducing persistent spiking. Finally, we were able to completely block the activity dependent plateau potential

and associated persistent activity by bath application of the muscarinic antagonist atropine (1μM; figure 4.1C; n=4) suggesting that muscarinic receptors are mediating the generation of the persistent spiking activity in the presence of carbachol.

The observations that in layer III LEC neurons the post-stimulus spiking was self-terminating after application of a prolonged supra-threshold depolarizing current pulse (longer than 8 seconds) suggest that the persistent activity in these neurons undergoes a desensitizing or adapting process during prolonged depolarization. Thus, we decided to test the effect of application of a second depolarizing current pulse during the persistent activity. As illustrated in figure 4.2A, we observed that in a majority of recorded neurons (~70% of total recorded neurons; n=41) application of a second 4-second pulse, identical to the first pulse, was sufficient to terminate the persistent activity with a delay of 6.28 ± 0.45 s (range = 0 to 15.6 s) after termination of the second depolarizing pulse (a movie of this effect is available at http://people.bu.edu/hasselmo/BabakCell.mpg). The ability to switch the persistent spiking activity "On" and "Off" in these neurons was a robust phenomenon since it was repeatable as long as recordings were maintained. However, in some cases (~25% of total recorded neurons; n= 16) longer duration pulses (6 to 10 s) or current pulses with higher intensity (0.1 to 0.2 nA more than the first pulse) were necessary to terminate the persistent activity. We were not able to turn off the persistent activity in three recorded neurons even with longer or stronger pulses.

We measured that in neurons with the "On/Off" ability the first ("On") and second ("Off") 4-second depolarizing pulses trigged action potentials with significantly different frequencies. The mean frequencies were 21.03 ± 0.47 Hz for the "On" pulse and 23.76 ± 0.52 Hz for the "Off" pulse ($P<0.001$; n=64). For these neurons, mean frequency during the period of persistent spiking was 6.61 ± 0.24 Hz (range from 3.1 to 12.6 Hz). Interestingly, we observed that there is a very strong frequency specificity for each individual neuron (figure 4.2B). Multiple tests in a single neuron induced persistent spiking with approximately the same firing frequency for that neuron. However, different neurons in the population of neurons in layer III of the LEC are able to generate persistent activity at frequencies that cover the theta range (ranging from 3 to 12 Hz) (figure 4.2C). We also observed that if step depolarizing current pulses were sufficient to trigger persistent spiking activity, frequency specificity of the persistent activity for each individual neuron was independent of the baseline membrane potential (figure 4.2A) or the intensity of the pulse (data not shown).

We also investigated the effect of step hyperpolarizing current pulses at variable durations and intensities on persistent spiking activity evoked by prior depolarizing current pulses in these neurons. Our data indicated that application of step hyperpolarizing currents with different duration (figure 4.3A; range from 0.5 to 30s; n=8), or different intensities (range from 0.05 to 0.5 nA; n=3; data not shown) is ineffective to either reduce or change the frequency of the persistent spiking activity in all tested neurons. However, a very prolonged hyperpolarizing current pulse (above 40s) can be effective to stop the persistent activity (three out

of three tested neurons). Thus, persistent activity in these neurons is insensitive to the hyperpolarizing pulse (up to 30 second pulses), however as depicted in figure 4.3A, the evoked persistent activity still has the ability to be turned "Off" by application of a depolarizing pulse.

Since the "On" and "Off" states of the persistent activity seem to be robust phenomena among the population of layer III LEC principal neurons, in the next step we wanted to test if induction and termination of persistent activity in these neurons was also achievable by synchronized synaptic activation. These neurons are the main targets of superficial cell layers of the perirhinal cortex (Burwell and Amaral, 1998b), and electrophysiological evidence has already shown that electrical stimulation of layers II/III of the perirhinal cortex evokes mono-synaptic excitatory post-synaptic potentials with the probability of triggering action potentials in layer III LEC neurons (de Villers-Sidani et al., 2004). Figure 4.3B shows a schematic diagram showing the locations of stimulating and recording electrodes in our slice preparation. These experiments were performed in the absence of kynurenic acid and picrotoxin. Figure 4.3B illustrates (left trace) a typical initiation and termination of the muscarinic mediated persistent spiking activity in a layer III LEC neuron following synchronized electrical stimulation of the PRC layers II/III. While we were able easily to initiate persistent activity with synaptic stimulation in all tested neurons (stimulus frequency 15-20 Hz; stimulus intensity 200-300 μA; stimulus duration 4s; n=6), we recognized that termination of the persistent activity through synaptic activation required higher intensity electrical stimulation (400-500 μA, stimulus duration 4s; n=6). With higher

intensity stimulation, we were able to terminate the persistent activity in all but one neuron with synaptic stimulation.

## 4.6 Discussion

In this study, we demonstrated that individual neurons in layer III of the LEC are able to switch "On" and "Off" their persistent spiking activity due to depolarizing inputs including both intracellular current injection and synaptic stimulation. The effect depends upon muscarinic receptor activation, as it was observed in the presence of the non-selective cholinergic agonist carbachol and was blocked by the muscarinic antagonist atropine. Data presented show that activity-dependent post-stimulus spiking in layer III depends on the baseline membrane potential voltage, and also depends on the duration of the excitatory depolarizing stimuli. We observed that short excitatory stimuli (0.5 and 1s) are not sufficient to induce persistent activity. Furthermore, very prolonged duration current stimuli (8 and 16s) also induce self-terminating post-stimulus spikes. However, stimuli with moderate duration (4s) are sufficient to induce post-stimulus spikes that usually generate persistent activity.

Previous studies showed muscarinic- and activity-dependent post-stimulus spikes in principal neurons of layer II (Klink and Alonso, 1997c; Magistretti et al., 2004) and layer V (Egorov et al., 2002; Fransen et al., 2006) of the medial entorhinal cortex (MEC). It has been shown that in layer II MEC principal neurons the post-stimulus spikes are always self-terminating and can last only up to a couple of tens of seconds (15.24 ± 0.97 and 29.52 ± 7.57s for

pyramidal and stellate neurons, respectively) (Magistretti et al., 2004). In contrast to those data, our data in layer III of the LEC show the existence of post-stimulus spiking which persists almost for an indefinite period of time (tested for many minutes). Graded persistent activity has been observed in single principal neurons of layer V of the MEC (Egorov et al., 2002; Fransen et al., 2006). In those neurons, it has been shown that the frequency of the persistent activity is able to be graded up and /or down depending on the nature of the stimuli and that a longer duration supra-threshold depolarizing pulse induces persistent activity at higher frequency in comparison with the frequency that is induced with a shorter duration pulse (Fransen et al., 2006). In contrast to the graded persistent activity, our current studies clearly show that layer III neurons can generate neither graded persistent activity nor persistent activity at a higher frequency following application of a prolonged step depolarizing current pulse.

We also observed that each individual layer III LEC principal neuron has very pronounced frequency specificity, which can be induced in repeated tests, and that the different frequencies of persistent activity for different neurons in the population of cells cover the theta frequency band. More interestingly, our data also indicate that the persistent activity in these neurons, in most cases, can be terminated following application of a second excitatory stimulus identical in intensity and duration to the first stimulation. Thus, the persistent activity in these neurons is able to toggle between two reliable states, one a state of persistent spiking activity ("On") and the other a silent ("Off"). In this respect these neurons can behave like a toggle switch by turning "On" and "Off" the activity-dependent

persistent spiking activity during muscarinic receptor activation. Furthermore, the persistent activity in these neurons can not be terminated by application of hyperpolarizing pulses. Switching "On" and "Off" the persistent activity in layer III neurons could be a plausible physiological mechanism involved in memory function, since we were able to induce and terminate persistent spiking by synaptic activation of superficial cell layers of the perirhinal cortex. Taken together, these data indicate that information in terms of persistent activity can be transferred easily between the LEC and PRC. This is consistent with neurophysiological, anatomical and lesion studies that indicate explicitly the importance of the integrity of the EC and highly inter-connected adjacent cortical regions in the communication between the neocortex and the hippocampus upon which long-term memory formation depends (reviewed in Buzsaki, 1996).

Recent studies have also shown that neurons in other brain areas can switch "On" and "Off" their electrical activity (Shu et al., 2003; Loewenstein et al., 2005). Loewenstien *et al.*, (2005) showed the transition of the cerebellar purkinje cells in an *in-vivo* preparation between hyperpolarized ("Down State") and stable depolarized states ("Up State"). In contrast to our findings; however, in that study termination of depolarized states was triggered by hyperpolarizing pulses. Turning "On" and "Off" the balance of recurrent synaptic activity has been observed in *in-vitro* prefrontal cortex circuits (Shu et al., 2003). That study showed how cortical "Up-states" and "Down-states" can be generated by a barrage of synaptic inputs in ferret slices in a modified extracellular Ringer solution. That mechanism does not contradict the parallel intrinsic mechanism

suggested here. Our intrinsic mechanism would add to the stability of network function. It is worthy to be noted that in those experiments the duration for each stable state was at most a couple of seconds. However, the intrinsic mechanism presented here would allow the network to maintain "Up-states" for expected periods of many seconds or minutes consistent with behavioral time-scales.

The mechanisms for sustained activity described here could play an important role in maintaining working memory for sensory stimuli in delayed match-to-sample tasks, and could also enhance encoding into long-term memory. This intrinsic mechanism for persistent spiking could underlie the delay period spiking observed during performance of delayed match and delayed non-match to sample tasks in rats and monkeys (Suzuki et al., 1997; Young et al., 1997). The dependence of persistent spiking on cholinergic modulation is consistent with cholinergic blockade impairing performance on delayed match-to-sample tasks (Penetar and McDonough, 1983). Because these intrinsic cellular mechanisms allow persistent spiking without prior synaptic modification, it could be particularly important for maintenance of novel stimuli. This is consistent with data showing that selective lesions of the cholinergic innervation of entorhinal cortex selectively impair delayed non match-to-sample function for novel but not familiar odors (McGaughy et al., 2005). In human subjects, maintenance and encoding of novel stimuli in a delayed match-to-sample task correlates with entorhinal and perirhinal activity during the delay period, as measured using fMRI (Schon et al., 2004), and this delay period activity is reduced by muscarinic blockade with scopolamine (Schon et al., 2005). Thus, persistent activity

provides an important mechanism of working memory for novel stimuli (Hasselmo and Stern, 2006).

While persistent activity is important for working memory, it requires mechanisms for termination of activity associated with repeated sequences of sensory input, to allow effective representation of new relations between events during an episode. These mechanisms for termination could be particularly relevant to experimental data on neural activity during delayed match to sample tasks (Suzuki et al., 1997). In this task, the subject must: 1) maintain memory of the sample stimulus during the delay period but not the inter-trial interval, 2) ignore intervening nonmatch distractors, 3) generate a response to the final stimulus (match stimulus), and 4) finally during the inter-trial interval must forget in order to prepare for a new sample stimulus on the next trial. The neural properties described here provide a cellular mechanism useful for this task. As shown here, the spiking activity associated with the sample will resist hyperpolarization caused by lateral inhibition induced by presentation of distractor stimuli during the delay period. When the test stimulus appears again as a match stimulus, the response can be generated, and the repetition would shut off persistent activity, allowing the system to respond to a new sample stimulus. This indicates the functional importance not only in the ability to activate persistent spiking, but in the ability of synaptic activation to toggle neurons between the plateau state and the resting state.

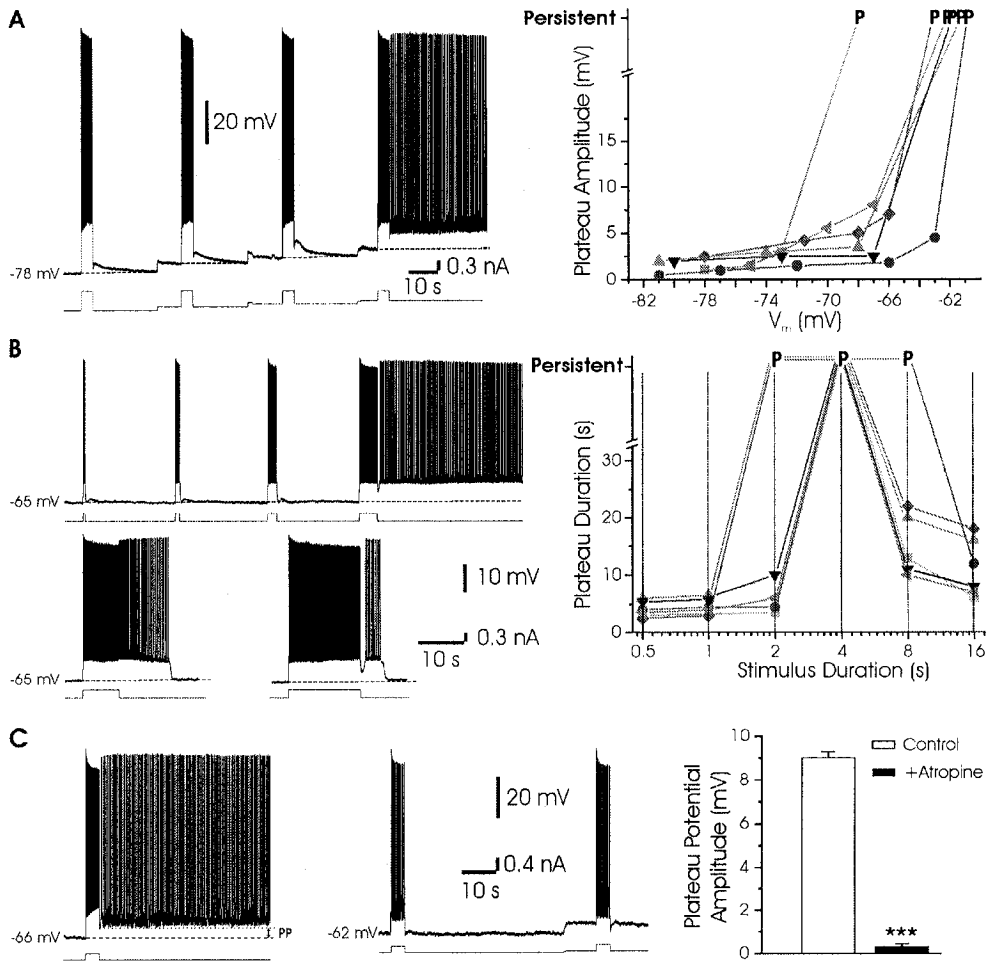


**Figure 4. 1.**

**Muscarinic-mediated persistent activity in layer III LEC neurons.** In this figure and all the subsequent figures recordings were performed with continuous bath perfusion of carbachol (10 μM) A. Induction of persistent activity is voltage dependent. Left, Membrane potential (upper trace) recorded during current injection (lower trace) that shows the spiking response to depolarizing steps at different membrane potentials. Note that persistent spiking activity appears after

the depolarizing step at the highest baseline potential (at this low temporal resolution, spiking appears as solid blocks). Right, Plot of plateau potential amplitude *vs.* baseline membrane potential in five different recorded neurons (different colors and symbols for different neurons). Most neurons show persistent activity (P) after current steps from baseline over ~ -68 mV. B. Duration of step depolarization current pulse has a strong influence on the duration of the plateau potential and post-stimulus spikes. Left, Membrane potential and associated current traces during stimulus pulses of 0.5, 1, 2, 4 (top) and 8 and 16 second duration (bottom). Persistent spiking appears after the 4 sec. pulse. Post-stimulus spiking terminates soon after 8 and 16 sec pulses. Right, Plot of plateau (or post-stimulus spiking) duration *vs.* stimulus duration in six different recorded neurons. All neurons show persistent activity (P) after 4 sec. pulses, and some neurons show the persistent activity after 2 and 8 sec. pulses. Different colors and symbols represent different neurons C. Persistent activity is mediated through muscarinic receptors. Membrane potential and associated current traces in carbochol condition (left traces) and after addition of atropine (right traces). Under our regular CCh conditions, a step depolarizing current pulse is followed by a depolarizing plateau potential (PP, arrow) and persistent firing that was fully blocked after addition of atropine (1μM) to the bath solution. Right, Bar graph shows the mean ± SE amplitude of the PP recorded under both conditions (*** denotes $P<0.001$; $n=4$).

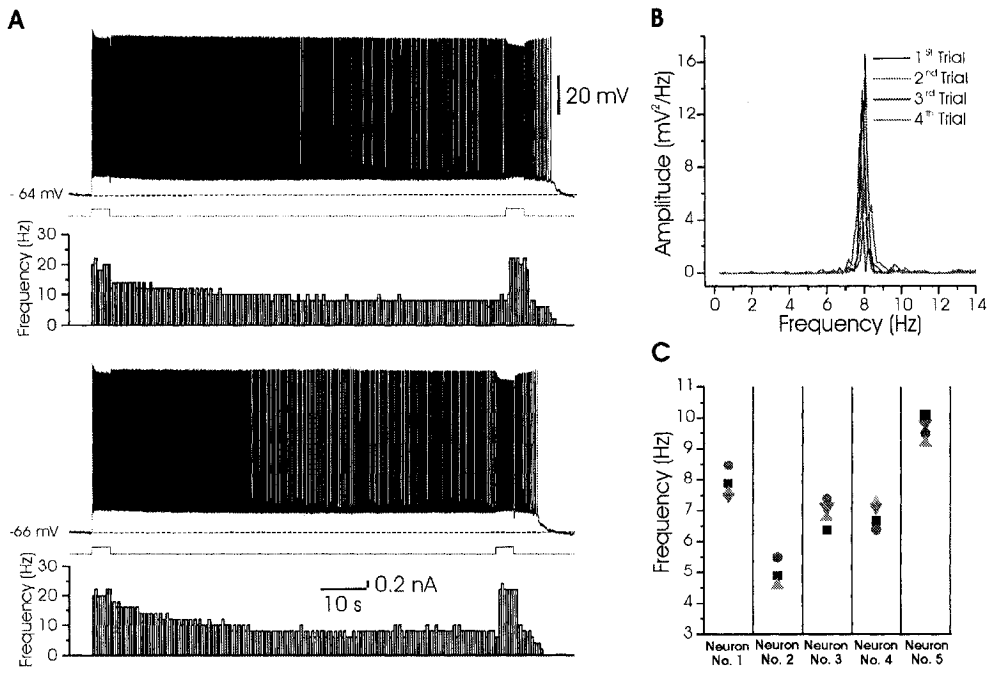


**Figure 4. 2.**

**Switching "On" and "Off" persistent activity in layer III LEC neurons.** A. Two typical recordings of membrane potential, current traces and the corresponding peri-stimulus spiking rate histogram (bin width=500ms) for a layer III LEC neuron. B. Power spectrum plot for the persistent activity of the same neuron shown in A for four different trials. Note there is a clear peak for a specific frequency in different trials C. Frequency of persistent activity is plotted for five different neurons in which "On" and "Off" states were repeated for several trials. Different colored symbols represent different trials for each individual neuron. While individual neurons show strong frequency specificity during sustained activity, the group of neurons displays frequencies that cover the theta range.

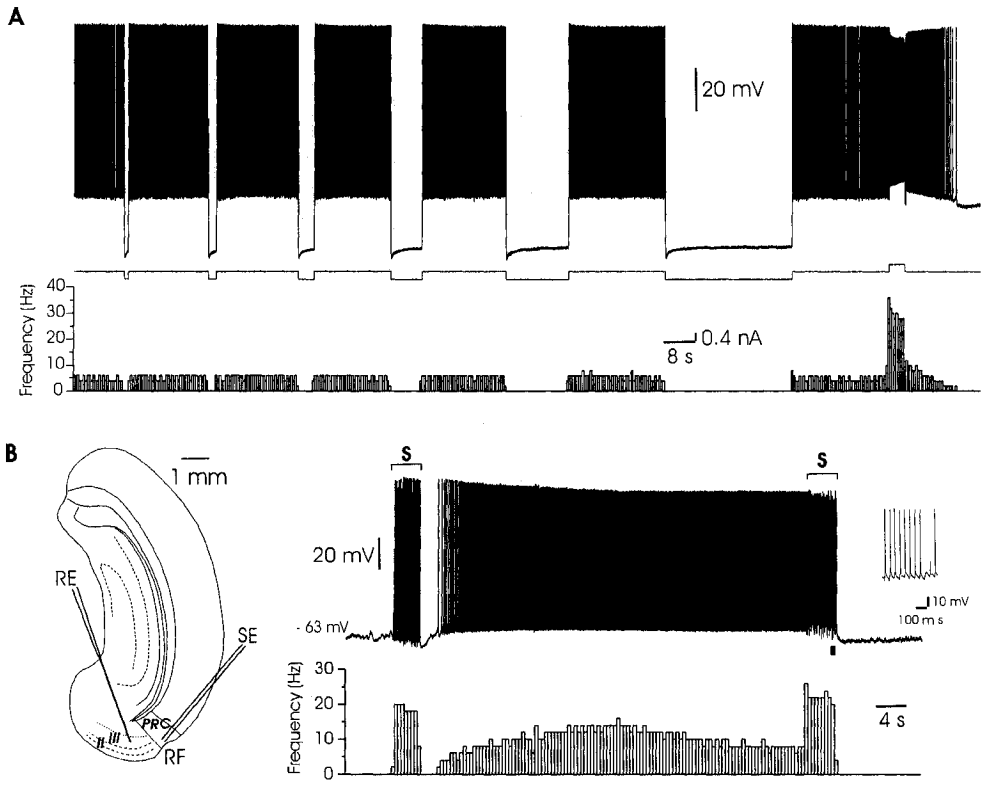


**Figure 4. 3.**

A. Persistent activity in layer III LEC neurons is resistant to a hyperpolarizing current pulse. Upper trace shows membrane potential of a neuron that previously received input inducing persistent spiking. The membrane potential is shown during a series of hyperpolarizing current injections (middle trace) of different durations (up to 32 seconds in this case). A peri-stimulus spike rate histogram (bin width=500ms) is shown at bottom indicating that the hyperpolarizing pulses can not reduce the frequency of the persistent activity or terminate it. However a step depolarizing pulse (at far right) was able to switch "Off" the persistent activity. Final membrane potential is -60 mV. B. Switching "On" and "Off" persistent activity by synaptic stimulation. In these experiments no synaptic blockers were

presented (n=6). Left, Schematic diagram shows locations of stimulating (SE) and recording (RE) electrodes in the slice preparation. RF and PRC represent rhinal fissure and perirhinal cortex, respectively. Right, Membrane potential trace and peri-stimulus spike rate histogram (bin width=500ms) showing induction and termination of the persistent activity in layer III LEC neuron by synaptic activation of PRC superficial layers. Inset corresponds to the section indicated by the black bar (below) showing generation of post-synaptic excitatory potentials and accompanying action potentials in layer III LEC neuron following synchronized electrical stimulation of the PRC at larger time scale. For clarity stimulus artifacts are removed. S represents period of synaptic stimulation.

**Movie 1.** Available at http://people.bu.edu/hasselmo/BabakCell.mpg. Oscilloscope display of the membrane potential of a single layer III LEC neuron during switching "On" and "Off" of persistent spiking activity with step depolarizing pulses. CCh, kynurenic acid and picrotoxin were presented.

# CHAPTER 5: Ionic basis of "On" and "Off" Persistent Activity in Layer III Lateral Entorhinal Cortical Principal Neurons

## 5.1 Preface

In chapter four, I provided the first evidence that principal neurons in layer III of the lateral entorhinal cortex (LEC) can generate "On" and "Off" persistent activity in the presence of a cholinergic agonist. It was observed that, in these neurons, persistent activity can both be induced and terminated in response to a brief (2-4 s) excitatory stimulus. Layer III LEC principal neurons exposed to a cholinergic agonist are therefore capable of producing a self-induced increase in firing rate that might contribute to delay firing, and to reset themselves in response to consecutive sensory stimuli. In this chapter, I performed experiments designed to clarify the intrinsic ionic mechanisms involved in the onset and termination of persistent firing in layer III LEC principal neurons by means of intracellular recording with sharp micro-electrode recordings.

## 5.2 Abstract

Principal neurons in layer III of the rat LEC generate a self-sustained plateau potential and persistent action potential firing following the application of a brief supra-threshold excitatory stimulus delivered in the presence of the muscarinic receptor agonist carbachol. This persistent activity can be terminated by application of a second excitatory stimulus, and these cells can be repeatedly

toggled between "On" and "Off" states by consecutive excitatory stimuli. The ionic mechanisms that underlie the production of "On" and "Off" states in Layer III LEC neurons are unknown, but appear to involve activity-dependent conductances, since they can be initiated by trains of action potentials evoked by either depolarizing current pulses applied to the cell, or by repetitive activation of excitatory synaptic inputs. In this study we obtained intracellular recordings from rat layer III LEC neurons *in-vitro*, and a series of pharmacological and ionic substitution experiments were performed to identify mechanisms involved in the induction and termination of persistent firing. Our data indicate that initiation of the "On" state depends on spike-evoked calcium influx and subsequent activation of calcium-activated non-selective current. Moreover, we show that termination of persistent firing in response to an excitatory stimulus can be blocked by tetraethylammonium or iberiotoxin, suggesting that the activation of calcium activated potassium current mediated by BK channels is required to induce the "Off" state.

## 5.3 Introduction

Previous studies in animals and humans have indicated that neurons of the LEC may generate a persistent increase in electrical activity following the presentation of a sensory stimulus (Suzuki et al., 1997; Young et al., 1997; Stern et al., 2001). In monkeys, for example, an increase in neural activity is observed during the delayed match-to-sample task, in which a subject is required to recognize that a second (i.e. "test") stimulus is identical to a "sample" sensory

stimulus after a brief delay (Suzuki et al., 1997). Neurophysiological (reviewed in Goldman-Rakic, 1995) and modeling studies (Fransen et al., 2002; Fransen et al., 2006) have suggested that this sustained activity may be important for maintaining information related to the sample sensory stimulus during the delay phase of the task. Interestingly, deafferentation of the cholinergic input to the entorhinal cortex significantly impairs the performance of short-term memory tasks (McGaughy et al., 2005; Turchi et al., 2005). Moreover, functional magnetic resonance imaging studies have revealed that activation of the medial temporal lobe during such tasks is reduced by systemic administration of scopolamine, a muscarinic cholinergic antagonist (Schon et al., 2005). These data suggest that generation of post-stimulus sustained activity in entorhinal cortex neurons may require cholinergic activation. Indeed, we have recently shown that principal neurons in layer III of the rat LEC can generate self-sustained persistent activity in presence of a cholinergic agonist (Tahvildari et al., 2007). This increase in electrical activity is expressed in the form of an after-discharge that is driven by a depolarizing plateau potential following a supra-threshold excitatory stimulus. Interestingly, post-stimulus sustained firing in LEC layer III principal neurons could be induced by triggering action potentials via injection of a depolarizing current pulse.

In order to be available for repeated trials, the increase in activity observed during the delay phase in LEC principal neurons should be terminated upon presentation of the test stimulus. Interestingly, we have shown that persistent firing initiated by a brief excitatory stimulus can be terminated by application of a

second excitatory stimulus. Moreover, both the "On" and "Off" phases of this activity could also be induced by a brief (4s) repetitive activation (~20 Hz) of excitatory synapses upon electrical stimulation of the perirhinal cortex, suggesting that toggled On/Off firing could be promoted by this pathway *in-situ* .

Previous studies in other cortical neurons have indicated that activation of a calcium dependent non-selective cation (CAN) current mediates the onset and maintenance of plateau potentials and after-discharges induced by depolarizing pulses applied in the presence of cholinergic agonists (Fraser and MacVicar, 1996; Haj-Dahmane and Andrade, 1996; Klink and Alonso, 1997b; Egorov et al., 2002; Shalinsky et al., 2002; Magistretti et al., 2004). Whether CAN channels are also involved in genesis of the persistent firing in layer III LEC principal neurons remains unknown. In this study we performed pharmacological and ionic-substitution experiments to identify ionic mechanisms contributing to the induction and termination of muscarinic receptor-dependent persistent firing in layer III LEC principal neurons.

## 5.4 Materials and methods

### 5.4.1 Preparation of brain slices

All experimental procedures were approved by the McGill University Animal Care Committee and were in compliance with the guidelines of the Canadian Council on Animal Care. Conventional sharp micro-electrode intracellular recordings were performed on brain slices obtained from adult Long-Evans rats (Male, 150-250 grams, Charles River Canada, Saint-Constant, Qc,

Canada). Semi-coronal *in-vitro* rat brain slices (450 μm thick) were prepared following the protocol explained in detail previously (de Villers-Sidani et al., 2004; Tahvildari and Alonso, 2005).

### 5.4.2 Recording procedures, drugs and analysis

All drugs and chemicals were purchased from Sigma Chemical Co. (Oakville, ON, Canada), except iberiotoxin (IBTX) which was purchased from Tocris Cookson Ltd. (Ellisville, MO). Carbachol (CCh), tetraethyl-ammonium chloride (TEA) and cadmium chloride ($CdCl_2$) were bath applied at the desired concentrations by dilution of stock solutions made in distilled water. Flufenamic acid (FFA) and IBTX were bath applied at the desired concentrations by dilution of stock solutions made in dimethyl sulfoxide (DMSO; Sigma) and distilled water, respectively. The final concentration of DMSO did not exceed 0.1%. Normal Ringer solution was prepared for daily requirements and contained (mM): 124 NaCl, 3 KCl, 1.6 $CaCl_2$, 1.8 $MgSO_4$, 26 $NaHCO_3$, 1.25 $NaH_2PO_4$ and 10 glucose [pH was adjusted at 7.4 by continuous application of $O_2/CO_2$ (95/5%)]. Since the muscarinic phenomenon studied here does not desensitize (Tahvildari et al., 2007), all neurons were directly impaled in the presence of CCh (10 μM). All recordings were also performed in the presence of Kynurenic acid (2 mM) and picrotoxin (100 μM) to inhibit glutamatergic and GABA-mediated neurotransmission, respectively.

Recordings were performed on slices maintained in an interface perfusion chamber (Fine Science Tools Inc., North Vancouver, BC, Canada). Borosilicate

glass electrodes (World Precision Instruments Inc., Sarasota, FL, USA) were pulled on a Brown Flaming puller (model P-97, Sutter Instruments Co., Novato, CA, USA), and backfilled with 2 M $K^+$-acetate and 2% biocytin (tip resistance of 80-120 MΩ). Electrical signals were amplified using an Axoclamp 2B amplifier (Axon Instruments Inc., Union City, Ca, USA), low-pass filtered at 5kHz, digitized at 10 kHz via a Digidata 1320 interface (Axon Instruments Inc.), and stored on a Pentium computer using Axoscope software (Axon Instruments Inc.) for off-line analysis. The location of each recording was determined by biocytin staining according to a protocol explained previously (Tahvildari and Alonso, 2005).

Electrophysiological data were analyzed using Clampfit 9.0 (Axon Instruments Inc.), and graphs were created using Origin 6.0 (Microcal Software Inc., North Hampton, MA, USA). Average values are expressed as means ± SE. Statistical significance was evaluated by means of the two-tail Student's *t*-test for paired data.

## 5.5 Results

Intracellular recordings with sharp microelectrodes were made from 34 pyramidal neurons in layer III of rat LEC slices maintained *in-vitro* in the continuous presence of CCh (10μM, see methods). The baseline membrane potential of these neurons was adjusted to a value between -65 and -60 mV by injection of continuous current (+ 0.02 to 0.15 nA). As reported previously, these neurons displayed a depolarizing plateau potential and persistent firing following

the application of a supra-threshold (0.1 to 0.3 nA, 4s) depolarizing current pulse (Tahvildari et al., 2007).

Previous studies in other cortical neurons have shown that induction and maintenance of muscarinic-receptor-dependent, post-excitation plateau potentials and after-discharges depend on influx of extracellular calcium through voltage-gated calcium channels (Fraser and MacVicar, 1996; Klink and Alonso, 1997b; Haj-Dahmane and Andrade, 1998; Egorov et al., 2002). We therefore examined if calcium influx was required for these features in LEC layer III neurons. Bath application of $CdCl_2$ (400 μM), a broad spectrum blocker of voltage-gated calcium channels, significantly inhibited the depolarizing plateau potential (10.62±0.94 mV in control *vs.* -0.4±0.18 mV in $Cd^{2+}$; n=8; P<0.001), and the accompanying persistent activity, that followed a depolarizing pulse (figure 5.1A). Similarly, the post-stimulus depolarizing plateau potential, and accompanying persistent activity, were eliminated in a $Ca^{2+}$-free solution containing 1mM EGTA and 4 mM $Mg^{2+}$ (10.33±1.22 mV in control *vs.* -0.25±0.28 mV in $Ca^{2+}$-free; n=6; P<0.001; figure 5.1B). Moreover, in three neurons impaled with micro-electrodes containing 200 mM EGTA, the ability to generate post-stimulus plateaus and after-discharges was gradually abolished over a period of 20-30 minutes following the impalement (figure 5.1C). These data suggest that the onset of persistent firing following an excitatory stimulus depends on influx of calcium through voltage-gated channels and on its accumulation inside the neuron.

Previous studies have shown that CAN channels commonly mediate the spike- and burst-evoked plateau potentials and after-discharges of neurons in different brain areas (Haj-Dahmane and Andrade, 1998; Egorov et al., 2002; Ghamari-Langroudi and Bourque, 2002). Since the induction of the "On" state of layer III LEC On/Off neurons is calcium-dependent, we next examined the possibility that a CAN current contributes to the generation of post-stimulus plateau potentials and persistent activity. As illustrated in figure 5.2, bath application of FFA (100 μM), a blocker of the CAN current (Partridge and Valenzuela, 2000), significantly reduced the depolarizing plateau potential (11.5±0.92 mV in control *vs.* 1.25±0.28 mV in FFA; n=6; $P<0.001$) and persistent activity that followed a depolarizing pulse.

The termination of on-going plateau potentials and persistent activity in response to the application of depolarizing pulse delivered during the "On" phase (i.e. onset of the "Off" phase), could be mediated by an activity-dependent reduction of the inward CAN current (e.g. Magistretti et al., 2004), or to the activation of an activity-dependent outward current. Although we did not examine the potential involvement of a down-regulation of the CAN current in the present study, we examined the possibility that calcium-activated potassium conductances contribute to the "Off" phase. Previous studies have shown that low concentrations of TEA (e.g. 1mM) can block calcium-activated potassium currents that flowing through large (i.e. BK) and intermediate conductance (i.e. IK) channels (Vogalis and Goyal, 1997). Under control conditions, application of a depolarizing pulse caused the emergence of a plateau potential and persistent

firing. In all of the neurons tested in this study (n=10), application of a second depolarizing pulse ~60 s after the onset of the after-discharge caused an immediate reduction in the amplitude of the plateau potential. This was followed by a further reduction of the plateau potential, a gradual decrease in firing frequency and, ultimately, by a complete cessation of firing (figure 5.3A). Bath application of 1 mM TEA abolished the effectiveness of a second depolarizing pulse to terminate the sustained activity (figure 5.3A). Indeed, whereas persistent firing always stopped within 16s of the second pulse under control conditions (figure 5.3A), neurons exposed to TEA continued to fire at a rate equivalent to the firing frequency observed prior to the second pulse (pre-pulse firing rate 7.58 ± 0.6 Hz *vs.* firing rate at 32s post-pulse 7.2 ± 0.55 Hz; n=7; P>0.05). Interestingly, the pre-pulse firing rate (i.e. basal rate of activity during persistent activity) was not affected by TEA (control 7.35 ± 0.49 Hz *vs.* TEA 7.58 ± 0.6 Hz; P>0.05).

Since TEA can block both BK and IK channels (Vogalis and Goyal, 1997), we examined the effects of IBTX, a specific BK channel antagonist. As illustrated in figure 5.3B, bath application of 100nM IBTX also abolished the ability of LEC layer III principal neurons to enter the "Off" phase following application of either single, or multiple, depolarizing pulses (figure 5.3B, n=3). Similar to TEA experiments, the persistent firing always stopped within 16s of the second pulse under control conditions (figure 5.3B), however, cells in presence of IBTX continued to fire at a rate equivalent to the firing frequency observed prior to the second pulse (pre-pulse firing rate 10.36±1.30 Hz *vs.* firing rate at 32s post-pulse 10.06 ± 1.54 Hz; n=3; P>0.05). Furthermore, the pre-pulse firing rate (i.e.

basal rate of activity during persistent activity) was not affected by IBTX (control 9.6± 1.92 Hz *vs.* IBTX 10.36±1.30 Hz).

## 5.2 Discussion

Recent studies have shown that a variety of neurons in the central nervous system can operate as toggle switches, where the electrical activity of the cell can be consecutively turned "On" and "Off" by identical stimuli (e.g. Shu et al., 2003; Loewenstein et al., 2005; Tahvildari et al., 2007). This property may play an important role in the short-term encoding or storage of information during signal processing in various parts of the brain. Neurophysiological and computational studies have shown that this On/Off behavior can be expressed through different mechanisms. For example, in ferret prefrontal cortical neurons, switching between "On" and "Off" states can be promoted by changing the proportional balance of excitation and inhibition generated through local recurrent synaptic connections (Shu et al., 2003). In contrast, the "On" and "Off" states of cerebellar Purkinje cells are each stabilized by intrinsic ionic conductances and On/Off transitions can be induced by stimuli which alternately promote changes in membrane potential toward depolarized and hyperpolarized voltages (Loewenstein et al., 2005). A recent study has shown that principal neurons in layer III of the LEC also display On/Off transitions in response to brief excitatory stimuli (Tahvildari et al., 2007), where it may play an important role in the encoding and storage of short-term memory (Goldman-Rakic, 1995). This phenomenon was retained even when glutamatergic and GABA-ergic synaptic transmission was blocked by

kynurenic acid and picrotoxin suggesting that On/Off transitions is due to an intrinsic process. However, the mechanisms supporting this behavior were not defined.

The results of this study show that induction of the "On" state, and maintenance of persistent firing, in pyramidal neurons of layer III of the LEC is inhibited by the blockade of $Ca^{2+}$ influx. Indeed, lowering extracellular $Ca^{2+}$, or blocking voltage-gated calcium channels with $Cd^{2+}$, prevented the emergence of plateau potential and the persistent firing following application of depolarizing pulse. Moreover, this process was also abolished by intracellular injection of EGTA. These observations indicate that the "On" state is triggered by the influx and accumulation of intracellular $Ca^{2+}$ that occurs during the action potentials evoked by depolarizing stimulus. Our experiments also showed that post-stimulus plateau potentials and persistent firing could be abolished by bath application of FFA, an inhibitor of CAN channels (Partridge and Valenzuela, 2000). Taken together, these data indicate that transition from the "Off" to the "On" state is due to the depolarizing effect of the inward current mediated by CAN channels that are activated in response to calcium influx during a depolarizing stimulus.

We also examined the basis for transitions from "On" to "Off" states in layer III LEC pyramidal neurons. Our data showed that blockade of BK channels, either by application of TEA or IBTX, prevented the suppression of plateau potentials and persistent firing that was normally induced by the application of a depolarizing stimulus in control solutions. Thus, an activity-dependent activation of BK channels is required to promote transitions from "On" to "Off" states in

these neurons. Indeed, immuno-histochemical and *in situ* hybridization studies have indicated that BK channels are highly expressed in the outer layers (i.e. layers II and III) of the cortex (Wanner et al., 1999), including the LEC (Knaus et al., 1996).

Our results suggest that depolarizing pulses promote transitions from the "Off" state to the "On" state by activating CAN channels, and transitions from the "On" state to the "Off" state by activation of BK channels. Although the mechanism by which identical depolarizing current pulses differentially regulate the extent to which CAN and BK channels are activated during the "On" or "Off" states is unknown, a number of factors are worthy of consideration. For example, it is possible that depolarizing stimuli applied during the "On" state activate CAN channels less effectively than during the "Off" state because they are already maximally activated. Alternately, CAN channels may be down regulated by depolarizing pulses applied during the "On" phase because of a higher pulse-induced increase in intracellular calcium concentration ($[Ca^{2+}]_i$) under these conditions (Magistretti et al., 2004) . The latter hypothesis is supported, in part, by the observation that significantly more action potentials are evoked during a depolarizing pulse applied during the "On" phase than during an identical current pulse delivered during the "Off" phase (Tahvildari et al., 2007), and see also figure 3 panels A and B, and by the higher basal $[Ca^{2+}]_i$ that may prevail during persistent firing. Moreover, it is possible that the higher $[Ca^{2+}]_i$ induced by depolarizing pulses applied during the "On" state, relative to that induced during the "Off" state, may activate BK channels more strongly under these conditions.

Indeed, the mean steady state firing frequency observed during "On" states recorded in the absence and presence of TEA or IBTX were not significantly different with those during control condition, suggesting that BK channels are not activated during persistent firing. Stronger activation of these channels in response to a depolarizing pulse applied during the "On" state may therefore promote transition to the "Off" state. Additional studies are needed to clarify the dynamics of currents mediated by CAN and BK channels during On/Off firing in currents in pyramidal neurons of layer III in the LEC.

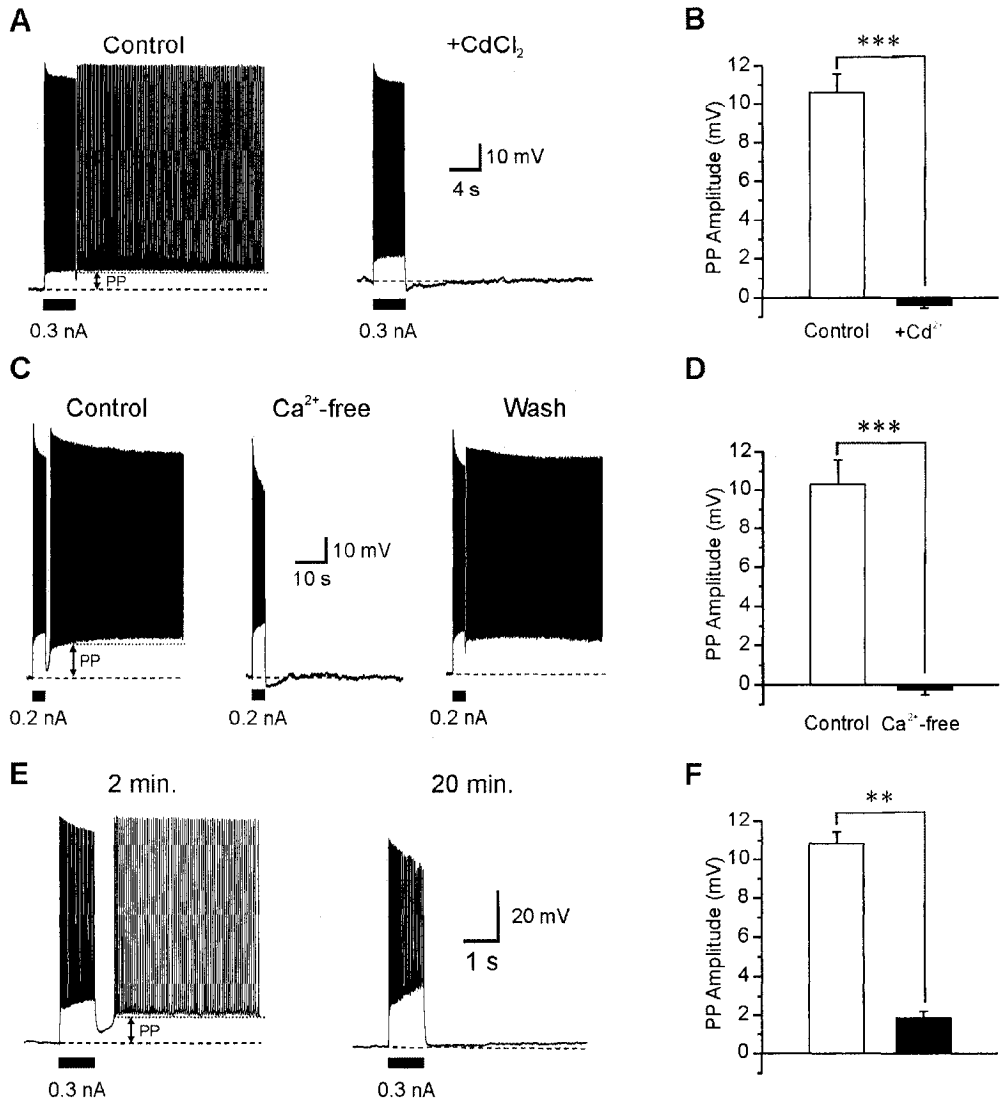


**Figure 5. 1.**

**The "On" state is a calcium dependent process.** In all panels voltage traces show the effects of depolarizing current pulses (bars) on LEC layer III pyramidal neurons recorded in the presence of 10 μM CCh. Dashed lines show baseline voltage. A. Under the control conditions the spike-train induced by the current pulse is followed by depolarizing plateau potential (PP, arrow) and persistent firing. Following addition of $CdCl_2$ the cell still fire action potentials in response

to the pulse, but the PP and persistent firing were eliminated. B. Bar graph shows the mean ± SE (n=8) amplitude of the PP recorded under both conditions (*** denotes P<0.001). C. As observed in the presence of cadmium (A) the post-pulse PP and persistent firing were abolished by removal of extracellular calcium ($Ca^{2+}$-free). D. Bar graph shows the mean ± SE (n=6) amplitude of the PP recorded under both conditions (*** denotes P<0.001). E. Recording obtained from a neuron impaled with a micro-electrode containing 200 mM EGTA. The two panels show the effects of depolarizing pulses applied 2 minute (left) and 20 minute (right) following impalement. Note after-discharges were eliminated after 20 minute F. Bar graph shows the mean ± SE (n=3) amplitude of the PP recorded at 2 and 20 min. after impalement (** denotes P<0.01). Intitial membrane potential in A, C and E is -60, -63 and -64 mV.

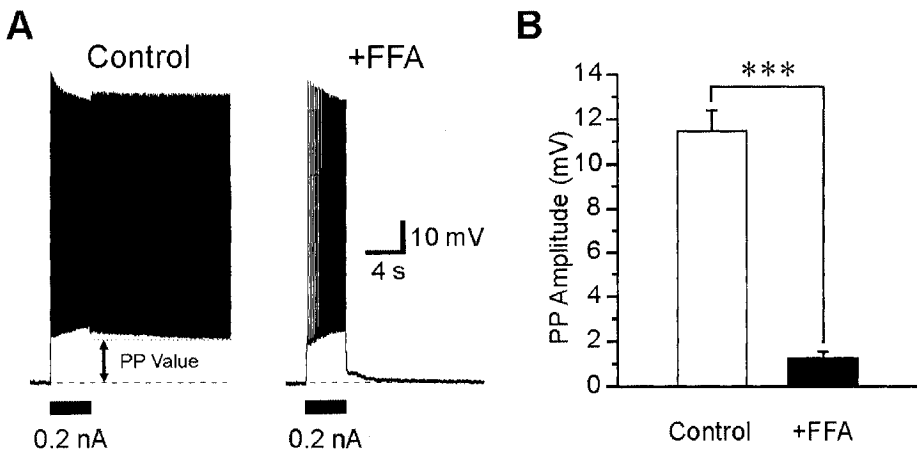


**Figure 5. 2**

**"Off"-"On" transitions are mediated by CAN channels.** A. Intracellular recordings of membrane voltage (upper traces) show the effects of depolarizing current pulses (lower bars) on firing in a layer III LEC pyramidal neuron recorded under control conditions (left) and in the presence of 100 μM FFA (right). CCh (10 μM) was present throughout the recording. Dashed lines show baseline voltage (initial membrane potential in A is -66 mV). Note that the post-pulse plateau potential (PP, arrow) and persistent firing are inhibited by FFA. B. Bar graph shows the mean ± SE (n=6) amplitude of the PP recorded under both conditions (*** denotes $P<0.001$).

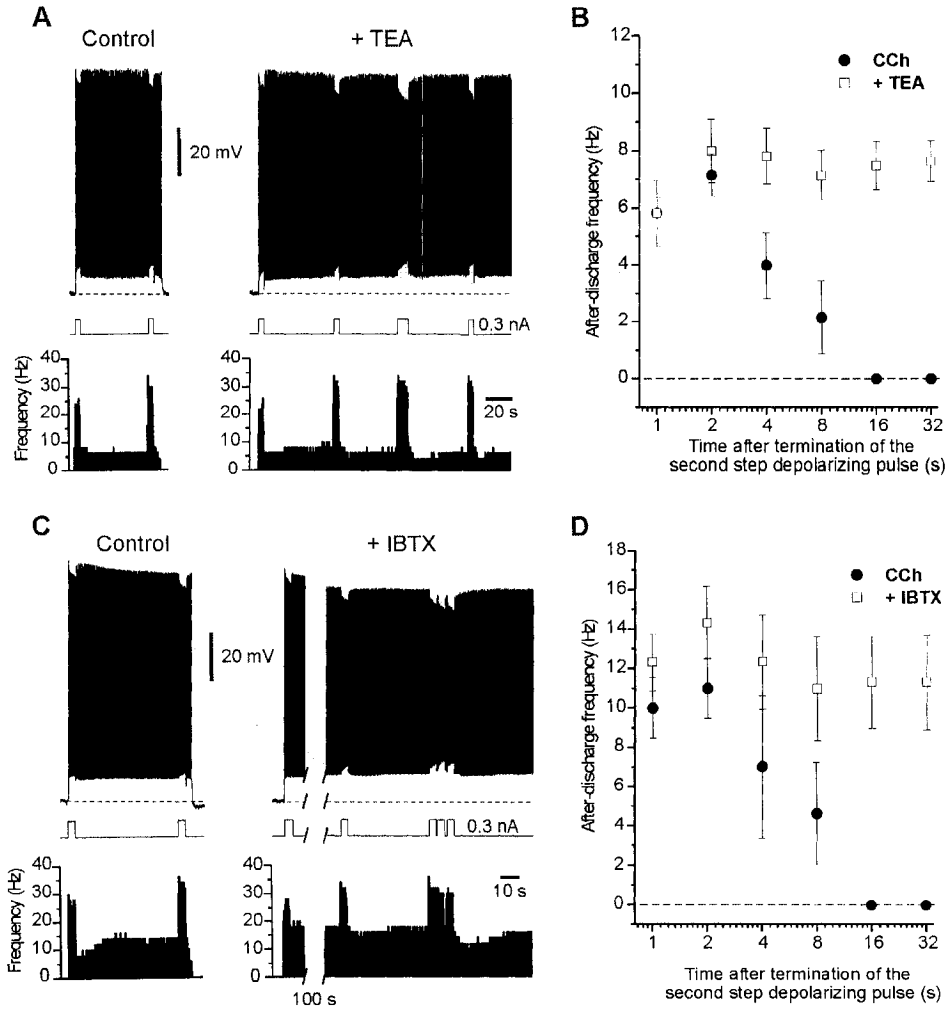


**Figure 5. 3**

**"On"-"Off" transitions are mediated by BK channels.** CCh (10 μM) was present in all conditions and dashed lines show baseline voltage. A. Intracellular recordings of membrane voltage (upper traces) and firing frequency (lower traces, bin width 500 ms) observed from a layer III LEC pyramidal neuron during current pulses (middle traces) injected under control conditions (left) and in the presence

of 1 mM TEA (right). Pulses applied during the "On" state fail to suppress persistent firing in the presence of TEA. Note that depolarizing pulses applied during the "On" state induce more action potential than those applied during the "Off" state under both conditions. B. Plots show the mean ± SE (n=7) frequency of firing observed at various time points following the application of a depolarizing pulse delivered during the "On" state under control conditions and in the presence of TEA. For this analysis, data were systematically obtained from pulses delivered ~ 60 s following the onset of the "On" state, and identical pulses were used for this comparison in the absence and presence of drug. C. Recording from another neuron (layout of traces as in A) shows the effects of 100 nM IBTX. Note that pulses applied during the "On" state fail to suppress persistent firing in the presence of IBTX. D. Plots show the mean ± SE (n=3) frequency of firing observed at various time points following the application of a depolarizing pulse delivered during the "On" state under control conditions and in the presence of IBTX. Initial membrane potential is A and C is -62 and -63 mV.

# CHAPTER 6: General Discussion

## 6.1 Summary

The experimental results reported in this thesis were obtained through a series of complementary research projects that were designed to increase our understanding of the contribution of the PRC-LEC circuit in MTL function (see result sections of chapters 2, 3, 4 and 5). They provide the first evidence that: (i) there is significant and reciprocal mono-synaptic excitatory interconnectivity between the PRC and LEC, (ii) principal neurons of layer II of the LEC possess heterogeneous intrinsic electrophysiological and morphological properties, whereas those in layer III display more homogenous properties, (iii) principal neurons of layer III of the LEC behave as toggle switches in the presence of a cholinergic agonist, switching between "On" and "Off" firing modes in response to brief excitatory stimuli, and (iv) transitions from the "Off" to the "On", and from the "On" to the "Off" states depend on activity dependent activation of CAN and BK channels, respectively. Novel findings related to each study were discussed separately (see discussion sections of chapters 2, 3, 4 and 5). In this final chapter, I will provide an updated discussion of my results that takes into account other recent findings that have been published concerning the functional organization of the PRC-LEC circuit (sections 6.2 and 6.3).

## 6.2 Reciprocal connectivity between the PRC and LEC

As explained in the introduction (section 1.3), long-term declarative memory depends on bidirectional communication between the NC and HC. Neuroanatomical studies, also reviewed in the introduction (section 1.4.1), have suggested that such communication occurs bi-directionally, through a sequence of MTL structures involving the PRC and LEC. Specifically, it is hypothesized that information flows in bi-directional NC ↔ PRC ↔ LEC ↔ HC circuits. Thus the PRC and LEC are hypothesized to serve as the first and second order relays, in the NC to HC pathway (see figure 1.1 and section 1.4.1). Although electrophysiological studies had provided partial support for this hypothesis, evidence for functional PRC ↔ LEC interactions remains controversial (see section 1.4.2). To address this issue we developed a new procedure permitting extracellular field potential recordings and CSD analysis *in-vivo*. Using this approach we showed the existence of bidirectional connections between PRC and LEC neurons (Chapter 2). Moreover, intracellular recordings obtained in a novel *in-vitro* preparation of the rat parahippocampal region, revealed dense mono-synaptic excitatory connections from the PRC to principal neurons in superficial layers of the LEC (~85% of the cells tested). More recently, preliminary data obtained using the same *in-vitro* preparation have revealed mono-synaptic excitatory connections from the deep layers of the LEC to three out three principal neurons in layers II/III of the PRC (Tahvildari et al, unpublished observations). Taken together, our novel *in-vivo* and *in-vitro* approaches allowed

us to obtain definitive evidence for the involvement of reciprocal of PRC-LEC connections in the NC-HC dialogue.

## 6.3 Organization of the bidirectional PRC-LEC circuit: An updated view

### 6.3.1 Forward (PRC→LEC) connection

As indicated in sections 1.4.1 and 1.4.2 previous anatomical and electrophysiological investigations have shown that the PRC can also inhibit LEC neurons via GABA containing terminals (e.g. Pinto et al., 2006). These synapses may be formed by direct mono-synaptic connections between the PRC and LEC neurons, or by the indirect activation of inhibitory neurons within the LEC. Indeed, it has been proposed that feed-forward inhibition could mediate a "wall of inhibition", preventing information transfer from the NC to the HC (de Curtis and Pare, 2004). Conceptually, this feed-forward inhibition could functionally oppose excitatory PRC-LEC connections, and thus information transfer from the NC to the HC would require relief of this inhibition or a facilitation of excitatory transmission between these regions. Interestingly Paz and colleagues (2006) have recently shown that PRC neurons can excite LEC neurons more reliably under conditions where neurons in the basal amygdala become activated. Indeed, these authors observed that during the early phase of an appetitive trace-conditioning task protocol action potentials generated by neurons in the basal amygdala appeared to facilitate impulse transmission from PRC to LEC neurons. Moreover, as learning proceeded, the effect of this facilitation decayed gradually. Taken

together these results indicate that forward excitatory projections from the PRC to the LEC are essential for NC-HC dialogue, and that a strengthening of these connections may be required during memory encoding. Whether this effect depends on a facilitation of excitatory PRC to LEC synapses or a removal of feed-forward inhibition remains to be determined.

### 6.3.2 Backward (LEC→PRC) connection

As described in section 1.3, connections from the HC to the NC are believed to play an important role in consolidation of short-term memories into long-term memories. In agreement with this hypothesis, electrical activity in HC neurons appears to induce spike discharges in NC neurons during periods of time associated with memory consolidation (e.g. during slow wave sleep, Siapas and Wilson, 1998). Although anatomical studies have suggested that the HC to NC dialogue progresses through HC→LEC→PRC→NC pathways (section 1.4.1), data supporting the existence of functional LEC-PRC connections were controversial. Specifically, despite field potential recordings suggesting the existence of mono-synaptic excitatory connections between LEC and PRC neurons (section 1.4.2, Ivanco and Racine, 2000), single unit recordings *in-vivo* have failed to show that firing in PRC neurons can be correlated to that of LEC neurons (Pelletier et al., 2004). As mentioned above the data presented in chapter 2, provide a direct evidence for excitatory LEC→PRC connections. How can these observations be reconciled? Interestingly, a recent study by Pare and colleagues (2006) has shown that firing in PRC neurons *in-vivo* can become correlated to that of LEC neurons during the late stages of a trace conditioning

task. Cross-correlation analysis of single unit activity recorded at multiple sites revealed that the facilitation of LEC→PRC connections is promoted by the electrical activity of neurons in the medial prefrontal cortex. Taken together, these findings suggest that bidirectional information propagation between the PRC and LEC might be under influence of other cortical and subcortical areas.

## 6.4 Concluding remarks: The contribution of cellular and synaptic neurophysiology to our understanding of the neurobiology of memory

The experimental results presented in this thesis aimed at clarifying the cellular and synaptic organization of forward and reverse neural connections between the PRC and the LEC, two essential relay stations within the MTL memory system. The bulk of this thesis research was performed under the supervision of the late Dr. Angel Alonso and, in my humble opinion, is quite representative of the unique and creative contributions of this great scientist to our understanding of memory.

Throughout his career Angel's goal was to clarify the mysteries of the entorhinal cortex through an extensive series of investigations of the intrinsic and synaptic properties of the neurons contained within this unique part of the brain using different *in-vivo* and *in-vitro* approaches. Indeed, his discoveries and those of his trainees have profoundly refined our understanding of the role of this structure in memory function. A major quest in his professional career was to demonstrate how the intrinsic cellular properties of neurons in different parts of the entorhinal cortex might contribute to memory *in-vivo*. Indeed, the

contributions of the numerous students and postdoctoral fellows who worked in his laboratory established an impressive database of information concerning the electrophysiological and morphological properties of different types of EC neurons. The usefulness of this approach is demonstrated by results of the present thesis which indicate that principal neurons in superficial layers of the LEC are distinct from those of neurons in corresponding portions of the MEC. This observation indicates that neurons in these areas can process neural information in different ways, a result that could not have been anticipated from anatomical or single unit recordings alone. In this respect, it is interesting to note that neurons in superficial layers of the MEC were recently shown to encode spatial cues more precisely than those in the LEC (Hargreaves et al., 2005). This *in-vivo* study therefore provided direct evidence showing that homologous neurons in different parts of the EC can perform different memory related tasks. The contributions of the different cellular properties of neurons in these areas to their respective network functions have yet to be established, but would surely have featured prominently in future work that could have been performed in Dr. Alonso's laboratory. Although Dr. Alonso passed away prematurely and unexpectedly in July 2005, his contributions to the field will continue through the future accomplishments of trainees and colleagues.

## References

Abe H, Ishida Y, Iwasaki T (2004) Perirhinal N-methyl-D-aspartate and muscarinic systems participate in object recognition in rats. Neurosci Lett 356:191-194.

Agrawal N, Hamam BN, Magistretti J, Alonso A, Ragsdale DS (2001) Persistent sodium channel activity mediates subthreshold membrane potential oscillations and low-threshold spikes in rat entorhinal cortex layer V neurons. Neuroscience 102:53-64.

Aigner TG, Mishkin M (1986) The effects of physostigmine and scopolamine on recognition memory in monkeys. Behav Neural Biol 45:81-87.

Aigner TG, Walker DL, Mishkin M (1991) Comparison of the effects of scopolamine administered before and after acquisition in a test of visual recognition memory in monkeys. Behav Neural Biol 55:61-67.

Alonso A, Kohler C (1984) A study of the reciprocal connections between the septum and the entorhinal area using anterograde and retrograde axonal transport methods in the rat brain. J Comp Neurol 225:327-343.

Alonso A, Llinas RR (1989) Subthreshold Na+-dependent theta-like rhythmicity in stellate cells of entorhinal cortex layer II. Nature 342:175-177.

Alonso A, Klink R (1993) Differential electroresponsiveness of stellate and pyramidal-like cells of medial entorhinal cortex layer II. J Neurophysiol 70:128-143.

Alvarez P, Zola-Morgan S, Squire LR (1995) Damage limited to the hippocampal region produces long-lasting memory impairment in monkeys. J Neurosci 15:3796-3807.

Andrade R (1991) Cell excitation enhances muscarinic cholinergic responses in rat association cortex. Brain Res 548:81-93.

Bartesaghi R (1994) Hippocampal-entorhinal relationships: electrophysiological analysis of the ventral hippocampal projections to the ventral entorhinal cortex. Neuroscience 61:457-466.

Bartesaghi R, Gessi T, Sperti L (1989) Electrophysiological analysis of the hippocampal projections to the entorhinal area. Neuroscience 30:51-62.

Beggs JM, Kairiss EW (1994) Electrophysiology and morphology of neurons in rat perirhinal cortex. Brain Res 665:18-32.

Biella G, Uva L, de Curtis M (2001) Network activity evoked by neocortical stimulation in area 36 of the guinea pig perirhinal cortex. J Neurophysiol 86:164-172.

Biella G, Uva L, de Curtis M (2002) Propagation of neuronal activity along the neocortical-perirhinal-entorhinal pathway in the guinea pig. J Neurosci 22:9972-9979.

Biella GR, Gnatkovsky V, Takashima I, Kajiwara R, Iijima T, de Curtis M (2003) Olfactory input to the parahippocampal region of the isolated guinea pig brain reveals weak entorhinal-to-perirhinal interactions. Eur J Neurosci 18:95-101.

Biscoe TJ, Duchen MR (1985) An intracellular study of dentate, CA1 and CA3 neurones in the mouse hippocampal slice. Q J Exp Physiol 70:189-202.

Blackstad TW (1956) Commissural connections of the hippocampal region in the rat, with special reference to their mode of termination. J Comp Neurol 105:417-537.

Boeijinga PH, Lopes da Silva FH (1988) Differential distribution of beta and theta EEG activity in the entorhinal cortex of the cat. Brain Res 448:272-286.

Bontempi B, Laurent-Demir C, Destrade C, Jaffard R (1999) Time-dependent reorganization of brain circuitry underlying long-term memory storage. Nature 400:671-675.

Bramham CR, Milgram NW, Srebro B (1991) Activation of AP5-sensitive NMDA Receptors is Not Required to Induce LTP of Synaptic Transmission in the Lateral Perforant Path. Eur J Neurosci 3:1300-1308.

Buckmaster PS, Alonso A, Canfield DR, Amaral DG (2004) Dendritic morphology, local circuitry, and intrinsic electrophysiology of principal neurons in the entorhinal cortex of macaque monkeys. J Comp Neurol 470:317-329.

Burwell RD (2000) The parahippocampal region: corticocortical connectivity. Ann N Y Acad Sci 911:25-42.

Burwell RD (2001) Borders and cytoarchitecture of the perirhinal and postrhinal cortices in the rat. J Comp Neurol 437:17-41.

Burwell RD, Amaral DG (1998a) Cortical afferents of the perirhinal, postrhinal, and entorhinal cortices of the rat. J Comp Neurol 398:179-205.

Burwell RD, Amaral DG (1998b) Perirhinal and postrhinal cortices of the rat: interconnectivity and connections with the entorhinal cortex. J Comp Neurol 391:293-321.

Burwell RD, Witter M (2002) Basic anatomy of the parahippocampal region in monkeys and rats. In: The parahippocampal region: organization and role in cognitive function (Witter M, Wouterlood FG, eds), pp 34-59. New York: Oxford University Press.

Burwell RD, Witter MP, Amaral DG (1995) Perirhinal and postrhinal cortices of the rat: a review of the neuroanatomical literature and comparison with findings from the monkey brain. Hippocampus 5:390-408.

Buzsaki G (1989) Two-stage model of memory trace formation: a role for "noisy" brain states. Neuroscience 31:551-570.

Buzsaki G (1996) The hippocampo-neocortical dialogue. Cereb Cortex 6:81-92.

Buzsaki G (1998) Memory consolidation during sleep: a neurophysiological perspective. J Sleep Res 7 Suppl 1:17-23.

Canning KJ, Wu K, Peloquin P, Kloosterman F, Leung LS (2000) Physiology of the entorhinal and perirhinal projections to the hippocampus studied by current source density analysis. Ann N Y Acad Sci 911:55-72.

Celesia GG, Jasper HH (1966) Acetylcholine released from cerebral cortex in relation to state of activation. Neurology 16:1053-1063.

Charpak S, Pare D, Llinas R (1995) The entorhinal cortex entrains fast CA1 hippocampal oscillations in the anaesthetized guinea-pig: role of the monosynaptic component of the perforant path. Eur J Neurosci 7:1548-1557.

Cho YH, Kesner RP (1996) Involvement of entorhinal cortex or parietal cortex in long-term spatial discrimination memory in rats: retrograde amnesia. Behav Neurosci 110:436-442.

Cho YH, Beracochea D, Jaffard R (1993) Extended temporal gradient for the retrograde and anterograde amnesia produced by ibotenate entorhinal cortex lesions in mice. J Neurosci 13:1759-1766.

Chrobak JJ, Buzsaki G (1996) High-frequency oscillations in the output networks of the hippocampal-entorhinal axis of the freely behaving rat. J Neurosci 16:3056-3066.

Chrobak JJ, Buzsaki G (1998) Gamma oscillations in the entorhinal cortex of the freely behaving rat. J Neurosci 18:388-398.

Craig S, Commins S (2006) The subiculum to entorhinal cortex projection is capable of sustaining both short- and long-term plastic changes. Behav Brain Res 174:281-288.

D'Antuono M, Biagini G, Tancredi V, Avoli M (2001) Electrophysiology of regular firing cells in the rat perirhinal cortex. Hippocampus 11:662-672.

de Curtis M, Pare D (2004) The rhinal cortices: a wall of inhibition between the neocortex and the hippocampus. Prog Neurobiol 74:101-110.

de Villers-Sidani E, Tahvildari B, Alonso A (2004) Synaptic activation patterns of the perirhinal-entorhinal inter-connections. Neuroscience 129:255-265.

Deacon TW, Eichenbaum H, Rosenberg P, Eckmann KW (1983) Afferent connections of the perirhinal cortex in the rat. J Comp Neurol 220:168-190.

Deadwyler SA, West JR, Cotman CW, Lynch G (1975) Physiological studies of the reciprocal connections between the hippocampus and entorhinal cortex. Exp Neurol 49:35-57.

Dickson CT, Mena AR, Alonso A (1997) Electroresponsiveness of medial entorhinal cortex layer III neurons in vitro. Neuroscience 81:937-950.

Dickson CT, Magistretti J, Shalinsky MH, Fransen E, Hasselmo ME, Alonso A (2000) Properties and role of I(h) in the pacing of subthreshold oscillations in entorhinal cortex layer II neurons. J Neurophysiol 83:2562-2579.

Dolorfo CL, Amaral DG (1998a) Entorhinal cortex of the rat: organization of intrinsic connections. J Comp Neurol 398:49-82.

Dolorfo CL, Amaral DG (1998b) Entorhinal cortex of the rat: topographic organization of the cells of origin of the perforant path projection to the dentate gyrus. J Comp Neurol 398:25-48.

Du F, Eid T, Lothman EW, Kohler C, Schwarcz R (1995) Preferential neuronal loss in layer III of the medial entorhinal cortex in rat models of temporal lobe epilepsy. J Neurosci 15:6301-6313.

Egorov AV, Hamam BN, Fransen E, Hasselmo ME, Alonso AA (2002) Graded persistent activity in entorhinal cortex neurons. Nature 420:173-178.

Eichenbaum H (2000) A cortical-hippocampal system for declarative memory. Nat Rev Neurosci 1:41-50.

Empson RM, Gloveli T, Schmitz D, Heinemann U (1995) Electrophysiology and morphology of a new type of cell within layer II of the rat lateral entorhinal cortex in vitro. Neurosci Lett 193:149-152.

Erchova I, Kreck G, Heinemann U, Herz AV (2004) Dynamics of rat entorhinal cortex layer II and III cells: characteristics of membrane potential resonance at rest predict oscillation properties near threshold. J Physiol 560:89-110.

Fransen E, Alonso AA, Hasselmo ME (2002) Simulations of the role of the muscarinic-activated calcium-sensitive nonspecific cation current INCM in entorhinal neuronal activity during delayed matching tasks. J Neurosci 22:1081-1097.

Fransen E, Tahvildari B, Egorov AV, Hasselmo ME, Alonso AA (2006) Mechanism of graded persistent cellular activity of entorhinal cortex layer v neurons. Neuron 49:735-746.

Fraser DD, MacVicar BA (1996) Cholinergic-dependent plateau potential in hippocampal CA1 pyramidal neurons. J Neurosci 16:4113-4128.

Freeman JA, Nicholson C (1975) Experimental optimization of current source-density technique for anuran cerebellum. J Neurophysiol 38:369-382.

Frey S, Petrides M (2002) Orbitofrontal cortex and memory formation. Neuron 36:171-176.

Fuster JM (1997) Network memory. Trends Neurosci 20:451-459.

Fyhn M, Molden S, Witter MP, Moser EI, Moser MB (2004) Spatial representation in the entorhinal cortex. Science 305:1258-1264.

Gauthier M, Destrade C, Soumireu-Mourat B (1983) Functional dissociation between lateral and medial entorhinal cortex in memory processes in mice. Behav Brain Res 9:111-117.

Germroth P, Schwerdtfeger WK, Buhl EH (1989) Morphology of identified entorhinal neurons projecting to the hippocampus. A light microscopical study combining retrograde tracing and intracellular injection. Neuroscience 30:683-691.

Germroth P, Schwerdtfeger WK, Buhl EH (1991) Ultrastructure and aspects of functional organization of pyramidal and nonpyramidal entorhinal projection neurons contributing to the perforant path. J Comp Neurol 305:215-231.

Ghamari-Langroudi M, Bourque CW (2002) Flufenamic acid blocks depolarizing afterpotentials and phasic firing in rat supraoptic neurones. J Physiol 545:537-542.

Gloveli T, Dugladze T, Schmitz D, Heinemann U (2001) Properties of entorhinal cortex deep layer neurons projecting to the rat dentate gyrus. Eur J Neurosci 13:413-420.

Gloveli T, Schmitz D, Empson RM, Dugladze T, Heinemann U (1997) Morphological and electrophysiological characterization of layer III cells of the medial entorhinal cortex of the rat. Neuroscience 77:629-648.

Goelet P, Castellucci VF, Schacher S, Kandel ER (1986) The long and the short of long-term memory--a molecular framework. Nature 322:419-422.

Goldman-Rakic PS (1995) Cellular basis of working memory. Neuron 14:477-485.

Gottfried JA, Smith AP, Rugg MD, Dolan RJ (2004) Remembrance of odors past: human olfactory cortex in cross-modal recognition memory. Neuron 42:687-695.

Haj-Dahmane S, Andrade R (1996) Muscarinic activation of a voltage-dependent cation nonselective current in rat association cortex. J Neurosci 16:3848-3861.

Haj-Dahmane S, Andrade R (1997) Calcium-activated cation nonselective current contributes to the fast afterdepolarization in rat prefrontal cortex neurons. J Neurophysiol 78:1983-1989.

Haj-Dahmane S, Andrade R (1998) Ionic mechanism of the slow afterdepolarization induced by muscarinic receptor activation in rat prefrontal cortex. J Neurophysiol 80:1197-1210.

Hamam BN, Amaral DG, Alonso AA (2002) Morphological and electrophysiological characteristics of layer V neurons of the rat lateral entorhinal cortex. J Comp Neurol 451:45-61.

Hamam BN, Kennedy TE, Alonso A, Amaral DG (2000) Morphological and electrophysiological characteristics of layer V neurons of the rat medial entorhinal cortex. J Comp Neurol 418:457-472.

Hargreaves EL, Rao G, Lee I, Knierim JJ (2005) Major dissociation between medial and lateral entorhinal input to dorsal hippocampus. Science 308:1792-1794.

Hasselmo ME (1999) Neuromodulation: acetylcholine and memory consolidation. Trends Cogn Sci 3:351-359.

Hasselmo ME, Bower JM (1993) Acetylcholine and memory. Trends Neurosci 16:218-222.

Hasselmo ME, Stern CE (2006) Mechanisms underlying working memory for novel information. Trends Cogn Sci 10:487-493.

Higuchi S, Miyashita Y (1996) Formation of mnemonic neuronal responses to visual paired associates in inferotemporal cortex is impaired by perirhinal and entorhinal lesions. Proc Natl Acad Sci U S A 93:739-743.

Himmelheber AM, Sarter M, Bruno JP (2000) Increases in cortical acetylcholine release during sustained attention performance in rats. Brain Res Cogn Brain Res 9:313-325.

Iijima T, Witter MP, Ichikawa M, Tominaga T, Kajiwara R, Matsumoto G (1996) Entorhinal-hippocampal interactions revealed by real-time imaging. Science 272:1176-1179.

Insausti R, Amaral DG, Cowan WM (1987) The entorhinal cortex of the monkey: II. Cortical afferents. J Comp Neurol 264:356-395.

Insausti R, Herrero MT, Witter MP (1997) Entorhinal cortex of the rat: cytoarchitectonic subdivisions and the origin and distribution of cortical efferents. Hippocampus 7:146-183.

Ivanco TL, Racine RJ (2000) Long-term potentiation in the reciprocal corticohippocampal and corticocortical pathways in the chronically implanted, freely moving rat. Hippocampus 10:143-152.

Jones RS (1994) Synaptic and intrinsic properties of neurons of origin of the perforant path in layer II of the rat entorhinal cortex in vitro. Hippocampus 4:335-353.

Kajiwara R, Takashima I, Mimura Y, Witter MP, Iijima T (2003) Amygdala input promotes spread of excitatory neural activity from perirhinal cortex to the entorhinal-hippocampal circuit. J Neurophysiol 89:2176-2184.

Klink R, Alonso A (1993) Ionic mechanisms for the subthreshold oscillations and differential electroresponsiveness of medial entorhinal cortex layer II neurons. J Neurophysiol 70:144-157.

Klink R, Alonso A (1997a) Morphological characteristics of layer II projection neurons in the rat medial entorhinal cortex. Hippocampus 7:571-583.

Klink R, Alonso A (1997b) Ionic mechanisms of muscarinic depolarization in entorhinal cortex layer II neurons. J Neurophysiol 77:1829-1843.

Klink R, Alonso A (1997c) Muscarinic modulation of the oscillatory and repetitive firing properties of entorhinal cortex layer II neurons. J Neurophysiol 77:1813-1828.

Kloosterman F, Witter MP, Van Haeften T (2003a) Topographical and laminar organization of subicular projections to the parahippocampal region of the rat. J Comp Neurol 455:156-171.

Kloosterman F, Van Haeften T, Witter MP, Lopes Da Silva FH (2003b) Electrophysiological characterization of interlaminar entorhinal connections: an essential link for re-entrance in the hippocampal-entorhinal system. Eur J Neurosci 18:3037-3052.

Knaus HG, Schwarzer C, Koch RO, Eberhart A, Kaczorowski GJ, Glossmann H, Wunder F, Pongs O, Garcia ML, Sperk G (1996) Distribution of high-

conductance Ca(2+)-activated K+ channels in rat brain: targeting to axons and nerve terminals. J Neurosci 16:955-963.

Knierim JJ, Lee I, Hargreaves EL (2006) Hippocampal place cells: parallel input streams, subregional processing, and implications for episodic memory. Hippocampus 16:755-764.

Kohler C (1988) Intrinsic connections of the retrohippocampal region in the rat brain: III. The lateral entorhinal area. J Comp Neurol 271:208-228.

Koulakov AA, Raghavachari S, Kepecs A, Lisman JE (2002) Model for a robust neural integrator. Nat Neurosci 5:775-782.

Krnjevic K (1993) Central cholinergic mechanisms and function. Prog Brain Res 98:285-292.

Lavenex P, Amaral DG (2000) Hippocampal-neocortical interaction: a hierarchy of associativity. Hippocampus 10:420-430.

Lavenex P, Suzuki WA, Amaral DG (2002) Perirhinal and parahippocampal cortices of the macaque monkey: projections to the neocortex. J Comp Neurol 447:394-420.

Leonard BW, Amaral DG, Squire LR, Zola-Morgan S (1995) Transient memory impairment in monkeys with bilateral lesions of the entorhinal cortex. J Neurosci 15:5637-5659.

Loewenstein Y, Mahon S, Chadderton P, Kitamura K, Sompolinsky H, Yarom Y, Hausser M (2005) Bistability of cerebellar Purkinje cells modulated by sensory stimulation. Nat Neurosci 8:202-211.

Lomo T (1971a) Potentiation of monosynaptic EPSPs in the perforant path-dentate granule cell synapse. Exp Brain Res 12:46-63.

Lomo T (1971b) Patterns of activation in a monosynaptic cortical pathway: the perforant path input to the dentate area of the hippocampal formation. Exp Brain Res 12:18-45.

Lopes da Silva FH, Witter MP, Boeijinga PH, Lohman AH (1990) Anatomic organization and physiology of the limbic cortex. Physiol Rev 70:453-511.

Magistretti J, Ma L, Shalinsky MH, Lin W, Klink R, Alonso A (2004) Spike Patterning by Ca2+-Dependent Regulation of a Muscarinic Cation Current in Entorhinal Cortex Layer-II Neurons. J Neurophysiol 92: 1644-57.

Major G, Tank D (2004) Persistent neural activity: prevalence and mechanisms. Curr Opin Neurobiol 14:675-684.

Marder E, Abbott LF, Turrigiano GG, Liu Z, Golowasch J (1996) Memory from the dynamics of intrinsic membrane currents. Proc Natl Acad Sci U S A 93:13481-13486.

Martina M, Royer S, Pare D (2001) Propagation of neocortical inputs in the perirhinal cortex. J Neurosci 21:2878-2888.

Maviel T, Durkin TP, Menzaghi F, Bontempi B (2004) Sites of neocortical reorganization critical for remote spatial memory. Science 305:96-99.

McClelland JL, McNaughton BL, O'Reilly RC (1995) Why there are complementary learning systems in the hippocampus and neocortex: insights from the successes and failures of connectionist models of learning and memory. Psychol Rev 102:419-457.

McCormick DA, Wang Z, Huguenard J (1993) Neurotransmitter control of neocortical neuronal activity and excitability. Cereb Cortex 3:387-398.

McGann JP, Moyer JR, Jr., Brown TH (2001) Predominance of late-spiking neurons in layer VI of rat perirhinal cortex. J Neurosci 21:4969-4976.

McGaughy J, Koene RA, Eichenbaum H, Hasselmo ME (2005) Cholinergic deafferentation of the entorhinal cortex in rats impairs encoding of novel but not familiar stimuli in a delayed nonmatch-to-sample task. J Neurosci 25:10273-10281.

McNaughton BL (1980) Evidence for two physiologically distinct perforant pathways to the fascia dentata. Brain Res 199:1-19.

Meunier M, Bachevalier J, Mishkin M, Murray EA (1993) Effects on visual recognition of combined and separate ablations of the entorhinal and perirhinal cortex in rhesus monkeys. J Neurosci 13:5418-5432.

Meunier M, Hadfield W, Bachevalier J, Murray EA (1996) Effects of rhinal cortex lesions combined with hippocampectomy on visual recognition memory in rhesus monkeys. J Neurophysiol 75:1190-1205.

Miller EK, Cohen JD (2001) An integrative theory of prefrontal cortex function. Annu Rev Neurosci 24:167-202.

Miller EK, Erickson CA, Desimone R (1996) Neural mechanisms of visual working memory in prefrontal cortex of the macaque. J Neurosci 16:5154-5167.

Milner B (1972) Disorders of learning and memory after temporal lobe lesions in man. Clin Neurosurg 19:421-446.

Milner B, Squire LR, Kandel ER (1998) Cognitive neuroscience and the study of memory. Neuron 20:445-468.

Mishkin M (1978) Memory in monkeys severely impaired by combined but not by separate removal of amygdala and hippocampus. Nature 273:297-298.

Mishkin M (1982) A memory system in the monkey. Philos Trans R Soc Lond B Biol Sci 298:83-95.

Moyer JR, Jr., McNay EC, Brown TH (2002) Three classes of pyramidal neurons in layer V of rat perirhinal cortex. Hippocampus 12:218-234.

Mumby DG, Pinel JP (1994) Rhinal cortex lesions and object recognition in rats. Behav Neurosci 108:11-18.

Murray EA, Mishkin M (1986) Visual recognition in monkeys following rhinal cortical ablations combined with either amygdalectomy or hippocampectomy. J Neurosci 6:1991-2003.

Naber PA, Witter MP, Lopes da Silva FH (2000) Differential distribution of barrel or visual cortex. Evoked responses along the rostro-caudal axis of the peri- and postrhinal cortices. Brain Res 877:298-305.

Naber PA, Lopes da Silva FH, Witter MP (2001) Reciprocal connections between the entorhinal cortex and hippocampal fields CA1 and the subiculum are in register with the projections from CA1 to the subiculum. Hippocampus 11:99-104.

Nadel L, Moscovitch M (1997) Memory consolidation, retrograde amnesia and the hippocampal complex. Curr Opin Neurobiol 7:217-227.

Naya Y, Yoshida M, Miyashita Y (2001) Backward spreading of memory-retrieval signal in the primate temporal cortex. Science 291:661-664.

Nemanic S, Alvarado MC, Bachevalier J (2004) The hippocampal/parahippocampal regions and recognition memory: insights from visual paired comparison versus object-delayed nonmatching in monkeys. J Neurosci 24:2013-2026.

Neumaier JF, Chavkin C (1989) Release of endogenous opioid peptides displaces [3H]diprenorphine binding in rat hippocampal slices. Brain Res 493:292-302.

O'Keefe J, Nadel L (1978) The hippocampus as a cognitive map. Oxford: Oxford University Press.

Otto T, Eichenbaum H (1992) Complementary roles of the orbital prefrontal cortex and the perirhinal-entorhinal cortices in an odor-guided delayed-nonmatching-to-sample task. Behav Neurosci 106:762-775.

Pare D, Bauer EP, Paz R (2006) Learning-related changes in the activity of medial prefrontal and rhinal neurons during the acquisition of a trace conditioning task. In: Soc. Neurosci. Abstr.

Partridge LD, Valenzuela CF (2000) Block of hippocampal CAN channels by flufenamate. Brain Res 867:143-148.

Paz R, Pelletier JG, Bauer EP, Pare D (2006) Emotional enhancement of memory via amygdala-driven facilitation of rhinal interactions. Nat Neurosci 9:1321-1329.

Pelletier JG, Apergis J, Pare D (2004) Low-probability transmission of neocortical and entorhinal impulses through the perirhinal cortex. J Neurophysiol 91:2079-2089.

Penetar DM, McDonough JH, Jr. (1983) Effects of cholinergic drugs on delayed match-to-sample performance of rhesus monkeys. Pharmacol Biochem Behav 19:963-967.

Penfield W, Perot P (1963) The Brain's Record of Auditory and Visual Experience. A Final Summary and Discussion. Brain 86:595-696.

Pennartz CM, Uylings HB, Barnes CA, McNaughton BL (2002) Memory reactivation and consolidation during sleep: from cellular mechanisms to human performance. Prog Brain Res 138:143-166.

Pinto A, Fuentes C, Pare D (2006) Feedforward inhibition regulates perirhinal transmission of neocortical inputs to the entorhinal cortex: ultrastructural study in guinea pigs. J Comp Neurol 495:722-734.

Ramón y Cajal S (1901) Sobre un ganglio especial de la corteza esfenooccipital. Trab del Lab de invest Biol Univ Madrid 1:189-201.

Rosene DL, Van Hoesen GW (1977) Hippocampal efferents reach widespread areas of cerebral cortex and amygdala in the rhesus monkey. Science 198:315-317.

Rosenzweig MR, Bennett EL, Colombo PJ, Lee DW, Serrano PA (1993) Short-term, intermediate-term, and long-term memories. Behav Brain Res 57:193-198.

Ruth RE, Collier TJ, Routtenberg A (1982) Topography between the entorhinal cortex and the dentate septotemporal axis in rats: I. Medial and intermediate entorhinal projecting cells. J Comp Neurol 209:69-78.

Ruth RE, Collier TJ, Routtenberg A (1988) Topographical relationship between the entorhinal cortex and the septotemporal axis of the dentate gyrus in rats: II. Cells projecting from lateral entorhinal subdivisions. J Comp Neurol 270:506-516.

Schmitz D, Gloveli T, Behr J, Dugladze T, Heinemann U (1998) Subthreshold membrane potential oscillations in neurons of deep layers of the entorhinal cortex. Neuroscience 85:999-1004.

Schon K, Hasselmo ME, Lopresti ML, Tricarico MD, Stern CE (2004) Persistence of parahippocampal representation in the absence of stimulus input enhances long-term encoding: a functional magnetic resonance imaging study of subsequent memory after a delayed match-to-sample task. J Neurosci 24:11088-11097.

Schon K, Atri A, Hasselmo ME, Tricarico MD, LoPresti ML, Stern CE (2005) Scopolamine reduces persistent activity related to long-term encoding in the parahippocampal gyrus during delayed matching in humans. J Neurosci 25:9112-9123.

Schwartz SP, Coleman PD (1981) Neurons of origin of the perforant path. Exp Neurol 74:305-312.

Scoville WB, Milner B (1957) Loss of recent memory after bilateral hippocampal lesions. J Neurol Neurosurg Psychiatry 20:11-21.

Scoville WB, Milner B (2000) Loss of recent memory after bilateral hippocampal lesions. 1957. J Neuropsychiatry Clin Neurosci 12:103-113.

Shah MM, Anderson AE, Leung V, Lin X, Johnston D (2004) Seizure-induced plasticity of h channels in entorhinal cortical layer III pyramidal neurons. Neuron 44:495-508.

Shalinsky MH, Magistretti J, Ma L, Alonso AA (2002) Muscarinic activation of a cation current and associated current noise in entorhinal-cortex layer-II neurons. J Neurophysiol 88:1197-1211.

Shu Y, Hasenstaub A, McCormick DA (2003) Turning on and off recurrent balanced cortical activity. Nature 423:288-293.

Siapas AG, Wilson MA (1998) Coordinated interactions between hippocampal ripples and cortical spindles during slow-wave sleep. Neuron 21:1123-1128.

Sirota A, Csicsvari J, Buhl D, Buzsaki G (2003) Communication between neocortex and hippocampus during sleep in rodents. Proc Natl Acad Sci U S A 100:2065-2069.

Skaggs WE, McNaughton BL (1996) Replay of neuronal firing sequences in rat hippocampus during sleep following spatial experience. Science 271:1870-1873.

Sorensen KE, Shipley MT (1979) Projections from the subiculum to the deep layers of the ipsilateral presubicular and entorhinal cortices in the guinea pig. J Comp Neurol 188:313-333.

Squire LR (1998) Memory systems. C R Acad Sci III 321:153-156.

Squire LR, Zola-Morgan S (1988) Memory: brain systems and behavior. Trends Neurosci 11:170-175.

Squire LR, Zola-Morgan S (1991) The medial temporal lobe memory system. Science 253:1380-1386.

Squire LR, Zola SM (1998) Episodic memory, semantic memory, and amnesia. Hippocampus 8:205-211.

Steffenach HA, Witter M, Moser MB, Moser EI (2005) Spatial memory in the rat requires the dorsolateral band of the entorhinal cortex. Neuron 45:301-313.

Stern CE, Sherman SJ, Kirchhoff BA, Hasselmo ME (2001) Medial temporal and prefrontal contributions to working memory tasks with novel and familiar stimuli. Hippocampus 11:337-346.

Stern CE, Corkin S, Gonzalez RG, Guimaraes AR, Baker JR, Jennings PJ, Carr CA, Sugiura RM, Vedantham V, Rosen BR (1996) The hippocampal formation participates in novel picture encoding: evidence from functional magnetic resonance imaging. Proc Natl Acad Sci U S A 93:8660-8665.

Steward O (1976) Topographic organization of the projections from the entorhinal area to the hippocampal formation of the rat. J Comp Neurol 167:285-314.

Steward O, Scoville SA (1976) Cells of origin of entorhinal cortical afferents to the hippocampus and fascia dentata of the rat. J Comp Neurol 169:347-370.

Sutherland GR, McNaughton B (2000) Memory trace reactivation in hippocampal and neocortical neuronal ensembles. Curr Opin Neurobiol 10:180-186.

Suzuki WA (1996) The anatomy, physiology and functions of the perirhinal cortex. Curr Opin Neurobiol 6:179-186.

Suzuki WA, Amaral DG (1994a) Topographic organization of the reciprocal connections between the monkey entorhinal cortex and the perirhinal and parahippocampal cortices. J Neurosci 14:1856-1877.

Suzuki WA, Amaral DG (1994b) Perirhinal and parahippocampal cortices of the macaque monkey: cortical afferents. J Comp Neurol 350:497-533.

Suzuki WA, Eichenbaum H (2000) The neurophysiology of memory. Ann N Y Acad Sci 911:175-191.

Suzuki WA, Amaral DG (2004) Functional neuroanatomy of the medial temporal lobe memory system. Cortex 40:220-222.

Suzuki WA, Miller EK, Desimone R (1997) Object and place memory in the macaque entorhinal cortex. J Neurophysiol 78:1062-1081.

Suzuki WA, Zola-Morgan S, Squire LR, Amaral DG (1993) Lesions of the perirhinal and parahippocampal cortices in the monkey produce long-lasting memory impairment in the visual and tactual modalities. J Neurosci 13:2430-2451.

Swanson LW, Cowan WM (1977) An autoradiographic study of the organization of the efferent connections of the hippocampal formation in the rat. J Comp Neurol 172:49-84.

Swanson LW, Kohler C (1986) Anatomical evidence for direct projections from the entorhinal area to the entire cortical mantle in the rat. J Neurosci 6:3010-3023.

Tahvildari B, Alonso A (2003) Electrophysiological and Morphological Properties of Neurons in Superficial Layers of Lateral Entorhinal Cortex in Rat Brain Slice. In: Soc. Neurosci. Abstr.

Tahvildari B, Alonso A (2005) Morphological and electrophysiological properties of lateral entorhinal cortex layers II and III principal neurons. J Comp Neurol 491:123-140.

Tahvildari B, Fransen E, Alonso AA, Hasselmo ME (2007) Switching between "On" and "Off" states of persistent activity in lateral entorhinal layer III neurons. Hippocampus 17:257-263.

Tamamaki N, Nojyo Y (1993) Projection of the entorhinal layer II neurons in the rat as revealed by intracellular pressure-injection of neurobiotin. Hippocampus 3:471-480.

Tang Y, Aigner TG (1996) Release of cerebral acetylcholine increases during visually mediated behavior in monkeys. Neuroreport 7:2231-2235.

Tang Y, Mishkin M, Aigner TG (1997) Effects of muscarinic blockade in perirhinal cortex during visual recognition. Proc Natl Acad Sci U S A 94:12667-12669.

Turchi J, Saunders RC, Mishkin M (2005) Effects of cholinergic deafferentation of the rhinal cortex on visual recognition memory in monkeys. Proc Natl Acad Sci U S A 102:2158-2161.

Uva L, Gruschke S, Biella G, De Curtis M, Witter MP (2004) Cytoarchitectonic characterization of the parahippocampal region of the guinea pig. J Comp Neurol 474:289-303.

van der Linden S, Lopes da Silva FH (1998) Comparison of the electrophysiology and morphology of layers III and II neurons of the rat medial entorhinal cortex in vitro. Eur J Neurosci 10:1479-1489.

Van Essen DC, Anderson CH, Felleman DJ (1992) Information processing in the primate visual system: an integrated systems perspective. Science 255:419-423.

van Haeften T, Jorritsma-Byham B, Witter MP (1995) Quantitative morphological analysis of subicular terminals in the rat entorhinal cortex. Hippocampus 5:452-459.

van Haeften T, Wouterlood FG, Witter MP (2000) Presubicular input to the dendrites of layer-V entorhinal neurons in the rat. Ann N Y Acad Sci 911:471-473.

Van Hoesen G, Pandya DN (1975a) Some connections of the entorhinal (area 28) and perirhinal (area 35) cortices of the rhesus monkey. I. Temporal lobe afferents. Brain Res 95:1-24.

Van Hoesen G, Pandya DN, Butters N (1975) Some connections of the entorhinal (area 28) and perirhinal (area 35) cortices of the rhesus monkey. II. Frontal lobe afferents. Brain Res 95:25-38.

Van Hoesen GW, Pandya DN (1975b) Some connections of the entorhinal (area 28) and perirhinal (area 35) cortices of the rhesus monkey. III. Efferent connections. Brain Res 95:39-59.

Vogalis F, Goyal RK (1997) Activation of small conductance Ca(2+)-dependent K+ channels by purinergic agonists in smooth muscle cells of the mouse ileum. J Physiol 502 ( Pt 3):497-508.

Wang X, Lambert NA (2003) Membrane properties of identified lateral and medial perforant pathway projection neurons. Neuroscience 117:485-492.

Wang XJ (2001) Synaptic reverberation underlying mnemonic persistent activity. Trends Neurosci 24:455-463.

Wanner SG, Koch RO, Koschak A, Trieb M, Garcia ML, Kaczorowski GJ, Knaus HG (1999) High-conductance calcium-activated potassium channels in rat brain: pharmacology, distribution, and subunit composition. Biochemistry 38:5392-5400.

Warburton EC, Koder T, Cho K, Massey PV, Duguid G, Barker GR, Aggleton JP, Bashir ZI, Brown MW (2003) Cholinergic neurotransmission is essential for perirhinal cortical plasticity and recognition memory. Neuron 38:987-996.

Wiig KA, Bilkey DK (1995) Lesions of rat perirhinal cortex exacerbate the memory deficit observed following damage to the fimbria-fornix. Behav Neurosci 109:620-630.

Wilson MA, McNaughton BL (1994) Reactivation of hippocampal ensemble memories during sleep. Science 265:676-679.

Wiltgen BJ, Brown RA, Talton LE, Silva AJ (2004) New circuits for old memories: the role of the neocortex in consolidation. Neuron 44:101-108.

Witter MP, Groenewegen HJ (1986) Connections of the parahippocampal cortex in the cat. IV. Subcortical efferents. J Comp Neurol 252:51-77.

Witter MP, Griffioen AW, Jorritsma-Byham B, Krijnen JL (1988) Entorhinal projections to the hippocampal CA1 region in the rat: an underestimated pathway. Neurosci Lett 85:193-198.

Witter MP, Groenewegen HJ, Lopes da Silva FH, Lohman AH (1989) Functional organization of the extrinsic and intrinsic circuitry of the parahippocampal region. Prog Neurobiol 33:161-253.

Witter MP, Wouterlood FG, Naber PA, Van Haeften T (2000) Anatomical organization of the parahippocampal-hippocampal network. Ann N Y Acad Sci 911:1-24.

Yeckel MF, Berger TW (1990) Feedforward excitation of the hippocampus by afferents from the entorhinal cortex: redefinition of the role of the trisynaptic pathway. Proc Natl Acad Sci U S A 87:5832-5836.

Young BJ, Otto T, Fox GD, Eichenbaum H (1997) Memory representation within the parahippocampal region. J Neurosci 17:5183-5195.

Ziakopoulos Z, Tillett CW, Brown MW, Bashir ZI (1999) Input-and layer-dependent synaptic plasticity in the rat perirhinal cortex in vitro. Neuroscience 92:459-472.

Zola-Morgan S, Squire LR (1984) Preserved learning in monkeys with medial temporal lesions: sparing of motor and cognitive skills. J Neurosci 4:1072-1085.

Zola-Morgan S, Squire LR (1985) Medial temporal lesions in monkeys impair memory on a variety of tasks sensitive to human amnesia. Behav Neurosci 99:22-34.

Zola-Morgan S, Squire LR, Amaral DG (1986) Human amnesia and the medial temporal region: enduring memory impairment following a bilateral lesion limited to field CA1 of the hippocampus. J Neurosci 6:2950-2967.

Zola-Morgan S, Squire LR, Amaral DG (1989a) Lesions of the amygdala that spare adjacent cortical regions do not impair memory or exacerbate the impairment following lesions of the hippocampal formation. J Neurosci 9:1922-1936.

Zola-Morgan S, Squire LR, Amaral DG, Suzuki WA (1989b) Lesions of perirhinal and parahippocampal cortex that spare the amygdala and hippocampal formation produce severe memory impairment. J Neurosci 9:4355-4370.

Zola-Morgan S, Squire LR, Clower RP, Rempel NL (1993) Damage to the perirhinal cortex exacerbates memory impairment following lesions to the hippocampal formation. J Neurosci 13:251-265.

Zola-Morgan SM, Squire LR (1990) The primate hippocampal formation: evidence for a time-limited role in memory storage. Science 250:288-290.

# Appendices

## Research compliance certificate

## Copyright waivers

Dear Dr Tahvildari

We hereby grant you permission to reproduce the material detailed below in your thesis at no charge subject to the following conditions:

1. If any part of the material to be used (for example, figures) has appeared in our publication with credit or acknowledgement to another source, permission must also be sought from that source. If such permission is not obtained then that material may not be included in your publication/copies.

2. Suitable acknowledgment to the source must be made, either as a footnote or in a reference list at the end of your publication, as follows: "Reprinted from Publication title, Vol number, Author(s), Title of article, Pages No., Copyright (Year), with permission from Elsevier".

3. Reproduction of this material is confined to the purpose for which permission is hereby given.

4. This permission is granted for non-exclusive world English rights only. For other languages please reapply separately for each one required. Permission excludes use in an electronic form. Should you have a specific electronic project in mind please reapply for permission.

5. This includes permission for the Library and Archives of Canada to supply single copies, on demand, of the complete thesis. Should your thesis be published commercially, please reapply for permission.

Yours sincerely,

Natalie David
Senior Rights Assistant

Your future requests will be handled more quickly if you complete the online form at www.elsevier.com/permissions <http://www.elsevier.com/permissions>

-----Original Message-----
From: babak.tahvildari@mcgill.ca [mailto:babak.tahvildari@mcgill.ca
mailto:babak.tahvildari@mcgill.ca
Sent: Monday, July 31, 2006 3:49 PM
To: healthpermissions@elsevier.com
Subject: Obtain Permission

This Email was sent from the Elsevier Corporate Web Site and is related to Obtain Permission form:

Product: Customer Support
Component: Obtain Permission
Web server: http://www.elsevier.com <http://www.elsevier.com>
IP address: 10.10.24.149
Client: Mozilla/4.0 (compatible; MSIE 6.0; Windows NT 5.1; SV1)
Invoked from:
http://www.elsevier.com/wps/find/obtainpermissionform.cws_home
http://www.elsevier.com/wps/find/obtainpermissionform.cws_home
?isSubmitted=yes&navigateXmlFileName=/store/prod_webcache_act/framework_support/obtainpermission.xml

Request From: Signed Waivers Babak Tahvildari
Montreal Neurological Institute, 3801 University St. Room 753, H3A 2B4, Montreal, Canada

Contact Details:
Telephone: (514) 398 8443
Fax:
Email Address: babak.tahvildari@mcgill.ca
To use the following material:
ISSN/ISBN:
Title: Neuroscience
Author(s): E. DE VILLERS-SIDANI, B. TAHVILDARI AND A. ALONSO
Volume: 129, Issue: 1, Year: 2004, Pages: 255 - 265
Article title: SYNAPTIC ACTIVATION PATTERNS OF THE PERIRHINAL/ENT
How much of the requested material is to be used:
The entire article
Are you the author: Yes
Author at institute: Yes
How/where will the requested material be used?
Details:
I am a PhD student at the Montreal Neurological Institute and in process of preparing my thesis. Since my thesis is going to be a manuscript-based thesis, I want to include the entire of the article mentioned as a chapter in my thesis. In this respect I need a signed waiver from the publisher

Additional Info:
- end -

Sara
Vanderwillik/Cana
da/Wiley

08/02/2006 02:15
PM

To: Bradley Johnson/P&T/Hoboken/Wiley@Wiley
cc:
Subject: Fw: Permission Request Form Canada

Hi Brad,
see below.
Sara

----- Forwarded by Sara Vanderwillik/Canada/Wiley on 02/08/2006 02:14 PM -----

svanderw@wiley.co
m

31/07/2006 04:21
PM

To: <svanderw@wiley.com>
cc:
Subject: Permission Request Form Canada

Please respond to
svanderw@wiley.co
m

A01_First_Name: Babak
A02_Last_Name: Tahvildari
A03_Company: Montreal Neurological Institute
A04_Address: 3801 University St. Room 753
A05_City: Montreal
A06_Province: Quebec
A07_Zip: H3A 2B4
A08_Country: Canada
A09_Phone: (514) 398 8443
A10_Fax: (514) 398 5871
A11_email: babak.tahvildari@mcgill.ca

Dear Mr. Tahvildari:

Please be advise permission is granted to reuse pages 257-263 from Hippocampus: 17(4) 2007 in your forthcoming Thesis which will be published by McGill University. Credit must appear on every copy using the material and must include the title; the author (s); and/or editor (s); Copyright (year and owner); and the statement "Reprinted with permission of Wiley-Liss, Inc. a subsidiary of John Wiley & Sons, Inc." Please Note: No rights are granted to use content that appears in the work with credit to another source.

Good luck with your thesis

Sincerely,

Brad Johnson, Permissions Assistant John Wiley & Sons, Inc. 111 River Street Hoboken, NJ 07030-5774 Permissions – Mail Stop 4-02 Tel: 201.748.6786 Fax: 201.748.6008 bjohns@wiley.com

Wiley Bicentennial: Knowledge for Generations 1807-2007

Visit our website @ www.wiley.com/go/permissions for permissions information

Dear Brad Johnson,

I am a PhD student and as the first author of the following manuscript I want to include it as a chapter of my PhD thesis entitled: "Functional Organizations of the Perirhinal-lateral entorhinal circuit".

Babak Tahvildari , Erik Fransén , Angel A. Alonso , Michael E. Hasselmo (2007) Switching between "On" and "Off" states of persistent activity in lateral entorhinal layer III neuron, Hippocampus 17(4): 257-63

Please provide the appropriate permission and copyright waiver.

Thanks,
Babak Tahvildari

Babak Tahvildari
PhD Student
Dept. of Neurology and Neurosurgery
Montreal Neurological Institute (MNI)
McGill Unversity
3801 University Street,
Montreal, Quebec
Canada H3A 2B4
Tel: (514) 398-8443
Fax: (514) 398-5871